The Role of Huntingtin in Fast Axonal Transport

by

Kurt R. Weiss

B.S. Biology
University of Wisconsin-Madison, 2005

SUBMITTED TO THE DEPARTMENT OF BIOLOGY IN PARTIAL FULFILLMENT OF THE
REQUIREMENTS FOR THE DEGREE OF

DOCTOR OF PHILOSOPHY

AT THE
MASSACHUSETTS INSTITUTE OF TECHNOLOGY

February 2012

Signature of Author: _____X
Department of Biology
November 9, 2011

Certified by: _____X
Dr. J. Troy Littleton
Professor of Biology
Thesis Advisor

Accepted by: _____X
Robert T. Sauer,
Luria Professor of Biology
Chairman of the Graduate Committee

The Role of Huntingtin in Fast Axonal Transport

by

Kurt R. Weiss

Submitted to the Department of Biology on January 17, 2012
in Partial Fulfillment of the Requirements for the Degree of
Doctor of Philosophy in Biology

ABSTRACT

Huntington's Disease (HD) is an autosomal dominant, neurodegenerative disease that occurs when an expansion of the polyQ tract of the *huntingtin* gene expands to greater than ~35 residues. This mutation leads to aggregation of the Huntingtin protein (Htt) and degeneration of striatal and cortex neurons, ultimately causing motor impairment and personality changes. Neither the mechanism by which mutant Htt causes toxicity, nor the endogenous function of wild-type Htt, are well understood.

To explore mechanisms of mutant Htt-induced toxicity, we generated and characterized a *Drosophila* model of HD by expressing a 588 amino acid N-terminal fragment of human Htt with 138 glutamines, and tagged with mRFP (Q138Htt-RFP). We used this model to conduct a screen for genes that modify cytoplasmic aggregation and/or toxicity phenotypes. We identified two classes of interacting suppressors in our screen: those that rescue viability while decreasing Htt expression and aggregation, and those that rescue viability independent of effects on Htt aggregation, suggesting that aggregation and toxicity can be separated.

To evaluate the putative function of Htt in fast axonal transport, we characterized the co-localization of the *Drosophila* Htt homolog tagged with mRFP (dHtt-RFP), and the alterations in axonal transport kinetics associated with a *dhtt* null. We find that dHtt co-localizes with a subset of cargos including synaptic vesicles and mitochondria, and acts locally on these cargos to increase transport processivity.

Finally, we evaluated the effects of Q138Htt-RFP expression on transport kinetics. We find that the majority of transport cargos bypass Q138Htt aggregates, indicating they are not complete blockages of axonal transport. We also observe reduced mitochondrial transport in the absence of aggregates, suggesting aggregate-independent transport defects.

Our observations of transport *in vivo* support a role for wild-type Htt in mediating fast axonal transport of membrane bound organelles, and suggest that mutant Htt can cause aggregation-dependent and -independent defects in axonal transport.

Thesis Advisor: J. Troy Littleton
Title: Professor of Biology

Acknowledgments

I thank everyone in the Littleton lab for years of personal and professional support. Specifically, I thank: Richard Cho for setting up the in *vivo* imaging chamber, Joost Schulte, Avital Rodal, and Zhou Guan for help with methods, and many useful Huntingtin related conversations. Dina Volfson and Charles Moss who are the gears that keep the lab running smoothly. My current and former graduate student peers, who have provided reagents, advice, and friendship. My girlfriend Carly, for her years of enduring support, and help editing this manuscript. And last, but not least, my advisor, Troy Littleton. Troy has seen our entire lab through thick and thin while remaining a strong leader, and showing wisdom, support, and generosity. His door, heart, and mind are always open, and he is always willing to help with any scientific or personal problem. I feel privileged to have the opportunity to work with him and know him as a person. Thank you all.

TABLE OF CONTENTS

Chapter 1

Introduction to Huntington's Disease

Kurt R. Weiss

Department of Biology and The Picower Institute for Learning and Memory, MIT,

Cambridge, MA 02139

Human pathology and genetics

Huntington's Disease (HD) is a neurodegenerative disorder first characterized as a hereditary, late-onset form of chorea by George Huntington in 1872 (Huntington 1872). An expansion in the polyglutamine (polyQ) tract of the *huntingtin* gene was identified as the genetic basis for the disease by the Huntington's Disease Collaborative Research Group in 1993 (HDCRG 1993). The disease manifests in an estimated 1 to 10 out of 100,000 people in the United States, resulting in chorea, cognitive defects, and ultimately death within 15-20 years of onset (Vonsattel, Myers et al. 1985; Walker 2007). The severity of the disease depends on the length of the glutamine repeat in exon 1 of the *IT15* gene encoding Huntingtin (Htt); under 35 glutamines is normal, 35-40 glutamines shows incomplete penetrance, and over 40 glutamines is fully penetrant, with increasing number of repeats resulting in earlier onset of the disease (Rubinsztein, Leggo et al. 1996; Rubinsztein and Carmichael 2003). Expansion beyond 70 residues results in a severe juvenile-onset form of HD (Duyao, Ambrose et al. 1993). Expansion of the glutamine tract occurs because polyQ tracts, especially those over 28 residues are unstable during meiotic and somatic DNA replication. PolyQ expansion mutations likely occur via formation of 'slipped,' or looped out secondary DNA structures on one strand during replication (Parniewski and Staczek 2002). The likelihood and severity of 'slipping' increases with tract length, resulting in expansion of the repeat in ~73% of occurrences and contraction in ~23% of occurrences (Ranen, Stine et al. 1995; Wheeler, Auerbach et al. 1999; Chattopadhyay, Ghosh et al. 2003). This leads to the phenomenon known as 'anticipation,' whereby the disease increases in severity in successive generations (McInnis 1996).

The Huntingtin protein is ubiquitously expressed throughout the body and brain; however, the pathology of HD is highly specific to the basal ganglia, cerebral cortex, and striatum (Vonsattel

and DiFiglia 1998). GABAergic type II medium spiny projection neurons are most severely

affected, while interneurons are largely spared (Hedreen, Peyser et al. 1991). Affected neurons

not only display selective atrophy in late-stage brains, but also demonstrate dysfunction in early

stages of HD (Gomez-Tortosa, MacDonald et al. 2001; Van Raamsdonk, Pearson et al. 2005).

Cortical neurons are found to have decreased levels of microtubule-associated protein-2 and

complexin-2, causing defects in axonal transport and synaptic signaling before patients display

symptoms (Modregger, DiProspero et al. 2002; DiProspero, Chen et al. 2004). Aberrant

signaling between the cortex and basal ganglia mediated by HD affected striatal neurons are the

likely cause of choreic movements seen in early stages of the disease (Albin, Reiner et al. 1990;

Albin, Young et al. 1990). In later stages, GABA/substance cells which project to the direct

pathway are also affected, resulting in decreased motor coordination (Glass, Dragunow et al.

2000). This cell specific toxicity leads to an overall reduction in brain mass of ~25-30% in late

stages of the disease, with the most significant loss in the striatum (Figure 1) (Aylward, Li et al.

1997; Kassubek, Juengling et al. 2004; Rosas, Salat et al. 2008).

Several neurodegenerative diseases show similar pathologies to HD, characterized by mutations

in a single causative gene that results in protein aggregation, late-onset neurodegeneration, and

selective vulnerability of a subset of neurons. This includes eight other diseases with expansions

in polyQ tracts: spinal and bulbar muscular atrophy (SBMA), dentatorubral and pallidoluysian

atrophy (DRPLA), and spinocerebellar ataxias (SCA) 1,2,3,6,7,17. There are also diseases with

similar pathologies that involve other classes of mutations which result in protein misfolding and

subsequent aggregation, including Parkinson's disease, amytrophic lateral sclerosis, and

Alzheimer's disease (Ross and Poirier 2004).

Aggregation and Post-translational modification of Htt

The discovery of inclusion bodies associated with HD was initially made by ultrastructural analysis of postmortem brains in 1979 (Roizin 1979), but was largely ignored until 1997 when Htt antibodies revealed intranuclear and dystrophic neurite aggregates, which co-localize with ubiquitin in the striatum and cortex of both human HD patients and mouse models. These aggregates in human samples were detected with an antibody to the N-terminal 17 amino acids, but not by an antibody to amino acids 585 to 725, suggesting proteolytic processing may be necessary for nuclear entry and aggregation (Davies, Turmaine et al. 1997; DiFiglia, Sapp et al. 1997). The role of cleavage was further validated by a targeted mutation of a caspase-6 cleavage site at amino acid 586 that resulted in reduced aggregation and toxicity in a YAC128 mouse model (Graham, Deng et al. 2006). Further cleavage of N-terminal fragments at amino acids 120-121 by uncharacterized proteases results in increased aggregation and toxicity associated with a redistribution of mutant Htt from the cytosol to the nucleus (Hackam, Singaraja et al. 1998; Hodgson, Agopyan et al. 1999; Juenemann, Weisse et al. 2011).

In addition to proteolytic cleavage, Htt is also phosphorylated at several residues within the N-terminus to alter its localization, cleavage, and degradation. Phosphorylation of ser16 reduces the interaction of Htt with the nuclear pore protein TPR, thus reducing its nuclear entry (Havel, Wang et al. 2011). Phosphorylation of ser421 results in reduced nuclear accumulation of caspase-6 cleavage fragments by reducing the activity of caspase-6 (Warby, Doty et al. 2009; Havel, Wang et al. 2011). Conversely, stress-induced phosphorylation of residues ser13 and ser16 causes increased nuclear localization of full-length Htt, and while this is a toxic event when applied to polyglutamine expanded Htt (polyQexHtt), it is beneficial for wild-type Htt (Atwal, Desmond et al. 2011). N-terminal Htt fragments can also be modified by small

ubiquitin-like modifier (SUMO)-1 or ubiquitin at lysine residues. SUMOylation of Htt stabilizes

N-terminal fragments, reduces aggregation, increases nuclear localization, and increases

neurodegeneration in a *Drosophila* model of HD (Steffan, Agrawal et al. 2004). Ubiquitination

targets Htt to the proteasome for degradation; however, misfolded forms of Htt are not

effectively degraded by this pathway, leading to global defects in the ubiquitination-proteasome

pathway that can result in increased levels of pro-apoptotic proteins (Jana, Zemskov et al. 2001).

Acetylation of mutant Htt at lysine 444 has been shown to increase its trafficking to

autophagosomes, decreasing overall levels and improving cell viability (Jeong, Then et al. 2009).

Together these results demonstrate the cellular processes and post-translational modifications

that act to modify toxicity, subcellular localization, and aggregation of Htt.

It is generally agreed at this point that cleavage events lead to monomeric, oligomerized, and

aggregated forms of polyQ-Htt that can misfold and contribute to cellular toxicity (Figure 2).

However, the role of aggregates in HD-mediated toxicity is still debated. Conflicting results

suggest aggregates may be toxic, neutral, or even beneficial to the cellular environment.

Evidence for aggregate-mediated toxicity comes from a strong correlation between the threshold

of >35glutamine residues for aggregation *in vitro* and disease manifestation *in vivo* (Davies,

Turmaine et al. 1997; Scherzinger, Sittler et al. 1999). Additionally, longer polyQ tracts have

faster *in vitro* aggregation kinetics and result in earlier disease onset (Scherzinger, Sittler et al.

1999). Suppression of aggregation via chaperone overexpression (Carmichael, Chatellier et al.

2000), and administration of small molecule aggregation inhibitors (Chopra, Fox et al. 2007),

have been shown to suppress cell death. *In vivo* and *in vitro* demonstrations of proteolytic

cleavage events of Htt also correlate aggregation with neurodegeneration. Cleavage of Htt at

amino acid 586 by caspase-6 cleavage produces an N-terminal fragment necessary for both aggregation and toxicity in mouse models (Graham, Deng et al. 2006).

Conversely, there is a body of evidence suggesting that aggregates are not correlated with neurotoxicity. Medium spiny projection neurons of the striatum exhibit fewer Htt aggregates than striatal interneurons, yet they are more vulnerable to neurodegeneration in HD (Kuemmerle, Gutekunst et al. 1999). Some mouse (Hodgson, Agopyan et al. 1999) and *Drosophila* (Romero, Cha et al. 2008) HD models expressing full-length polyQ-Htt show selective neurodegeneration and behavioral phenotypes without obvious aggregation. Additionally, the 'short-stop' mouse model expresses an N-terminal Htt fragment with a 128 glutamine repeat, resulting in aggregation, but no neuronal dysfunction or neurodegeneration (Slow, Graham et al. 2005). In cultured striatal neurons, neuronal cell death associated with transient expression of mutant Htt is inversely proportional to Htt aggregate formation (Arrasate, Mitra et al. 2004), suggesting that inclusion body formation may decrease levels of other toxic forms of Htt and promote neuronal survival. There is also evidence suggesting that oligomers precede aggregate formation, and these are the toxic species in HD (Lam, Chan et al. 2008; Lajoie and Snapp 2010). These contradictory results in different cellular contexts and HD models have led to confusion over the toxicity of aggregates, and subsequently, over whether therapeutic approaches in HD should focus on reducing or enhancing aggregate formation. It seems that aggregation toxicity is highly dependent on cellular context. For cell culture and yeast HD models, cytoplasmic aggregates appear to be beneficial, as they may reduce levels of toxic soluble Htt monomers and oligomers. Likewise, aggregates in the cell bodies of neurons may act similarly and reduce HD mediated toxicity. Aggregates forming in axonal processes or nuclei, however, appear to be toxic because they can bind transcription factors and impede axonal transport.

These results, along with cell specificity in HD, suggest a significant role for modifier genes such as proteases, kinases, and chaperones involved in HD-mediated toxicity. Such modifier loci are informative to both the endogenous role of Htt, the cellular processes affected in HD, and for potential drug targets in treatment of HD. Indeed, roughly 70% of the variability in age of HD onset can be accounted for by genetics, while the remaining 30% is due to modifier genes and environmental factors (Wexler, Lorimer et al. 2004).

The endogenous function of Huntingtin

Genetic Knockouts**:** Although the gene encoding Htt was first cloned over 18 years ago and several functions have been proposed, its endogenous function is still unclear. Mutant analysis of Htt suggests functions in nervous system maintenance, transport, and iron utilization. The constitutive genetic knockout of *htt* in mice leads to early embryonic lethality (Duyao, Auerbach et al. 1995; Nasir, Floresco et al. 1995; Zeitlin, Liu et al. 1995). The lethality is rescued by wild-type extraembyronic tissue expression, and data suggests a role for Htt in transport of essential ferric ions to the embryo (Dragatsis, Efstratiadis et al. 1998). This non-neural effect may represent an ancient function of Htt that evolved in organisms without nervous systems. Indeed, zebrafish Htt is known to have an essential role in iron utilization which is not involved in the nervous system (Lumsden, Henshall et al. 2007). Conditional knockouts in the Central Nervous System (CNS) of adult mice lead to late-onset neurodegeneration and decreased lifespan, confirming a role for Htt in maintaining neuronal health (O'Kusky, Nasir et al. 1999; Dragatsis, Levine et al. 2000).

Functional domains suggest functions in transcription and transport: The structure of the *huntingtin* gene and protein indicates several clues to its biological function, and suggests roles in transcriptional regulation and intracellular transport. The *huntingtin* gene is highly conserved

across evolution and has little sequence homology to any other known protein. Htt is ubiquitously expressed throughout development and adulthood in humans, with the highest levels in neurons of the CNS and testes. Mammalian *huntingtin* consists of a 180 kb open reading frame with 67 exons that encode a 3144 amino acid protein with a molecular weight of 348 kDa. The gene consists of three highly conserved regions containing several HEAT (huntingtin, elongation factor 3, PR65/A subunit of protein phosphatase 2a and mTor) domains present in all known homologs (Figure3) (Li, Karlovich et al. 1999; Tartari, Gissi et al. 2008). HEAT repeats are roughly 40 amino acid domains that repeat several times within a protein and are known to mediate protein-protein interactions by forming hydrophobic alpha-helices which act as a binding pockets for other proteins (Andrade, Petosa et al. 2001). HEAT domains are commonly found in proteins involved in axonal transport, chromosome segregation, and entry/exit from the nuclear pore complex (Neuwald and Hirano 2000; Andrade, Perez-Iratxeta et al. 2001). Vertebrate Htt homologs have a polyQ region that is postulated to play a role in mediating protein-protein interactions, especially among other proteins with polyQ regions. The polyQ region ranges from four glutamines in zebrafish, to seven in mice, to ~20-35 glutamines in humans, where it is most polymorphic (Karlovich, John et al. 1998; Cattaneo, Zuccato et al. 2005; Tartari, Gissi et al. 2008). *Drosophila* do not have a polyQ stretch (Li, Karlovich et al. 1999). Evolutionary analysis suggests the polyQ region has a specific role in complex nervous systems because the polyQ co-evolved and continued expanding with the appearance of complex nervous systems (Tartari, Gissi et al. 2008). Immediately following the polyQ region is a polyproline stretch which is well conserved, with a role in protein-protein interactions between Htt and Src3 homology-3 domains of proteins such as p53 (Steffan, Kazantsev et al. 2000) and PSD-95 (Sun, Savanenin et al. 2001; Fan, Cowan et al. 2009) The polyproline tract size and location has also been shown to alter polyQ misfolding and toxicity (Darnell, Orgel et al. 2007).

PolyQ and polyproline regions have also been demonstrated to form polar zipper structures and interact with DNA directly, suggesting Htt may function as a transcriptional activator (Gerber, Seipel et al. 1994; Perutz, Johnson et al. 1994).

The N-terminal 17 amino acid region of Htt, immediately adjacent to the polyQ region, is another highly conserved domain with important functions in localization and aggregation. This N17 domain has been demonstrated to act as a cytoplasmic retention signal and/or nuclear export signal, and has been demonstrated to control the association of Htt to membrane bound structures such as the Golgi, ER, mitochondria, and vesicles (Cornett, Cao et al. 2005; Atwal, Xia et al. 2007; Rockabrand, Slepko et al. 2007). N17 has also been demonstrated *in vitro* to enhance aggregation of N-terminal Htt fragments, an aggregation which can be suppressed by an N17 interacting chaperonin, TRiC (Tam, Spiess et al. 2009; Thakur, Jayaraman et al. 2009).

Biochemical screening techniques have been used to identify novel binding partners for Htt and determine the cellular processes in which Htt is involved. These experiments have generally used the yeast two-hybrid and/or pull-down followed by mass spec methods. A brief summary of the Htt proteomics data produced from these complimentary methods is presented in Figure 4. Together, this data suggest that Htt is involved in a diverse array of cellular processes, and many of these pathways may be affected in HD. Indeed, when a subset of these interacting proteins (n=60) were tested for their ability to modify HD-mediated neurodegeneration in a *Drosophila* HD model, at 45% hit rate was obtained, compared to the expected 1-4% expected from a random library, thus confirming the important role of these interacting proteins in HD (Kaltenbach, Romero et al. 2007).

Htt as a pro-survival factor: Overexpression studies have demonstrated that Htt has a role in maintaining cell viability in response to acute toxic stimuli and excitotoxicity. Wild-type Htt can

suppress apoptosis *in vitro* in response to exogenous toxic stimuli such as 3-nitroproprionicacid, which selectively damages the striatum, presumably by preventing activation of proaspase-9 (Rigamonti, Sipione et al. 2001). Similarly, Htt can protect against excitotoxicity after quinolic acid injection *in vitro* and *in vivo,* by mediating apoptosome complex activity and inhibiting caspase activation downstream of cytochrome-c release (Rigamonti, Bauer et al. 2000; Leavitt, van Raamsdonk et al. 2006).

Overexpression and knockout studies suggest Htt regulates the cellular levels of brain-derived neurotrophic factor (BDNF), which is a survival factor produced by cortical neurons and transported to striatal neurons where it is necessary for proper cellular function. Wild-type Htt was found to bind a BDNF transcription repressor element, REST/NRSF, and retain it in the cytoplasm permitting transcription of BDNF. This function is abolished in polyQex-Htt, permitting the repressor to enter the nucleus and decrease BDNF transcription (Zuccato, Ciammola et al. 2001; Zuccato, Tartari et al. 2003). Htt has also been shown to regulate BDNF levels by promoting its transport (Humbert and Saudou 2004) through its interaction with HAP1 (Wu, Fan et al. 2010).

Htt has also been implicated in the stress response system because phosphorylation of Htt by CDK5 in response to DNA damage prevents Htt from inducing p53 dependent apoptosis (Anne, Saudou et al. 2007). Htt is also implicated in anti-apoptosis due to its interaction with HIP1, which reduces HIP1 and Hippi's ability to mediate procaspase-8 cleavage and apoptosis (Gervais, Singaraja et al. 2002). Additionally, phosphorylation of the N17 region of Htt regulates nuclear entry and association with chromatin in response to heat shock (Atwal, Desmond et al. 2011).

Htt as a regulator of intracellular transport: Much of the information gleaned from analysis of Htt interacting proteins suggests a role in intracellular transport. Yeast two-hybrid screens have implicated Htt in binding HAP1 (Li, Li et al. 1995), which is involved in axonal transport via its interaction with kinesin (McGuire, Rong et al. 2006) and dynein (Engelender, Sharp et al. 1997; Rong, Li et al. 2007), and HIP1 and HIP14, which have roles in endocytosis, suggesting a role for Htt in various aspects of microtubule and actin based intracellular transport (Kalchman, Koide et al. 1997; Wanker, Rovira et al. 1997). Additionally, a direct interaction between Htt and dynein was suggested by yeast two-hybrid, and validated in cell culture, by demonstrating that reduced Htt expression leads to disruption of Golgi stacks, a hallmark dynein-mediated defect (Caviston, Ross et al. 2007; Pardo, Molina-Calavita et al. 2010).

 Htt has been suggested to act as a 'molecular switch' in controlling anterograde and retrograde transport of BDNF and amyloid precursor protein (APP). Experiments in cell culture measuring transport of BDNF demonstrate that phosphorylation of ser421 favors anterograde transport, while unphosphorylated ser421 favors retrograde transport (Colin, Zala et al. 2008). A similar 'switching' mechanism has been attributed to Htt by its interaction with HAP40, a Rab5 associated protein, suggesting that Htt functions to transfer endosomes from microtubules to F-actin tracks (Peters and Ross 2001; Pal, Severin et al. 2008). Htt has also been implicated in actin-based transport by its interaction with optineurin, which may physically link Htt to the actin motor myosin-VI (Sahlender, Roberts et al. 2005).

Htt in synaptic signaling: Htt is localized post-synaptically with PSD-95, a membrane-associated guanylate kinase (MAGUK) protein that binds the NMDA and kainate receptors at the postsynaptic density (Sun, Savanenin et al. 2001; Fan, Cowan et al. 2009). Htt is also localized pre-synaptically through its interactions with synaptic vesicles, HIP1, and HIP14, suggesting

roles in synaptic signaling and vesicle recycling (Waelter, Scherzinger et al. 2001; Stowers and

Isacoff 2007).

Theories of polyQexHtt-mediated toxicity

Supporting the evidence that wild-type Htt is involved in many diverse cellular processes,

polyQex-Htt toxicity has also been attributed to defects in a wide array of cellular processes. HD

has been suggested to impair transcriptional regulation, fast axonal transport, mitochondrial

energy metabolism and calcium buffering, protein degradation pathways, and synaptic signaling

(Figure 5).

While there is good evidence for a gain-of-function in HD due to the presence of aggregation and

dominant inheritance phenotypes, the degree to which loss of Htt function contributes to HD is

not clear. There are examples of loss-of-function in HD, including reduced BDNF-mediated

transcription (Zuccato, Ciammola et al. 2001; del Toro, Canals et al. 2006), and reduced axonal

transport of BDNF, mitochondria, and synaptic vesicles (Trushina, Dyer et al. 2004).

Additionally, overexpression of wild-type Htt in a polyQexHtt background has been

demonstrated to improve striatal cell neuropathology, potentially due to its anti-apoptotic

properties, but it does not significantly improve motor dysfunction (Leavitt, Guttman et al. 2001;

Van Raamsdonk, Pearson et al. 2006).

The majority of evidence, however, supports gain-of-function as the primary cause of toxicity in

HD. Additionally, human genetic data suggests the polyQ mutation does not render the Htt

protein entirely defective. HD patients homozygous for the mutant *htt* allele only show a slightly

more severe disease progression than heterozygotes, and the age of onset is the same (Squitieri,

Gellera et al. 2003). Patients who are hemizygous for *htt* do not develop any symptoms of HD

(Ambrose, Duyao et al. 1994). Additional evidence against a complete loss-of-function is derived from the finding that polyQex-Htt expression can rescue the lethality in *htt* null mice (White, Auerbach et al. 1997).

Mitochondrial-based Defects: Mitochondria play important roles in many cellular pathways, especially in neurons where they provide ATP necessary to supply ion pumps to establish chemical gradients and buffer calcium at nerve terminals (Grunewald and Beal 1999; Beal, Palomo et al. 2000; Hollenbeck and Saxton 2005). Mutant Htt has been found to bind directly to mitochondria, altering its metabolic activity, calcium buffering, apoptotic properties, and motility (Choo, Johnson et al. 2004; Trushina, Dyer et al. 2004; Orr, Li et al. 2008).

Defects in mitochondrial energy metabolism: HD patient post mortem brain slices and mouse models demonstrate decreased levels of cAMP and ATP/ADP ratios, indicating defective mitochondrial energy metabolism (Gines, Seong et al. 2003). PET imaging in the striatum of patients during presymptomatic or early stages of HD revealed increased oxygen over glucose utilization, suggesting early defects in glycolysis (Powers, Videen et al. 2007). The R6/2 mouse model shows increased oxygen consumption and increased uncoupling protein-2 mRNA levels in the brown adipose tissue, which suggests inefficient coupling of the electron transport and ATP synthesis (van der Burg, Bacos et al. 2008). Similarly, HD patients often demonstrate severe chorea-independent weight loss (Djousse, Knowlton et al. 2002). Defects in the mitochondrial respiratory chain complex II and III have been observed specifically in the caudate and putamen, but not cerebellum or cortex of HD patients (Brennan, Bird et al. 1985; Gu, Gash et al. 1996; Tabrizi, Cleeter et al. 1999). Together these results point to cell specific defects associated with mitochondrial energy production in areas of the brain prone to neurodegeneration

in HD; because many of these effects are seen pre-symptomatically, defects may represent early events in pathogenesis which could provide useful targets for therapeutics.

Defective calcium buffering, mitochondrial membrane potential, and increased oxidative stress: Mitochondria isolated from HD patient lymphocytes have lower membrane potential and depolarize at lower calcium concentrations than controls (Almeida, Sarmento-Ribeiro et al. 2008). A *Drosophila* model of HD expressing full-length human Htt with an expanded polyQ also demonstrated increased resting levels of intracellular calcium (Romero, Cha et al. 2008). HD mice display increased mitochondrial permeability transition pore (mPTP) opening correlated with polyQ length. mPTP opening results in several detrimental events for a cell including mitochondrial depolarization and release of reactive oxygen species, calcium, and caspases. Aberrant mPTP opening likely occurs via a direct interaction of polyQexHtt with the mPTP (Panov, Obertone et al. 1999; Choo, Johnson et al. 2004). Additional i*n vivo* evidence for overall degradation of mitochondria comes from HD brain slices illustrating ultrastructural abnormalities (Goebel, Heipertz et al. 1978), and from mitochondrial DNA fragmentation/deletion, a common marker for oxidative stress (Panov, Gutekunst et al. 2002). This overall degradation and 'leakyness' of mitochondria results in the release of reactive oxygen species (ROS) produced via redox reactions in the electron transport chain, which are generally contained in inter-membrane space of mitochondria. ROS inhibitors have been shown to decrease striatal degeneration, and include mitochondrial antioxidant enzymes Cu/Zn and manganese superoxide dismutases (SOD1 and SOD2) (Albers and Beal 2000). Notably, SOD1 mutations are present in some familial forms of the motor neuron specific neurodegenerative disease ALS (Rosen, Siddique et al. 1993).

Mitochondrial energy metabolism defects are especially relevant in HD because defects in oxidative phosphorylation have been demonstrated to be selectively detrimental to the striatum compared to the cortex or hippocampus (Pickrell, Fukui et al. 2011). Overall, these results suggest that mitochondria become 'leaky' and weakened by the association of polyQexHtt with the outer membrane, ultimately leading to decreased energy metabolism, oxidative stress, and aberrant calcium buffering.

Axonal Transport defects: Neurons are highly dependent on anterograde axonal transport to carry nuclear products to the synapse, and retrograde transport to return neurotrophic factors to the cell body. Thus, axonal transport defects may contribute neuron specificity to HD pathology. In addition to steric impediments to transport caused aggregated polyQex-Htt, soluble polyQex-Htt is also postulated alter axonal transport because wild-type Htt likely functions as a regulator of fast axonal transport (FAT) (Velier, Kim et al. 1998; Gunawardena, Her et al. 2003; Trushina, Dyer et al. 2004; Wu, Fan et al. 2010). FAT defects have been demonstrated in several neurodegenerative diseases including Alzheimer's Disease (Gunawardena and Goldstein 2001), ALS (Warita, Itoyama et al. 1999), and hereditary spastic paraplegias (Salinas, Proukakis et al. 2008). Additionally, mutations in kinesin and dynein motors also cause neurodegenerative disease-like phenotypes as a result of defective FAT (Hurd and Saxton 1996). Htt-mediated transport of APP and BDNF is impaired in striatal and hippocampal cells, but not cortical cultured neurons, suggesting a striatal specific defect in transport (Her and Goldstein 2008). PolyQex-Htt expression has been shown to alter axonal transport of mitochondria (Lee, Yoshihara et al. 2004; Sinadinos, Burbidge-King et al. 2009), synaptic vesicles (Lee, Yoshihara et al. 2004), neurotrophic factors (Gauthier et al, 2004), and other organelles (Chang, Rintoul et al. 2006).

Mitochondrial transport defects: Mitochondrial transport defects have been demonstrated in several models of HD. Results suggest aggregation-independent defects owing to a role for wild-type Htt in mediating fast axonal transport of mitochondria (Trushina, Dyer et al. 2004; Li, Orr et al. 2010), as well as aggregation-dependent defects resulting from large Htt aggregates blocking axonal transport in nueritic processes (Lee, Yoshihara et al. 2004). Axonal transport experiments done in striatal culture confirmed a polyQexHtt effect on mitochondrial transport resulting in decreased processivity, flux, and velocity (Trushina, Dyer et al. 2004). One possible mechanism by which polyQexHtt may alter transport suggests that a neuron specific cJun N-terminal Kinase (JNK3) becomes activated by mutant Htt, phosphorylates kinesin-1, and reduces kinesin binding to microtubules (Morfini, You et al. 2009). Reduced transport processivity, along with results demonstrating that mitochondria have defective membrane potential, calcium buffering, and energy metabolism suggests a model of mitochondrial-mediated toxicity whereby multiple mitochondrial defects become cumulative, resulting in increased toxicity to neurons. In this model, transport defects are compounded by the observation that mitochondria that become trapped along axons at the sites of aggregates are prone to becoming depolarized and breaking down, thus releasing reactive oxygen species and pro-apoptotic signals which contribute to cell death (Kiechle, Dedeoglu et al. 2002; Chang, Rintoul et al. 2006). Mitochondria are postulated to produce ~90% of the cellular ATP to neurons, which if reduced, could affect any ATP dependent process, from organelle transport to ion pumping (Lee and Peng 2008). Indeed, ATP-dependent ubiquitin-proteasomal defects are especially severe at the synapses and distal regions of axons of mice where ATP levels are reduced in HD (Orr, Li et al. 2008; Wang, Wang et al. 2008).

Axonal transport defects for synaptic vesicles and neurotrphic factors: Htt has a well-established role in transport of brain derived neurotrophic factor (BDNF) in neurons (Reilly

2001; Gauthier, Charrin et al. 2004; Zuccato and Cattaneo 2007; Pardo, Molina-Calavita et al. 2010). BDNF transport mechanisms are especially important to striatal neurons which depend on anterograde transport of BDNF in cortical neurons to the nerve terminals where it is released and activates downstream effectors and growth factors via the TrkB receptor in striatal neurons. These downstream effector growth factors must then be transported retrograde to the cell body (Mizuno, Carnahan et al. 1994). HD patients and mouse models demonstrate reduced BDNF levels in the striatum, but not cortex, suggesting some aspect of the release, uptake, or transport of BDNF is defective in striatal cells (Spires, Grote et al. 2004; Ciammola, Sassone et al. 2007). Decreased BDNF results in toxicity because BDNF is known to help protect against excitotoxic stresses (Bemelmans, Horellou et al. 1999), and generally acts as a growth factor required for viability (Zuccato and Cattaneo 2007).

Transcriptional dysregulation: In addition to BDNF transport defects, BDNF transcription is also affected in HD. Wild-type Htt is known to bind the RE1-silencing transcription factor/neuron-restrictive silencer factor (REST/NRSF) complex. This interaction is likely mediated by HAP1, dynactin, and the REST/NRSF-interacting LIM domain protein (RILP) (Shimojo 2008). The interaction between Htt and REST/NRSF is reduced in HD, allowing translocation of REST/NRSF into the nucleus and reducing transcription of BDNF, as well as many other neuronal genes under the control of the REST complex, which is a global regulator of neuronal gene transcription (Zuccato, Belyaev et al. 2007; Zuccato and Cattaneo 2007; Zuccato, Marullo et al. 2008).

Both wild-type and polyQexHtt are cleaved by caspases, resulting in N-terminal fragments that enter the nucleus and alter transcription (DiFiglia, Sapp et al. 1997; Steffan, Kazantsev et al. 2000). PolyQ tracts and glutamine rich regions are common in transcription factors, arguing that

wild-type Htt may act in a similar manner, and the expanded polyQ could alter its endogenous interactions with transcription factors and DNA. In agreement with this hypothesis, nuclear polyQexHtt aggregates have been shown to accumulate CBP (cAMP-responsive element binding protein) in mouse models and human brains (Steffan, Kazantsev et al. 2000; Nucifora, Sasaki et al. 2001), as well as TAFII-130, a cofactor for CREB dependent transcription (Shimohata, Nakajima et al. 2000; Dunah, Jeong et al. 2002). Accumulation of CBP into aggregates reduces its effective concentration in the nucleus and results in decreased CREB-mediated transcription of BDNF and other neurotrophins (Shimohata, Shimohata et al. 2005). Injection and overexpression of BDNF via viral vector in rat brains has been shown to protect striatal neurons against excitotoxicity from quinolic acid injection and improve motor function (Martinez-Serrano and Bjorklund 1996; Kells, Fong et al. 2004).

Global changes in transcription are suggested by results indicating that polyQexHtt can interact with proteins involved in histone acetylation (McCampbell and Fischbeck 2001). A *Drosophila* model suggests these defects are responsible for HD mediated toxicity by demonstrating that neurodegeneration and lethality caused by polyQexHtt expression can be reduced with expression of histone de-actylase inhibitors (Steffan, Bodai et al. 2001). Alteration of histone acetylation suggests broad transcriptional defects are possible in HD. Indeed, a large microarray-based study of expression data in HD mouse models revealed decreases in mRNA related to intracellular transport, cytoskeletal components, neurotransmitter receptors, synaptic transmission, calcium homeostasis, and most cellular processes which were postulated to involve Htt. The majority of changes were seen pre-symptomatically or at early onset, suggesting a causative role in HD, though the magnitude of mRNA changes did also increase with disease progression (Fossale, Wheeler et al. 2002; Luthi-Carter, Hanson et al. 2002).

Defective protein degradation pathways: Cells utilize three major pathways to ensure proper

folding of proteins. First, molecular chaperones, which are small scaffolding proteins associate

with nascent polypeptide chains and some fully-folded proteins to maintain proper tertiary

structure. These include heat shock proteins which are expressed during increased temperature

and other environmental stresses that lead to protein misfolding. As a second level of control,

misfolded proteins can be degraded by tagging them with ubiquitin and targeting them to the

proteasome (Sherman and Goldberg 2001). Finally, autophagocytosis can be activated to

remove large protein complexes that cannot be repaired or degraded by other means.

The initial studies which identified Htt aggregates also noted that they co-localize with ubiquitin,

suggesting that polyQex-Htt is not being properly targeted or degraded to the proteasome in HD

(Davies, Turmaine et al. 1997; DiFiglia, Sapp et al. 1997). It has been demonstrated that

polyQexHtt misfolds as a result of its expanded polyQ tract. This in turn activates chaperones

and the ubiquitin-proteasome pathway, reducing the amount of these proteins available for other

misfolding events. Additionally, long term inactivation of the ubiquitin-proteasome pathway is

likely, as many aggregate prone proteins with polyQ regions are not effectively degraded by the

proteasome, and may clog the machinery rendering it nonfunctional (Holmberg, Staniszewski et

al. 2004; Venkatraman, Wetzel et al. 2004). Indeed, only one proteasomal isoform, the

puromycin-sensitive aminopeptidase (PSA), is capable of degrading polyQ regions entirely

(Bhutani, Venkatraman et al. 2007). PSA, found primarily in brain tissues, becomes upregulated

in polyQ diseases, and has been shown to reduce neurodegeneration in a fly model of tauopathy

(Venkatraman, Wetzel et al. 2004; Sengupta, Horowitz et al. 2006). Additionally,

overexpression of chaperone proteins in the context of polyQ expansion diseases have been

demonstrated to reduce aggregation and toxicity in mice (Cummings, Sun et al. 2001),

Drosophila (Kazemi-Esfarjani and Benzer 2000; Fayazi, Ghosh et al. 2006), and cell culture models (Howarth, Kelly et al. 2007), by both increasing chaperone expression, and increasing ubiquitination.

A third level of control on protein degradation exists at the level of the autophagy. Autophagy is the bulk degradation process whereby aggregated proteins, any associated structures, and cytosol are endocytosed in a double-membrane structure which is then degraded by the lysosome (Ravikumar, Duden et al. 2002; Ventruti and Cuervo 2007). Autophagy is activated by Htt aggregates, and negatively regulated by mTOR, which is found in Htt aggregates (Ravikumar, Duden et al. 2002). Htt aggregates, therefore, cause a drastic increase in cellular autophagy, which reduces aggregation and has been shown to be beneficial to neurons in mouse and *Drosophila* models (Ravikumar, Vacher et al. 2004). Activation of autophagy via deletion of alpha-synuclein, a negative regulator of autophagy, or addition of rapamycin, results in decreased aggregation and increased viability in *Drosophila* and cell-culture models of HD (Sarkar, Ravikumar et al. 2009; Corrochano, Renna et al. 2011).

Excitotoxicity: Excitotoxicty occurs from either overactive glutamate release, reduced glutamate uptake by glial cells, or glutamate hypersensitivity of NMDA receptors (NMDAR) or downstream signaling pathways in the striatal cells. Thus, excitotoxicity is an appealing mechanism of HD-mediated toxicity in striatal cells because striatal cells depend on glutamatergic activation from cortical cells. Early evidence for this model came from human patient brain slices demonstrating reduced NMDAR binding specifically in the striatum (Young, Greenamyre et al. 1988). YAC128 mouse models expressing full-length mutant Htt also display excitotoxic sensitivity in striatal cells (Benn, Slow et al. 2007), however, shorter N-terminal Htt fragment models of HD do not, and conversely, demonstrate resistance to chemical induced

excitotoxicity (Morton and Leavens 2000; Fan and Raymond 2007; Zhang, Li et al. 2008). This suggests full-length, or a unique cleavage fragment of Htt, is required for NMDAR-mediated excitotoxicity in striatal cells. Possible mechanisms for this effect include changes in NMDAR protein levels or post-translational modifications, though conflicting results have not produced a definitive answer (Cepeda, Ariano et al. 2001; Ali and Levine 2006). Defective glutamate clearance from the synaptic cleft by glia has also been suggested as a possible cause of excitotoxicity. The transporter GLT1, a glial glutamine transporter, appears down-regulated in some mouse models of HD, increasing levels of glutamine in the synaptic cleft (Estrada-Sanchez, Montiel et al. 2009).

Model systems and screens for HD modifiers

Human subject based studies of HD focused on genetic association studies to coordinate phenotypes and genotypes, and characterize polyglutamine repeat length-dependence effects. In particular, a Venezuelan kindred of over 18,000 individuals spanning 10 generations has yielded many informative results on genetic modifiers and environmental factors in HD (Wexler, Lorimer et al. 2004). In addition, post mortem brain slices have been used for molecular and ultrastructural analyses. Today, methods such as MRI and PET imaging allow *in vivo* imaging of brain function and structure. Additionally, lymphoblast cell lines have been generated from human patients to facilitate *in vitro* experimentation.

Mouse models have been the most utilized model organism for HD research and have the distinct advantage over non-vertebrate models of demonstrating the striatal specific effects endemic to HD. Mouse models of HD have been generated by introducing the human polyQexHtt transgene as either an N-terminal fragment, e.g. the R6/1 and R6/2 models (Mangiarini, Sathasivam et al. 1996), or full-length human Htt, e.g. YAC128 (Reddy, Charles et al. 1999).

These models recapitulate certain aspects of HD such as aggregation and neurodegeneration, but the severity, cell specificity, and subcellular localization patterns vary greatly with transgene size, expression, and repeat length, reinforcing the importance of Htt cleavage events in HD pathology. Another set of mouse models was generated using homologous recombination at the endogenous mouse *htt* locus to expand the mouse polyQ tract to the pathogenic range. One such knock-in model with 150 glutamines demonstrates striatal specific aggregation and behavioral defects, but not enhanced striatal specific degeneration (Lin, Tallaksen-Greene et al. 2001). Invertebrate models of HD generated by overexpression of human polyQexHtt transgenes demonstrate aggregation and toxicity that increases with transgene expression and polyQ length similar to mammalian systems. Transgenes which contain significant genomic context surrounding the polyQ show intergenerational instability in polyQ repeat length (Mangiarini, Sathasivam et al. 1997; Jung and Bonini 2007). For all transgenic mouse and non-vertebrate models, increased expression of polyQexHtt and increased polyQ length is correlated with increased toxicity. Increased transgene size is generally negatively correlated with toxicity, likely due to incomplete caspase and protease cleavage in the host organism, which has been shown to be essential for toxicity (Graham, Deng et al. 2006).

Cell culture and invertebrate models have been primarily used for screening and characterization of specific protein-protein interactions. Forward genetic screens in the *Drosophila* eye have identified chaperone proteins as being effective in reducing polyQ-mediated toxicity (Kazemi-Esfarjani and Benzer 2000). Another screen identified the *Drosophila* homolog of human myeloid leukemia factor-1 as a suppressor of toxicity that had no effect on aggregation, though the exact mechanism of suppression was not determined (Kazemi-Esfarjani and Benzer 2002). A screen was conducted to identify novel Htt interacting proteins and modifiers of HD-mediated

toxicity using yeast two-hybrid and pull-down mass spectroscopy to identify proteins that interact with mutant or wild-type Htt. Gain- or loss-of-function mutations for these interactors were obtained in *Drosophila*, and 45% of these interactors were able to enhance or suppress polyQexHtt mediated toxicity in a *Drosophila* eye model of HD (Kaltenbach, Romero et al. 2007). Hits were found in pathways for most cellular processes in which Htt is postulated to be involved, including axonal transport, synaptic transmission, transcriptional regulation, and proteolysis (Figure 6). Cell culture based RNAi screens have also been carried out to uncover genetic modifiers of aggregation and toxicity. One such screen further confirmed the role of chaperones in protection against aggregation and identified a novel transcription factor Tra1, which reduces aggregation through an undefined mechanism (Zhang, Binari et al. 2010). A similar screen used genome wide RNAi and a small molecule library to screen for modifiers of toxicity and aggregation. Several small molecule compounds known to function as Topoisomerase inhibitors were able to reduce aggregation and increase viability *in vivo* in a *Drosophila* model of HD. In addition, an upstream kinase in the mTOR/Insulin pathway, *lkb,* was found to decrease aggregation. However, a direct correlation between reduced aggregation and increased viability was not established in this or any other toxicity/aggregation screen (Schulte, Sepp et al. 2011).

Fast axonal transport overview

Considering the focus on the role of wild-type Htt and polyQexHtt aggregates in fast axonal transport (FAT) in this paper, this section will serve to introduce the current models and questions in the field of FAT. FAT involves the anterograde movement of cargos such as mitochondria, synaptic vesicles, lysosomes other proteins or organelles which are synthesized in the cell body and must be transported to the synapse. Additionally, neurotrophic factors,

organelles, as well as proteins and membranes which need repair or degradation, are transported in the retrograde direction via FAT. FAT occurs on microtubule tracks and microtubule motors throughout the length of the axon at a rate of roughly 0.1 to 1 µm/s (Morris and Hollenbeck 1993; Louie 2008). Shorter range movements near the synapse and Golgi are mediated by Myosin-V actin-based transport (Langford 2002). Cargos move in the anterograde direction via microtubule plus-end directed kinesin motors, and in retrograde direction via microtubule minus-end directed dynein motors (Hirokawa and Takemura 2004). These motor proteins move by an ATP hydrolysis and ADP release, which results in a conformational change that confers motion (Pfister, Wagner et al. 1989).

There are likely 15-30 unique members of the kinesin family which may yield even greater variety considering splice isoforms (Endow and Hatsumi 1991). Different motor isoforms have different specificities for cargos. KIF5 (conventional kinesin-1 heavy chain) and KIF1-B are responsible for anterograde mitochondrial transport (Pilling, Horiuchi et al. 2006), while KIF1-A (*Drosophila* UNC-104) is the primary motor for anterograde transport of dense core vesicles and synaptic vesicles (Pack-Chung, Kurshan et al. 2007; Barkus, Klyachko et al. 2008). Cytoplasmic dynein is the only known retrograde motor. To ensure proper cargo localization, FAT is a tightly regulated process which requires highly organized cytoskeletal tracks, motor coordination, and proper cargo attachment.

An important aspect of fast axonal transport is the highly specific delivery of components such as sodium/potassium channels to nodes of Ranvier and synaptic vesicles to synapses. The exact mechanisms that control organelle movement and localization are not clear, though it has been suggested that adapter molecules, which mediate binding of cargos to motors, are necessary to regulate the movement of organelles such as mitochondria (Hollenbeck and Saxton 2005).

Several adapter molecules have been identified as being specific for mitochondria, including HAP1, *Drosophila* Milton, which is required for mitochondrial localization to the axon in *Drosophila* (Stowers, Megeath et al. 2002). Miro is another adaptor protein necessary for mitochondrial transport that been shown to control mitochondrial responses to calcium (Russo, Louie et al. 2009). While HAP1 controls binding of mitochondria to the motor, Miro has been shown to control binding of the motor to the microtubule track. This demonstrates two methods whereby adapter molecules can alter movement of a cargo. Adapter molecules have also been characterized for synaptic and dense core vesicle transport. In *Drosophila* lacking the App-like interacting protein-1 (APLIP-1), synaptic and dense core vesicles are highly concentrated in the cell body because they do not properly bind kinesin, though mitochondria transport is normal (Horiuchi, Barkus et al. 2005). Another kinesin motor adaptor protein is kinesin light chain (KLC), which binds both cargos and kinesin heavy chain and links them together. Direct interaction between the cargo and the kinesin heavy chain C-terminus is also possible (Gauger and Goldstein 1993). In the retrograde direction, dynein has several adapter molecules such as dynein light chain, dynein intermediate chain, and the dynactin complex which binds dynein through the P150$^{\text{GLUED}}$ complex. These function to both bind cargos and increase motor processivity (King and Schroer 2000). In addition to adapters which bind and release cargos, local signaling molecules are also required to induce this action. Synapsin-1 is one such protein that is localized to synapses by an unknown mechanism. Synapsin-1 binds both actin and synaptic vesicles in an unphosphorylated state, thus arresting vesicular transport at the synapse (McGuinness, Brady et al. 1989).

Different cargos move through the axons at different speeds. While this may be partially mediated by differential motor use, often multiple cargos utilize the same motor proteins but

exhibit different velocities. The exact mechanisms regulating motor velocity are not well understood, but motor movement has been shown to be cooperative, allowing increased force and velocity with increasing concentration (Gagliano, Walb et al. 2010). Motor velocity is also known to be affected by load (Svoboda and Block 1994), the presence of microtubule-associated proteins, such as the p150Glued subunit of dynactin (Culver-Hanlon, Lex et al. 2006), and efficiency of ATP hydrolysis (De Vos, Chapman et al. 2007).

Precise coordination between motors is also required for proper axonal transport. Since both kinesin and dynein are likely bound to the same cargo during transport (Martin, Iyadurai et al. 1999), mechanisms are required to coordinate their movement allowing stoppage and bidirectional movement (Martin, Iyadurai et al. 1999). Additionally, at the beginning and end of microtubule tracks, cargos must transfer from the long range microtubule tracks to the shorter range actin-based tracks, requiring coordination between kinesin, dynein, and myosin motors (Naisbitt, Valtschanoff et al. 2000).

Defective FAT caused by kinesin and dynein mutations manifests in 'tail flipping' phenotypes in *Drosophila* resulting from distal paralysis (Hurd and Saxton 1996). This phonotype is strikingly similar to the 'dying back' phenotype described in HD, whereby a neuron recedes from the distal end, potentially due to defective fast axonal transport defects that accumulate over the lifetime of the organism.

Conclusions

Current models suggest the Htt protein is a scaffold-like protein involved in mediating protein-protein interactions in a diverse array of cellular processes and subcellular compartments. These Htt-mediated interactions are not essential for maintenance of organismal viability, but rather

specifically increase viability of neuronal cells. Specific roles for Htt in transport and synaptic signaling are suggested by the neuronal specificity of Htt phenotypes. The binding and localization properties of Htt are strongly mediated by post-translational modifications such as cleavage and phosphorylation. When the polyQ tract in Htt expands beyond ~35 residues, Htt misfolds, aggregates, and causes neuron specific degeneration. Cleavage and localization of Htt fragments strongly impact their toxicity. By some unknown mechanism, these mutant Htt fragments induce a slow, steady program of neurodegeneration in a subset of neurons in the brain.

Outstanding problems regarding Htt in disease include elucidation of molecular mechanisms linking protein misfolding and neuronal toxicity, as well as the nature of late onset effect, and striatal cell specificity. Outstanding questions regarding the endogenous function of Htt include determining which interacting proteins target Htt to a specific subset of motors and cargos, and determining if there is functional redundancy between Htt and any other proteins that mask defects in Htt null model organisms.

Here, we focus on the role of Htt in fast axonal transport in health and disease and search for novel Htt interacting proteins by screening for suppressors of viability and aggregation in a *Drosophila* model of HD. *Drosophila* provides an effective model organism with a simple nervous system, permitting *in vivo* analysis of transport kinetics in a genetic background with less redundancy than mammalian systems. This system allows clearer assessment of the role of wild-type and polyQex-Htt in fast axonal transport.

Figure 1
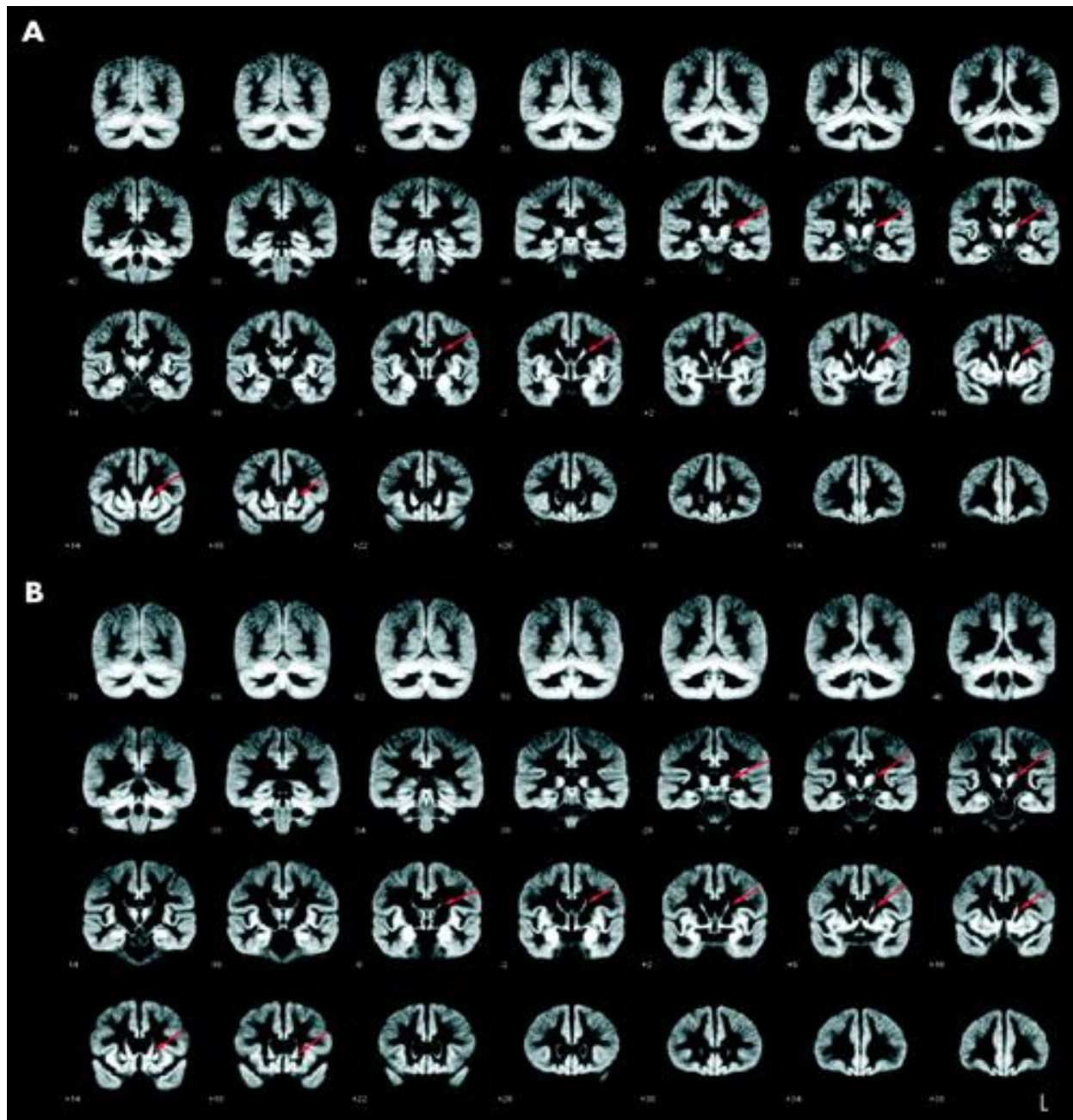
Figure 1. Cell specific neurodegeneration occurs in HD. MRI brain images from control (A) and HD affected (B) individuals. Images were quantified for changes in cerebral grey matter. Increased atrophy of cerebral grey matter was correlated with larger repeat lengths and more advanced stages of the disease. The most affected regions of the brain were the caudate nuclei of the striatum as indicated by arrows. Image reproduced from Kassubek et al 2004.

Figure 2
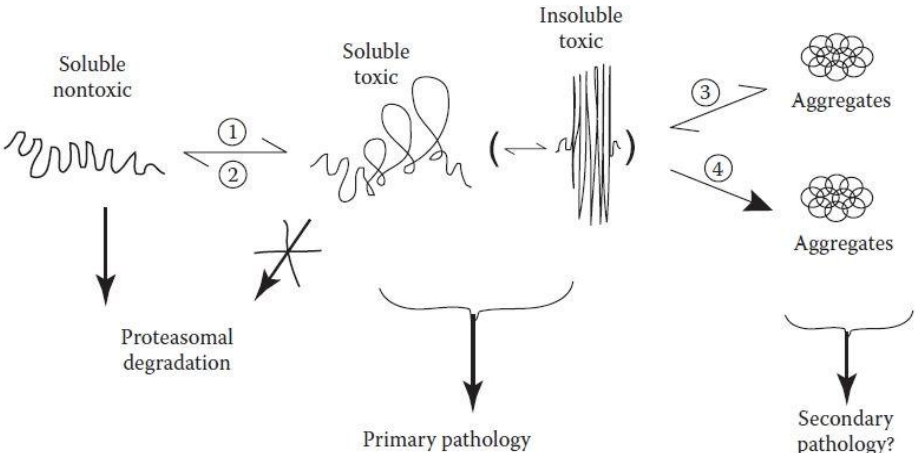
Figure 2. Models of Htt processing and aggregation. Soluble nontoxic Htt is in equilibrium with

a toxic misfolded form. This equilibrium favors the nontoxic form in the presence of

chaperones, and the toxic form in the presence of caspases (Grote and La Spada 2003). Once the

monomer misfolds, the polyQ region can no longer be degraded by the proteasome. These

misfolded monomers and oligomers likely represent one toxic species, while aggregation likely

forms another toxic species in certain cellular contexts, such as the axonal and dendritic

processes. Image reproduced from Grote and La Spada 2003.

Figure 3
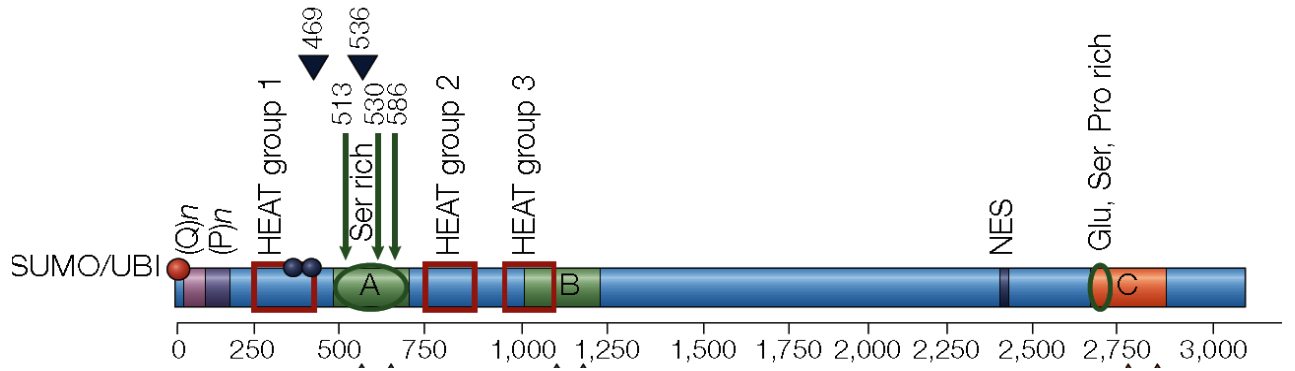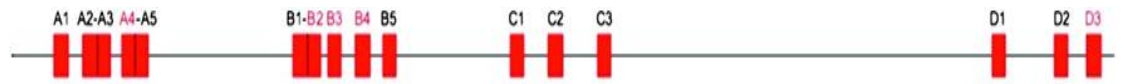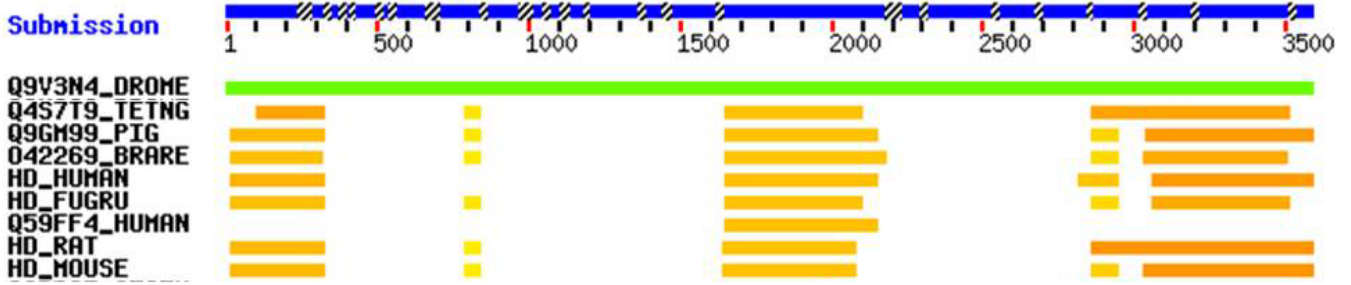
Figure 3. Schematics and alignments of Htt. (A) Schematic depicting well characterized domains of the Htt protein, arrows represent cleavage sites, B identifies the regions cleaved preferentially in the cerebral cortex, C indicates those cleaved mainly in the striatum, and A indicates regions cleaved in both (Reproduced from Catteano et al 2005). (B) Schematic showing the conserved regions in mammals and (C) highly (>50% similarity) conserved regions from all metazoans (B and C reproduced from Tartari et al 2008). (D) An NCBI BLAST alignment of a *Drosophila* Htt entry demonstrating regions of high homology with other Htt model organisms. Overall this figure illustrates highly conserved regions and the associated structural components in the Htt protein. This data illustrates the fact that while the N-terminus is indeed highly conserved and known to mediate many interactions, there are at least two other regions of high homology which have not been characterized.

Figure 4

A

Name[b]	Function	Region in htt for binding	PolyQ-length influence[c]	Identification method
Transcription				
CA150	Transcription activator	Unknown	None	Y2-H
CBP	Transcription activator	Amino acid 1–588	Enhances	GST-pull down
CtBP	Transcription repressor	Unknown	Decreases	Y2-H
HYP-A, B	RNA splicing factors	Polyproline	Enhances	Y2-H
HYP-C	Transcription factor	Polyproline	Enhances	Y2-H
NCOR	Transcription repressor	Amino acid 1–171	Enhances	Y2-H
NF-κB	Transcription factor	HEAT repeats	Unknown	Co-IP
SP1	Transcription activator	Amino acid 1–171	Enhances	GST-pull down, Y2-H
TAFII130	Transcription activator	Amino acid 1–480	None	Y2-H
TBP	Basal transcription factor	Unknown	Unknown	Filter assay
P53	Transcription factor	Polyproline	None	Inclusion isolation
REST–NRSE	Transcription suppressor	Amino acid 1–548	Decreases	Co-IP
Trafficking and endocytosis				
HAP1	Trafficking, endocytosis	Amino acid 1–230	Enhances	Y2-H
HIP1	Endocytosis, pro-apoptotic	Amino acid 1–540	Decreases	Y2-H
HIP14	Trafficking, endocytosis	Amino acid 1–550	Decreases	Y2-H
PACSIN1	Endocytosis	Polyproline	Enhances	Y2-H
PSD-95	Synaptic scaffolding	Unknown	Decreases	Co-IP
Signaling				
Calmodulin	Calcium-binding regulatory protein	Unknown	Enhances	Affinity chromatography
CIP-4	Cdc42-related signaling	Amino acid 1–152	Enhances	Y2-H
FIP2 (also known as HYP-L)	GTPase Rab8 interactor	Amino acid 1–550	Unknown	Y2-H
GRb2	Growth factor signaling	Polyproline	Unknown	Co-IP
IP₃1	Calcium release channel	Amino acid 1–158	Enhances	Co-IP
SH3GL3	Endocytosis and vesicle recycling	Polyproline	Enhances	Y2-H
RasGAP	Ras GTPase-activating protein	Polyproline	Unknown	Co-IP
Metabolism				
Cystathionine β-synthase	Generation of cysteine	Amino acid 1–171	None	Y2-H
GAPDH	Glycolitic enzyme	Polyproline	Enhances	Affinity chromatography
HIP2	Ubiquitin-conjugated enzyme	Amino acid 1–540	None	Y2-H

B
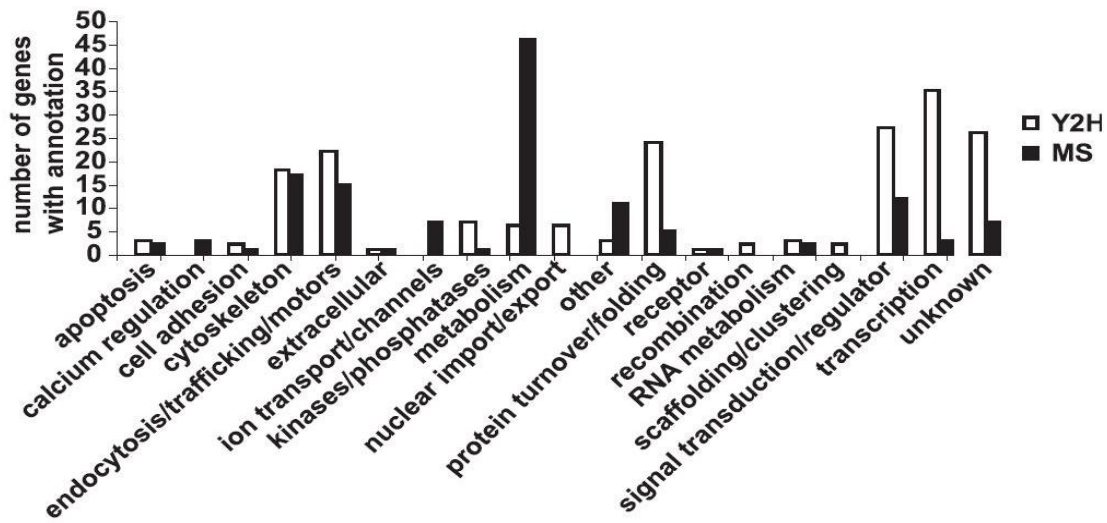
Figure 4. Summary of select hits from screens for Htt interacting proteins using yeast two hybrid, co-IP, and affinity purification with mass spectroscopy. (A) Yeast two-hybrid screens have identified many of the confirmed Htt interacting proteins to date. These screens generally use N-terminal fragments, leaving much of the C-terminal region uncharacterized; however, screens from Kaltenbach et al 2007 revealed no positive interactions in yeast two-hybrid assays from five separate clones representing fragments from the C-terminal 2,000 amino acid region of Htt. Image reproduced from Li and Li 2004. (B) A summary of yeast two-hybrid and affinity pull down mass spec data signifying the complementarity of the two approaches and the broad range of cellular processes that may be mediated by Htt. Image reproduced from Kaltenbach et al 2007.

Figure 5
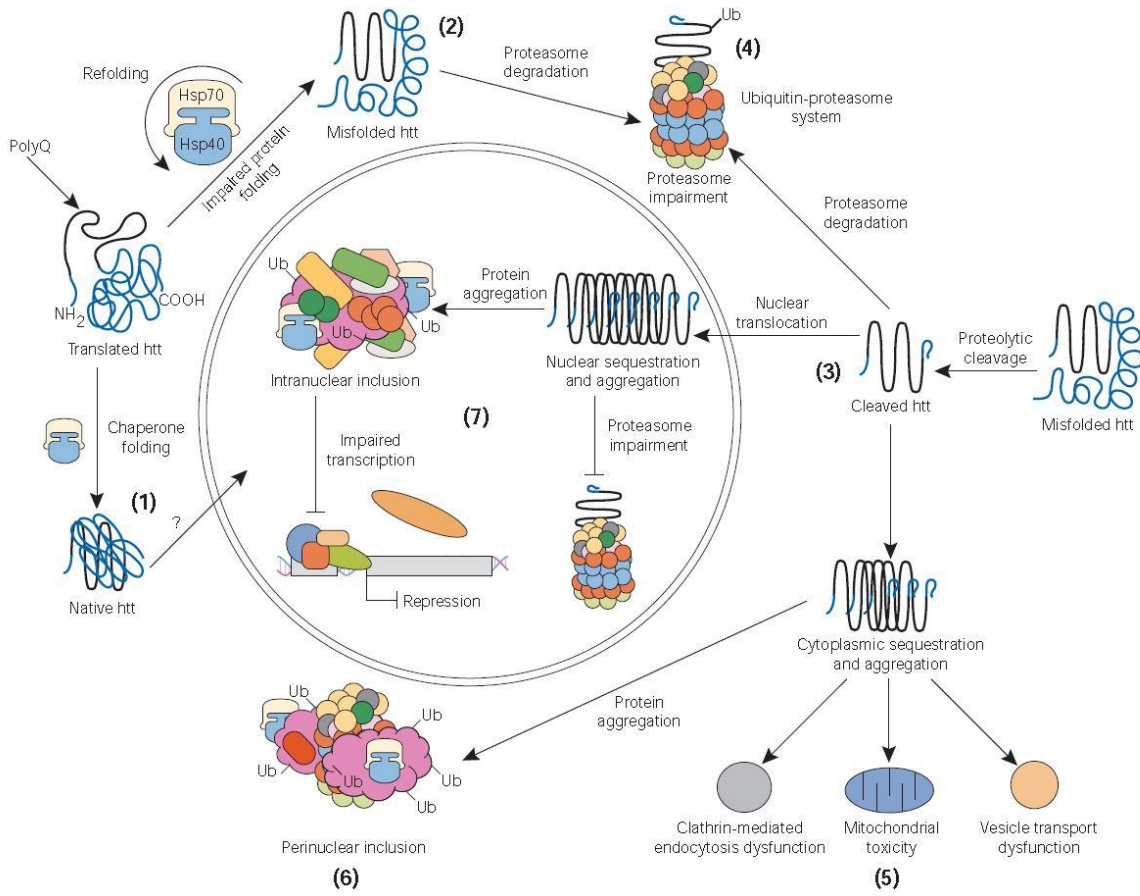
Figure 5. Models of Htt-mediated toxicity. (1) Increased stress on chaperones increases misfolding of Htt and other proteins. (2) Misfolded proteins are targeted to the proteasome but cannot be effectively degraded. (3) Cleavage events lead to nuclear localization and nuclear aggregate formation. (4) UPS system becomes defective due to increased load and decreased ATP production from defective mitochondria. (5) Defective mitochondria also release pro-apoptotic proteins. (6) Aggregate formation can sequester proteins and impede axonal transport. (7) Nuclear entry of Htt fragments results in transcriptional dysregulation. HD is likely to encompass many or all of these mechanisms. Image reproduced from Cattaneo et al 2005.

Figure 6

Functional Category	Human Gene Symbol	Source	*Drosophila* Ortholog	Biological Process	Over-Expression Allele(s)	E/S	Loss-of-Function Allele(s)	E/S
Cytoskeletal organization and biogenesis	ADD3	Y2H	hts	Structural constituent of the cytoskeleton	NA	NA	01103, k06121, KG06777	S
	CEP36 (FLJ13386)	Y2H	zipper	Cytoskeletal protein binding, structural constituent of the cytoskeleton	NA	NA	02957, IIX62	E
	CTNNB1	Y2H	armadillo	Wnt receptor signaling pathway, adherens junction	NA	NA	G0192, G0234, 2, 3	S
	GFAP	MS	Lamin C	Cytoskeletal organization	NA	NA	G00158, k11904	E
	GPM6[a]	MS	M6	Cytoskeletal organization, transmission of nerve impulse	EY07032	E	BG00390	S
	KIAA1229	Y2H	CLIP-190	Structural constituent of the cytoskeleton	NA	NA	KG07837, KG06490	E
	KIF5C[a]	MS	Khc	Structural constituent of the cytoskeleton	NA	NA	E02141,8, k1331,4	S
	PPL	Y2H	short stop	Actin cytoskeletal organization, axonogenesis	NA	NA	3, 65–2	E
	SEPT7 (CDC10)	MS	peanut	Actin binding, structural constituent of the cytoskeleton	NA	NA	XP, 02502, KG00478	S
	SORBS1	Y2H	CAP	Cytoskeletal constituent	NA	NA	BG02184, KG0083, KG00308	E
Signal transduction	GNAZ	MS	G-iα65A	G-protein coupled receptor signaling pathway	EY10355, EY09376b	E	KG01907	S
	ITPR1	MS	Itp-r83A	Calcium ion transport; signal transduction	EY02522	E	05616	S
	NEGR1	MS	Lachesin	Axonogenesis, signal transduction	NA	NA	G00044, BG01462	E
	PTK6	Y2H	Src42A	Protein amino acid phosphorylation	UAS-Src42A.CA	S	KG02515, k10108, E1	E
	YWHAB	MS	14-3-3ζ	Ras protein signal transduction	EY06147, EY03325	E	NA	NA
	YWHAE[a]	MS	14-3-3ε	Ras protein signal transduction	UAS:14-3-3, UAS:14-3-3(weak)	E	j2B10	S
Synaptic transmission	CLTC	MS	Chc	Intracellular protein transport, neurotransmitter secretion	NA	NA	1, G0438, BG02593a	S
	NAPA[a]	MS	SNAP	Intracellular protein transport, neurotransmitter secretion	S102C#2D	E	SNAP[G8], SNAP[J1], SNAP[I65], SNAP[M3], SNAP[M4], SNAP[P2]	S
	STX1A	MS	Syntaxin 1A	t-SNARE, neurotransmitter secretion	EP3215	E	Delta229, 06737	S
Proteolysis/peptidolysis or ubiquitin cycle	ASPH	MS	Asph	Proteolysis and peptidolysis, tyrosine kinase signaling pathway	NA	NA	ZCL1605, KG09881	E
	DNCH1	Y2H	Dhc64C	Intracellular protein transport, proteolysis and peptidolysis	NA	NA	4–19, KG08838	E
	PSMC2[a]	Y2H	Rpt1	Proteolysis and peptidolysis	EP2153	E	43Ed-1, 05643	S
	USP9X	Y2H	fat facets	Proteolysis and peptidolysis, protein deubiquitination	EP381	S	Bx4	E
Regulation of transcription or translation	MEF2D	Y2H	Mef2	Regulation of transcription from Pol II promoter	NA	NA	X1, KG01211a	S
	PPARG	Y2H	Eip75B	Regulation of transcription from Pol II; fatty acid metabolism	NA	NA	BG02576, KG00139, KG09026, 07041	S
	ZNF91	Y2H	crooked legs	RNA Polymerase II transcription factor activity	EY08953	S	04418, k05025	E
Other	CACNA2D1	MS	CG12455	Calcium channel activity, voltage-gated calcium channel activity	EY09750	E	KG00260	S
	FEZ1	Y2H/LIT	Unc-76	Axon cargo transport	NA	NA	G0310, G0333, G0423a	E
	GAPDH	MS/Y2H/LIT	Gpdh	Carbohydrate metabolism	NA	NA	N0, n1–4, n1–5	S
	GPI[a]	MS	Pgi	Gluconeogenesis, glycolysis	nNC1,2	E	NA	NA
	NDUFB10	MS	Pdsw	Mitochondrial electron transport	NA	NA	K10101	S
	VDAC2	MS	porin	Voltage-gated ion channel	NA	NA	k05123, f03616	S

Functional classification as in Table 2. E, enhancer; S, suppressor.
[a]Genes tested in *Drosophila* prior to statistical filtering.
doi:10.1371/journal.pgen.0030082.t003

Figure 6. Proteins that interact with Htt in yeast two-hybrid and pull down mass spectrometry experiments were tested for their ability to suppress (S) or enhance (E) Htt-mediated toxicity in a *Drosophila* eye model of HD. Image reproduced from Kaltenbach et al 2007.

References

Albers, D. S. and M. F. Beal (2000). "Mitochondrial dysfunction and oxidative stress in aging and neurodegenerative disease." J Neural Transm Suppl **59**: 133-154.

Albin, R. L., A. Reiner, et al. (1990). "Striatal and nigral neuron subpopulations in rigid Huntington's disease: implications for the functional anatomy of chorea and rigidity-akinesia." Ann Neurol **27**(4): 357-365.

Albin, R. L., A. B. Young, et al. (1990). "Abnormalities of striatal projection neurons and N-methyl-D-aspartate receptors in presymptomatic Huntington's disease." N Engl J Med **322**(18): 1293-1298.

Ali, N. J. and M. S. Levine (2006). "Changes in expression of N-methyl-D-aspartate receptor subunits occur early in the R6/2 mouse model of Huntington's disease." Dev Neurosci **28**(3): 230-238.

Almeida, S., A. B. Sarmento-Ribeiro, et al. (2008). "Evidence of apoptosis and mitochondrial abnormalities in peripheral blood cells of Huntington's disease patients." Biochem Biophys Res Commun **374**(4): 599-603.

Ambrose, C. M., M. P. Duyao, et al. (1994). "Structure and expression of the Huntington's disease gene: evidence against simple inactivation due to an expanded CAG repeat." Somat Cell Mol Genet **20**(1): 27-38.

Andrade, M. A., C. Perez-Iratxeta, et al. (2001). "Protein repeats: structures, functions, and evolution." J Struct Biol **134**(2-3): 117-131.

Andrade, M. A., C. Petosa, et al. (2001). "Comparison of ARM and HEAT protein repeats." J Mol Biol **309**(1): 1-18.

Anne, S. L., F. Saudou, et al. (2007). "Phosphorylation of huntingtin by cyclin-dependent kinase 5 is induced by DNA damage and regulates wild-type and mutant huntingtin toxicity in neurons." J Neurosci **27**(27): 7318-7328.

Arrasate, M., S. Mitra, et al. (2004). "Inclusion body formation reduces levels of mutant huntingtin and the risk of neuronal death." Nature **431**(7010): 805-810.

Atwal, R. S., C. R. Desmond, et al. (2011). "Kinase inhibitors modulate huntingtin cell localization and toxicity." Nat Chem Biol **7**(7): 453-460.

Atwal, R. S., J. Xia, et al. (2007). "Huntingtin has a membrane association signal that can modulate huntingtin aggregation, nuclear entry and toxicity." Hum Mol Genet **16**(21): 2600-2615.

Aylward, E. H., Q. Li, et al. (1997). "Longitudinal change in basal ganglia volume in patients with Huntington's disease." Neurology **48**(2): 394-399.

Barkus, R. V., O. Klyachko, et al. (2008). "Identification of an axonal kinesin-3 motor for fast anterograde vesicle transport that facilitates retrograde transport of neuropeptides." Mol Biol Cell **19**(1): 274-283.

Beal, M. F., T. Palomo, et al. (2000). "Neuroprotective and neurorestorative strategies for neuronal injury." Neurotox Res **2**(2-3): 71-84.

Bemelmans, A. P., P. Horellou, et al. (1999). "Brain-derived neurotrophic factor-mediated protection of striatal neurons in an excitotoxic rat model of Huntington's disease, as demonstrated by adenoviral gene transfer." Hum Gene Ther **10**(18): 2987-2997.

Benn, C. L., E. J. Slow, et al. (2007). "Glutamate receptor abnormalities in the YAC128 transgenic mouse model of Huntington's disease." Neuroscience **147**(2): 354-372.

Bhutani, N., P. Venkatraman, et al. (2007). "Puromycin-sensitive aminopeptidase is the major peptidase responsible for digesting polyglutamine sequences released by proteasomes during protein degradation." EMBO J **26**(5): 1385-1396.

Brennan, W. A., Jr., E. D. Bird, et al. (1985). "Regional mitochondrial respiratory activity in Huntington's disease brain." J Neurochem **44**(6): 1948-1950.

Carmichael, J., J. Chatellier, et al. (2000). "Bacterial and yeast chaperones reduce both aggregate formation and cell death in mammalian cell models of Huntington's disease." Proceedings of the National Academy of Sciences of the United States of America **97**(17): 9701-9705.

Cattaneo, E., C. Zuccato, et al. (2005). "Normal huntingtin function: an alternative approach to Huntington's disease." Nat Rev Neurosci **6**(12): 919-930.

Caviston, J. P., J. L. Ross, et al. (2007). "Huntingtin facilitates dynein/dynactin-mediated vesicle transport." Proc Natl Acad Sci U S A **104**(24): 10045-10050.

Cepeda, C., M. A. Ariano, et al. (2001). "NMDA receptor function in mouse models of Huntington disease." J Neurosci Res **66**(4): 525-539.

Chang, D. T., G. L. Rintoul, et al. (2006). "Mutant huntingtin aggregates impair mitochondrial movement and trafficking in cortical neurons." Neurobiol Dis.

Chang, D. T., G. L. Rintoul, et al. (2006). "Mutant huntingtin aggregates impair mitochondrial movement and trafficking in cortical neurons." Neurobiol Dis **22**(2): 388-400.

Chattopadhyay, B., S. Ghosh, et al. (2003). "Modulation of age at onset in Huntington's disease and spinocerebellar ataxia type 2 patients originated from eastern India." Neurosci Lett **345**(2): 93-96.

Choo, Y. S., G. V. Johnson, et al. (2004). "Mutant huntingtin directly increases susceptibility of mitochondria to the calcium-induced permeability transition and cytochrome c release." Hum Mol Genet **13**(14): 1407-1420.

Chopra, V., J. H. Fox, et al. (2007). "A small-molecule therapeutic lead for Huntington's disease: preclinical pharmacology and efficacy of C2-8 in the R6/2 transgenic mouse." Proceedings of the National Academy of Sciences of the United States of America **104**(42): 16685-16689.

Ciammola, A., J. Sassone, et al. (2007). "Low brain-derived neurotrophic factor (BDNF) levels in serum of Huntington's disease patients." Am J Med Genet B Neuropsychiatr Genet **144B**(4): 574-577.

Colin, E., D. Zala, et al. (2008). "Huntingtin phosphorylation acts as a molecular switch for anterograde/retrograde transport in neurons." EMBO J **27**(15): 2124-2134.

Cornett, J., F. Cao, et al. (2005). "Polyglutamine expansion of huntingtin impairs its nuclear export." Nat Genet **37**(2): 198-204.

Corrochano, S., M. Renna, et al. (2011). "Alpha-synuclein levels modulate Huntington's disease in mice." Hum Mol Genet.

Culver-Hanlon, T. L., S. A. Lex, et al. (2006). "A microtubule-binding domain in dynactin increases dynein processivity by skating along microtubules." Nat Cell Biol **8**(3): 264-270.

Cummings, C. J., Y. Sun, et al. (2001). "Over-expression of inducible HSP70 chaperone suppresses neuropathology and improves motor function in SCA1 mice." Hum Mol Genet **10**(14): 1511-1518.

Darnell, G., J. P. Orgel, et al. (2007). "Flanking polyproline sequences inhibit beta-sheet structure in polyglutamine segments by inducing PPII-like helix structure." J Mol Biol **374**(3): 688-704.

Davies, S. W., M. Turmaine, et al. (1997). "Formation of neuronal intranuclear inclusions underlies the neurological dysfunction in mice transgenic for the HD mutation." Cell **90**(3): 537-548.

De Vos, K. J., A. L. Chapman, et al. (2007). "Familial amyotrophic lateral sclerosis-linked SOD1 mutants perturb fast axonal transport to reduce axonal mitochondria content." Hum Mol Genet **16**(22): 2720-2728.

del Toro, D., J. M. Canals, et al. (2006). "Mutant huntingtin impairs the post-Golgi trafficking of brain-derived neurotrophic factor but not its Val66Met polymorphism." J Neurosci **26**(49): 12748-12757.

DiFiglia, M., E. Sapp, et al. (1997). "Aggregation of huntingtin in neuronal intranuclear inclusions and dystrophic neurites in brain." Science **277**(5334): 1990-1993.

DiProspero, N. A., E. Y. Chen, et al. (2004). "Early changes in Huntington's disease patient brains involve alterations in cytoskeletal and synaptic elements." J Neurocytol **33**(5): 517-533.

Djousse, L., B. Knowlton, et al. (2002). "Weight loss in early stage of Huntington's disease." Neurology **59**(9): 1325-1330.

Dragatsis, I., A. Efstratiadis, et al. (1998). "Mouse mutant embryos lacking huntingtin are rescued from lethality by wild-type extraembryonic tissues." Development **125**(8): 1529-1539.

Dragatsis, I., M. S. Levine, et al. (2000). "Inactivation of Hdh in the brain and testis results in progressive neurodegeneration and sterility in mice." Nat Genet **26**(3): 300-306.

Dunah, A. W., H. Jeong, et al. (2002). "Sp1 and TAFII130 transcriptional activity disrupted in early Huntington's disease." Science **296**(5576): 2238-2243.

Duyao, M., C. Ambrose, et al. (1993). "Trinucleotide repeat length instability and age of onset in Huntington's disease." Nat Genet **4**(4): 387-392.

Duyao, M. P., A. B. Auerbach, et al. (1995). "Inactivation of the mouse Huntington's disease gene homolog Hdh." Science **269**(5222): 407-410.

Endow, S. A. and M. Hatsumi (1991). "A multimember kinesin gene family in Drosophila." Proc Natl Acad Sci U S A **88**(10): 4424-4427.

Engelender, S., A. H. Sharp, et al. (1997). "Huntingtin-associated protein 1 (HAP1) interacts with the p150Glued subunit of dynactin." Hum Mol Genet **6**(13): 2205-2212.

Estrada-Sanchez, A. M., T. Montiel, et al. (2009). "Glutamate toxicity in the striatum of the R6/2 Huntington's disease transgenic mice is age-dependent and correlates with decreased levels of glutamate transporters." Neurobiol Dis **34**(1): 78-86.

Fan, J., C. M. Cowan, et al. (2009). "Interaction of postsynaptic density protein-95 with NMDA receptors influences excitotoxicity in the yeast artificial chromosome mouse model of Huntington's disease." J Neurosci **29**(35): 10928-10938.

Fan, M. M. and L. A. Raymond (2007). "N-methyl-D-aspartate (NMDA) receptor function and excitotoxicity in Huntington's disease." Prog Neurobiol **81**(5-6): 272-293.

Fayazi, Z., S. Ghosh, et al. (2006). "A Drosophila ortholog of the human MRJ modulates polyglutamine toxicity and aggregation." Neurobiol Dis **24**(2): 226-244.

Fossale, E., V. C. Wheeler, et al. (2002). "Identification of a presymptomatic molecular phenotype in Hdh CAG knock-in mice." Hum Mol Genet **11**(19): 2233-2241.

Gagliano, J., M. Walb, et al. (2010). "Kinesin velocity increases with the number of motors pulling against viscoelastic drag." Eur Biophys J **39**(5): 801-813.

Gauger, A. K. and L. S. Goldstein (1993). "The Drosophila kinesin light chain. Primary structure and interaction with kinesin heavy chain." J Biol Chem **268**(18): 13657-13666.

Gauthier, L. R., B. C. Charrin, et al. (2004). "Huntingtin controls neurotrophic support and survival of neurons by enhancing BDNF vesicular transport along microtubules." Cell **118**(1): 127-138.

Gerber, H. P., K. Seipel, et al. (1994). "Transcriptional activation modulated by homopolymeric glutamine and proline stretches." Science **263**(5148): 808-811.

Gervais, F. G., R. Singaraja, et al. (2002). "Recruitment and activation of caspase-8 by the Huntingtin-interacting protein Hip-1 and a novel partner Hippi." Nat Cell Biol **4**(2): 95-105.

Gines, S., I. S. Seong, et al. (2003). "Specific progressive cAMP reduction implicates energy deficit in presymptomatic Huntington's disease knock-in mice." Hum Mol Genet **12**(5): 497-508.

Glass, M., M. Dragunow, et al. (2000). "The pattern of neurodegeneration in Huntington's disease: a comparative study of cannabinoid, dopamine, adenosine and GABA(A) receptor alterations in the human basal ganglia in Huntington's disease." Neuroscience **97**(3): 505-519.

Goebel, H. H., R. Heipertz, et al. (1978). "Juvenile Huntington chorea: clinical, ultrastructural, and biochemical studies." Neurology **28**(1): 23-31.

Gomez-Tortosa, E., M. E. MacDonald, et al. (2001). "Quantitative neuropathological changes in presymptomatic Huntington's disease." Ann Neurol **49**(1): 29-34.

Graham, R. K., Y. Deng, et al. (2006). "Cleavage at the caspase-6 site is required for neuronal dysfunction and degeneration due to mutant huntingtin." Cell **125**(6): 1179-1191.

Grote, S. K. and A. R. La Spada (2003). "Insights into the molecular basis of polyglutamine neurodegeneration from studies of a spinocerebellar ataxia type 7 mouse model." Cytogenet Genome Res **100**(1-4): 164-174.

Grunewald, T. and M. F. Beal (1999). "Bioenergetics in Huntington's disease." Ann N Y Acad Sci **893**: 203-213.

Gu, M., M. T. Gash, et al. (1996). "Mitochondrial defect in Huntington's disease caudate nucleus." Ann Neurol **39**(3): 385-389.

Gunawardena, S. and L. S. Goldstein (2001). "Disruption of axonal transport and neuronal viability by amyloid precursor protein mutations in Drosophila." Neuron **32**(3): 389-401.

Gunawardena, S., L. S. Her, et al. (2003). "Disruption of axonal transport by loss of huntingtin or expression of pathogenic polyQ proteins in Drosophila." Neuron **40**(1): 25-40.

Hackam, A. S., R. Singaraja, et al. (1998). "The influence of huntingtin protein size on nuclear localization and cellular toxicity." J Cell Biol **141**(5): 1097-1105.

Havel, L. S., C. E. Wang, et al. (2011). "Preferential accumulation of N-terminal mutant huntingtin in the nuclei of striatal neurons is regulated by phosphorylation." Hum Mol Genet **20**(7): 1424-1437.

HDCRG (1993). "A novel gene containing a trinucleotide repeat that is expanded and unstable on Huntington's disease chromosomes. The Huntington's Disease Collaborative Research Group." Cell **72**(6): 971-983.

Hedreen, J. C., C. E. Peyser, et al. (1991). "Neuronal loss in layers V and VI of cerebral cortex in Huntington's disease." Neurosci Lett **133**(2): 257-261.

Hirokawa, N. and R. Takemura (2004). "Molecular motors in neuronal development, intracellular transport and diseases." Curr Opin Neurobiol **14**(5): 564-573.

Hodgson, J. G., N. Agopyan, et al. (1999). "A YAC mouse model for Huntington's disease with full-length mutant huntingtin, cytoplasmic toxicity, and selective striatal neurodegeneration." Neuron **23**(1): 181-192.

Hollenbeck, P. J. and W. M. Saxton (2005). "The axonal transport of mitochondria." J Cell Sci 118(Pt 23): 5411-5419.

Holmberg, C. I., K. E. Staniszewski, et al. (2004). "Inefficient degradation of truncated polyglutamine proteins by the proteasome." EMBO J 23(21): 4307-4318.

Horiuchi, D., R. V. Barkus, et al. (2005). "APLIP1, a kinesin binding JIP-1/JNK scaffold protein, influences the axonal transport of both vesicles and mitochondria in Drosophila." Curr Biol 15(23): 2137-2141.

Howarth, J. L., S. Kelly, et al. (2007). "Hsp40 molecules that target to the ubiquitin-proteasome system decrease inclusion formation in models of polyglutamine disease." Mol Ther 15(6): 1100-1105.

Humbert, S. and F. Saudou (2004). "[Stimulation of BDNF transport by huntingtin]." Med Sci (Paris) 20(11): 952-954.

Huntington, G. (1872). "On Chorea." The Medical and Surgical Reporter: A Weekly Journal 26(15): 317-321.

Hurd, D. D. and W. M. Saxton (1996). "Kinesin mutations cause motor neuron disease phenotypes by disrupting fast axonal transport in Drosophila." Genetics 144(3): 1075-1085.

Jana, N. R., E. A. Zemskov, et al. (2001). "Altered proteasomal function due to the expression of polyglutamine-expanded truncated N-terminal huntingtin induces apoptosis by caspase activation through mitochondrial cytochrome c release." Hum Mol Genet 10(10): 1049-1059.

Jeong, H., F. Then, et al. (2009). "Acetylation targets mutant huntingtin to autophagosomes for degradation." Cell 137(1): 60-72.

Juenemann, K., C. Weisse, et al. (2011). "Modulation of mutant huntingtin N-terminal cleavage and its effect on aggregation and cell death." Neurotox Res 20(2): 120-133.

Jung, J. and N. Bonini (2007). "CREB-binding protein modulates repeat instability in a Drosophila model for polyQ disease." Science 315(5820): 1857-1859.

Kalchman, M. A., H. B. Koide, et al. (1997). "HIP1, a human homologue of S. cerevisiae Sla2p, interacts with membrane-associated huntingtin in the brain." Nat Genet 16(1): 44-53.

Kaltenbach, L. S., E. Romero, et al. (2007). "Huntingtin interacting proteins are genetic modifiers of neurodegeneration." PLoS Genet 3(5): e82.

Karlovich, C. A., R. M. John, et al. (1998). "Characterization of the Huntington's disease (HD) gene homologue in the zebrafish Danio rerio." Gene 217(1-2): 117-125.

Kassubek, J., F. D. Juengling, et al. (2004). "Topography of cerebral atrophy in early Huntington's disease: a voxel based morphometric MRI study." J Neurol Neurosurg Psychiatry 75(2): 213-220.

Kazemi-Esfarjani, P. and S. Benzer (2000). "Genetic suppression of polyglutamine toxicity in Drosophila." Science 287(5459): 1837-1840.

Kazemi-Esfarjani, P. and S. Benzer (2002). "Suppression of polyglutamine toxicity by a Drosophila homolog of myeloid leukemia factor 1." Hum Mol Genet 11(21): 2657-2672.

Kells, A. P., D. M. Fong, et al. (2004). "AAV-mediated gene delivery of BDNF or GDNF is neuroprotective in a model of Huntington disease." Mol Ther 9(5): 682-688.

Kiechle, T., A. Dedeoglu, et al. (2002). "Cytochrome C and caspase-9 expression in Huntington's disease." Neuromolecular Med 1(3): 183-195.

King, S. J. and T. A. Schroer (2000). "Dynactin increases the processivity of the cytoplasmic dynein motor." Nat Cell Biol 2(1): 20-24.

Kuemmerle, S., C. A. Gutekunst, et al. (1999). "Huntington aggregates may not predict neuronal death in Huntington's disease." Annals of neurology **46**(6): 842-849.

Lajoie, P. and E. L. Snapp (2010). "Formation and toxicity of soluble polyglutamine oligomers in living cells." PLoS One **5**(12): e15245.

Lam, W., W. M. Chan, et al. (2008). "Human receptor for activated protein kinase C1 associates with polyglutamine aggregates and modulates polyglutamine toxicity." Biochemical and biophysical research communications **377**(2): 714-719.

Langford, G. M. (2002). "Myosin-V, a versatile motor for short-range vesicle transport." Traffic **3**(12): 859-865.

Leavitt, B. R., J. A. Guttman, et al. (2001). "Wild-type huntingtin reduces the cellular toxicity of mutant huntingtin in vivo." Am J Hum Genet **68**(2): 313-324.

Leavitt, B. R., J. M. van Raamsdonk, et al. (2006). "Wild-type huntingtin protects neurons from excitotoxicity." J Neurochem **96**(4): 1121-1129.

Lee, C. W. and H. B. Peng (2008). "The function of mitochondria in presynaptic development at the neuromuscular junction." Mol Biol Cell **19**(1): 150-158.

Lee, W. C., M. Yoshihara, et al. (2004). "Cytoplasmic aggregates trap polyglutamine-containing proteins and block axonal transport in a Drosophila model of Huntington's disease." Proc Natl Acad Sci U S A **101**(9): 3224-3229.

Li, X. J., S. H. Li, et al. (1995). "A huntingtin-associated protein enriched in brain with implications for pathology." Nature **378**(6555): 398-402.

Li, X. J., A. L. Orr, et al. (2010). "Impaired mitochondrial trafficking in Huntington's disease." Biochim Biophys Acta **1802**(1): 62-65.

Li, Z., C. A. Karlovich, et al. (1999). "A putative Drosophila homolog of the Huntington's disease gene." Hum Mol Genet **8**(9): 1807-1815.

Lin, C. H., S. Tallaksen-Greene, et al. (2001). "Neurological abnormalities in a knock-in mouse model of Huntington's disease." Hum Mol Genet **10**(2): 137-144.

Louie, K., Gary J. Russo , David B. Salkoff , Andrea Wellington , Konrad E. Zinsmaier (2008). "Effects of imaging conditions on mitochondrial transport and length in larval motor

axons of Drosophila." Comp Biochem Physiol A Comp Physiol **151**(151): 159-172.

Lumsden, A. L., T. L. Henshall, et al. (2007). "Huntingtin-deficient zebrafish exhibit defects in iron utilization and development." Hum Mol Genet **16**(16): 1905-1920.

Luthi-Carter, R., S. A. Hanson, et al. (2002). "Dysregulation of gene expression in the R6/2 model of polyglutamine disease: parallel changes in muscle and brain." Hum Mol Genet **11**(17): 1911-1926.

Mangiarini, L., K. Sathasivam, et al. (1997). "Instability of highly expanded CAG repeats in mice transgenic for the Huntington's disease mutation." Nat Genet **15**(2): 197-200.

Mangiarini, L., K. Sathasivam, et al. (1996). "Exon 1 of the HD gene with an expanded CAG repeat is sufficient to cause a progressive neurological phenotype in transgenic mice." Cell **87**(3): 493-506.

Martin, M., S. J. Iyadurai, et al. (1999). "Cytoplasmic dynein, the dynactin complex, and kinesin are interdependent and essential for fast axonal transport." Mol Biol Cell **10**(11): 3717-3728.

Martinez-Serrano, A. and A. Bjorklund (1996). "Protection of the neostriatum against excitotoxic damage by neurotrophin-producing, genetically modified neural stem cells." J Neurosci **16**(15): 4604-4616.

McCampbell, A. and K. H. Fischbeck (2001). "Polyglutamine and CBP: fatal attraction?" <u>Nat Med</u> **7**(5): 528-530.

McGuire, J. R., J. Rong, et al. (2006). "Interaction of Huntingtin-associated protein-1 with kinesin light chain: implications in intracellular trafficking in neurons." <u>J Biol Chem</u> **281**(6): 3552-3559.

McInnis, M. G. (1996). "Anticipation: an old idea in new genes." <u>Am J Hum Genet</u> **59**(5): 973-979.

Mizuno, K., J. Carnahan, et al. (1994). "Brain-derived neurotrophic factor promotes differentiation of striatal GABAergic neurons." <u>Dev Biol</u> **165**(1): 243-256.

Modregger, J., N. A. DiProspero, et al. (2002). "PACSIN 1 interacts with huntingtin and is absent from synaptic varicosities in presymptomatic Huntington's disease brains." <u>Hum Mol Genet</u> **11**(21): 2547-2558.

Morfini, G. A., Y. M. You, et al. (2009). "Pathogenic huntingtin inhibits fast axonal transport by activating JNK3 and phosphorylating kinesin." <u>Nat Neurosci</u> **12**(7): 864-871.

Morris, R. L. and P. J. Hollenbeck (1993). "The regulation of bidirectional mitochondrial transport is coordinated with axonal outgrowth." <u>J Cell Sci</u> **104 (Pt 3)**: 917-927.

Morton, A. J. and W. Leavens (2000). "Mice transgenic for the human Huntington's disease mutation have reduced sensitivity to kainic acid toxicity." <u>Brain Res Bull</u> **52**(1): 51-59.

Naisbitt, S., J. Valtschanoff, et al. (2000). "Interaction of the postsynaptic density-95/guanylate kinase domain-associated protein complex with a light chain of myosin-V and dynein." <u>J Neurosci</u> **20**(12): 4524-4534.

Nasir, J., S. B. Floresco, et al. (1995). "Targeted disruption of the Huntington's disease gene results in embryonic lethality and behavioral and morphological changes in heterozygotes." <u>Cell</u> **81**(5): 811-823.

Neuwald, A. F. and T. Hirano (2000). "HEAT repeats associated with condensins, cohesins, and other complexes involved in chromosome-related functions." <u>Genome Res</u> **10**(10): 1445-1452.

Nucifora, F. C., Jr., M. Sasaki, et al. (2001). "Interference by huntingtin and atrophin-1 with cbp-mediated transcription leading to cellular toxicity." <u>Science</u> **291**(5512): 2423-2428.

O'Kusky, J. R., J. Nasir, et al. (1999). "Neuronal degeneration in the basal ganglia and loss of pallido-subthalamic synapses in mice with targeted disruption of the Huntington's disease gene." <u>Brain Res</u> **818**(2): 468-479.

Orr, A. L., S. Li, et al. (2008). "N-terminal mutant huntingtin associates with mitochondria and impairs mitochondrial trafficking." <u>J Neurosci</u> **28**(11): 2783-2792.

Pack-Chung, E., P. T. Kurshan, et al. (2007). "A Drosophila kinesin required for synaptic bouton formation and synaptic vesicle transport." <u>Nat Neurosci</u> **10**(8): 980-989.

Pal, A., F. Severin, et al. (2008). "Regulation of endosome dynamics by Rab5 and Huntingtin-HAP40 effector complex in physiological versus pathological conditions." <u>Methods Enzymol</u> **438**: 239-257.

Panov, A., T. Obertone, et al. (1999). "Ca(2+)-dependent permeability transition and complex I activity in lymphoblast mitochondria from normal individuals and patients with Huntington's or Alzheimer's disease." <u>Ann N Y Acad Sci</u> **893**: 365-368.

Panov, A. V., C. A. Gutekunst, et al. (2002). "Early mitochondrial calcium defects in Huntington's disease are a direct effect of polyglutamines." <u>Nat Neurosci</u> **5**(8): 731-736.

Pardo, R., M. Molina-Calavita, et al. (2010). "pARIS-htt: an optimised expression platform to study huntingtin reveals functional domains required for vesicular trafficking." <u>Mol Brain</u> **3**: 17.

Parniewski, P. and P. Staczek (2002). "Molecular mechanisms of TRS instability." Adv Exp Med Biol **516**: 1-25.

Perutz, M. F., T. Johnson, et al. (1994). "Glutamine repeats as polar zippers: their possible role in inherited neurodegenerative diseases." Proc Natl Acad Sci U S A **91**(12): 5355-5358.

Peters, M. F. and C. A. Ross (2001). "Isolation of a 40-kDa Huntingtin-associated protein." J Biol Chem **276**(5): 3188-3194.

Pfister, K. K., M. C. Wagner, et al. (1989). "Modification of the microtubule-binding and ATPase activities of kinesin by N-ethylmaleimide (NEM) suggests a role for sulfhydryls in fast axonal transport." Biochemistry **28**(23): 9006-9012.

Pickrell, A. M., H. Fukui, et al. (2011). "The striatum is highly susceptible to mitochondrial oxidative phosphorylation dysfunctions." J Neurosci **31**(27): 9895-9904.

Pilling, A. D., D. Horiuchi, et al. (2006). "Kinesin-1 and Dynein are the primary motors for fast transport of mitochondria in Drosophila motor axons." Mol Biol Cell **17**(4): 2057-2068.

Powers, W. J., T. O. Videen, et al. (2007). "Selective defect of in vivo glycolysis in early Huntington's disease striatum." Proc Natl Acad Sci U S A **104**(8): 2945-2949.

Ranen, N. G., O. C. Stine, et al. (1995). "Anticipation and instability of IT-15 (CAG)n repeats in parent-offspring pairs with Huntington disease." Am J Hum Genet **57**(3): 593-602.

Ravikumar, B., R. Duden, et al. (2002). "Aggregate-prone proteins with polyglutamine and polyalanine expansions are degraded by autophagy." Hum Mol Genet **11**(9): 1107-1117.

Ravikumar, B., C. Vacher, et al. (2004). "Inhibition of mTOR induces autophagy and reduces toxicity of polyglutamine expansions in fly and mouse models of Huntington disease." Nat Genet **36**(6): 585-595.

Reddy, P. H., V. Charles, et al. (1999). "Transgenic mice expressing mutated full-length HD cDNA: a paradigm for locomotor changes and selective neuronal loss in Huntington's disease." Philos Trans R Soc Lond B Biol Sci **354**(1386): 1035-1045.

Reilly, C. E. (2001). "Wild-type huntingtin up-regulates BDNF transcription in Huntington's disease." J Neurol **248**(10): 920-922.

Rigamonti, D., J. H. Bauer, et al. (2000). "Wild-type huntingtin protects from apoptosis upstream of caspase-3." J Neurosci **20**(10): 3705-3713.

Rigamonti, D., S. Sipione, et al. (2001). "Huntingtin's neuroprotective activity occurs via inhibition of procaspase-9 processing." J Biol Chem **276**(18): 14545-14548.

Rockabrand, E., N. Slepko, et al. (2007). "The first 17 amino acids of Huntingtin modulate its sub-cellular localization, aggregation and effects on calcium homeostasis." Hum Mol Genet **16**(1): 61-77.

Roizin, L., Stellar, S., and Liu, J.C (1979). "Neuronal nuclear-cytoplasmic changes in Huntingtons chorea: electron microscope investigations." Advances in Neurology **23**: 95–122.

Romero, E., G. H. Cha, et al. (2008). "Suppression of neurodegeneration and increased neurotransmission caused by expanded full-length huntingtin accumulating in the cytoplasm." Neuron **57**(1): 27-40.

Rong, J., S. H. Li, et al. (2007). "Regulation of intracellular HAP1 trafficking." J Neurosci Res **85**(14): 3025-3029.

Rosas, H. D., D. H. Salat, et al. (2008). "Cerebral cortex and the clinical expression of Huntington's disease: complexity and heterogeneity." Brain **131**(Pt 4): 1057-1068.

Rosen, D. R., T. Siddique, et al. (1993). "Mutations in Cu/Zn superoxide dismutase gene are associated with familial amyotrophic lateral sclerosis." Nature **362**(6415): 59-62.

Ross, C. A. and M. A. Poirier (2004). "Protein aggregation and neurodegenerative disease." <u>Nat Med</u> **10 Suppl**: S10-17.

Rubinsztein, D. C. and J. Carmichael (2003). "Huntington's disease: molecular basis of neurodegeneration." <u>Expert Rev Mol Med</u> **5**(20): 1-21.

Rubinsztein, D. C., J. Leggo, et al. (1996). "Phenotypic characterization of individuals with 30-40 CAG repeats in the Huntington disease (HD) gene reveals HD cases with 36 repeats and apparently normal elderly individuals with 36-39 repeats." <u>Am J Hum Genet</u> **59**(1): 16-22.

Russo, G. J., K. Louie, et al. (2009). "Drosophila Miro is required for both anterograde and retrograde axonal mitochondrial transport." <u>J Neurosci</u> **29**(17): 5443-5455.

Sahlender, D. A., R. C. Roberts, et al. (2005). "Optineurin links myosin VI to the Golgi complex and is involved in Golgi organization and exocytosis." <u>J Cell Biol</u> **169**(2): 285-295.

Salinas, S., C. Proukakis, et al. (2008). "Hereditary spastic paraplegia: clinical features and pathogenetic mechanisms." <u>Lancet Neurol</u> **7**(12): 1127-1138.

Sarkar, S., B. Ravikumar, et al. (2009). "Rapamycin and mTOR-independent autophagy inducers ameliorate toxicity of polyglutamine-expanded huntingtin and related proteinopathies." <u>Cell Death Differ</u> **16**(1): 46-56.

Scherzinger, E., A. Sittler, et al. (1999). "Self-assembly of polyglutamine-containing huntingtin fragments into amyloid-like fibrils: implications for Huntington's disease pathology." <u>Proc Natl Acad Sci U S A</u> **96**(8): 4604-4609.

Scherzinger, E., A. Sittler, et al. (1999). "Self-assembly of polyglutamine-containing huntingtin fragments into amyloid-like fibrils: implications for Huntington's disease pathology." <u>Proceedings of the National Academy of Sciences of the United States of America</u> **96**(8): 4604-4609.

Schulte, J., K. J. Sepp, et al. (2011). "High-content chemical and RNAi screens for suppressors of neurotoxicity in a Huntington's disease model." <u>PLoS One</u> **6**(8): e23841.

Sengupta, S., P. M. Horowitz, et al. (2006). "Degradation of tau protein by puromycin-sensitive aminopeptidase in vitro." <u>Biochemistry</u> **45**(50): 15111-15119.

Sherman, M. Y. and A. L. Goldberg (2001). "Cellular defenses against unfolded proteins: a cell biologist thinks about neurodegenerative diseases." <u>Neuron</u> **29**(1): 15-32.

Shimohata, M., T. Shimohata, et al. (2005). "Interference of CREB-dependent transcriptional activation by expanded polyglutamine stretches--augmentation of transcriptional activation as a potential therapeutic strategy for polyglutamine diseases." <u>J Neurochem</u> **93**(3): 654-663.

Shimohata, T., T. Nakajima, et al. (2000). "Expanded polyglutamine stretches interact with TAFII130, interfering with CREB-dependent transcription." <u>Nat Genet</u> **26**(1): 29-36.

Shimojo, M. (2008). "Huntingtin regulates RE1-silencing transcription factor/neuron-restrictive silencer factor (REST/NRSF) nuclear trafficking indirectly through a complex with REST/NRSF-interacting LIM domain protein (RILP) and dynactin p150 Glued." <u>J Biol Chem</u> **283**(50): 34880-34886.

Sinadinos, C., T. Burbidge-King, et al. (2009). "Live axonal transport disruption by mutant huntingtin fragments in Drosophila motor neuron axons." <u>Neurobiol Dis</u> **34**(2): 389-395.

Slow, E. J., R. K. Graham, et al. (2005). "Absence of behavioral abnormalities and neurodegeneration in vivo despite widespread neuronal huntingtin inclusions." <u>Proc Natl Acad Sci U S A</u> **102**(32): 11402-11407.

Spires, T. L., H. E. Grote, et al. (2004). "Dendritic spine pathology and deficits in experience-dependent dendritic plasticity in R6/1 Huntington's disease transgenic mice." Eur J Neurosci **19**(10): 2799-2807.

Squitieri, F., C. Gellera, et al. (2003). "Homozygosity for CAG mutation in Huntington disease is associated with a more severe clinical course." Brain **126**(Pt 4): 946-955.

Steffan, J. S., N. Agrawal, et al. (2004). "SUMO modification of Huntingtin and Huntington's disease pathology." Science **304**(5667): 100-104.

Steffan, J. S., L. Bodai, et al. (2001). "Histone deacetylase inhibitors arrest polyglutamine-dependent neurodegeneration in Drosophila." Nature **413**(6857): 739-743.

Steffan, J. S., A. Kazantsev, et al. (2000). "The Huntington's disease protein interacts with p53 and CREB-binding protein and represses transcription." Proc Natl Acad Sci U S A **97**(12): 6763-6768.

Stowers, R. S. and E. Y. Isacoff (2007). "Drosophila huntingtin-interacting protein 14 is a presynaptic protein required for photoreceptor synaptic transmission and expression of the palmitoylated proteins synaptosome-associated protein 25 and cysteine string protein." J Neurosci **27**(47): 12874-12883.

Stowers, R. S., L. J. Megeath, et al. (2002). "Axonal transport of mitochondria to synapses depends on milton, a novel Drosophila protein." Neuron **36**(6): 1063-1077.

Sun, Y., A. Savanenin, et al. (2001). "Polyglutamine-expanded huntingtin promotes sensitization of N-methyl-D-aspartate receptors via post-synaptic density 95." J Biol Chem **276**(27): 24713-24718.

Svoboda, K. and S. M. Block (1994). "Force and velocity measured for single kinesin molecules." Cell **77**(5): 773-784.

Tabrizi, S. J., M. W. Cleeter, et al. (1999). "Biochemical abnormalities and excitotoxicity in Huntington's disease brain." Ann Neurol **45**(1): 25-32.

Tam, S., C. Spiess, et al. (2009). "The chaperonin TRiC blocks a huntingtin sequence element that promotes the conformational switch to aggregation." Nat Struct Mol Biol **16**(12): 1279-1285.

Tartari, M., C. Gissi, et al. (2008). "Phylogenetic comparison of huntingtin homologues reveals the appearance of a primitive polyQ in sea urchin." Mol Biol Evol **25**(2): 330-338.

Thakur, A. K., M. Jayaraman, et al. (2009). "Polyglutamine disruption of the huntingtin exon 1 N terminus triggers a complex aggregation mechanism." Nat Struct Mol Biol **16**(4): 380-389.

Trushina, E., R. B. Dyer, et al. (2004). "Mutant huntingtin impairs axonal trafficking in mammalian neurons in vivo and in vitro." Mol Cell Biol **24**(18): 8195-8209.

van der Burg, J. M., K. Bacos, et al. (2008). "Increased metabolism in the R6/2 mouse model of Huntington's disease." Neurobiol Dis **29**(1): 41-51.

Van Raamsdonk, J. M., J. Pearson, et al. (2006). "Wild-type huntingtin ameliorates striatal neuronal atrophy but does not prevent other abnormalities in the YAC128 mouse model of Huntington disease." BMC Neurosci **7**: 80.

Van Raamsdonk, J. M., J. Pearson, et al. (2005). "Cognitive dysfunction precedes neuropathology and motor abnormalities in the YAC128 mouse model of Huntington's disease." J Neurosci **25**(16): 4169-4180.

Velier, J., M. Kim, et al. (1998). "Wild-type and mutant huntingtins function in vesicle trafficking in the secretory and endocytic pathways." Exp Neurol **152**(1): 34-40.

Venkatraman, P., R. Wetzel, et al. (2004). "Eukaryotic proteasomes cannot digest polyglutamine sequences and release them during degradation of polyglutamine-containing proteins." Mol Cell **14**(1): 95-104.

Ventruti, A. and A. M. Cuervo (2007). "Autophagy and neurodegeneration." Curr Neurol Neurosci Rep **7**(5): 443-451.

Vonsattel, J. P. and M. DiFiglia (1998). "Huntington disease." J Neuropathol Exp Neurol **57**(5): 369-384.

Vonsattel, J. P., R. H. Myers, et al. (1985). "Neuropathological classification of Huntington's disease." J Neuropathol Exp Neurol **44**(6): 559-577.

Waelter, S., E. Scherzinger, et al. (2001). "The huntingtin interacting protein HIP1 is a clathrin and alpha-adaptin-binding protein involved in receptor-mediated endocytosis." Hum Mol Genet **10**(17): 1807-1817.

Walker, F. O. (2007). "Huntington's disease." Lancet **369**(9557): 218-228.

Wanker, E. E., C. Rovira, et al. (1997). "HIP-I: a huntingtin interacting protein isolated by the yeast two-hybrid system." Hum Mol Genet **6**(3): 487-495.

Warby, S. C., C. N. Doty, et al. (2009). "Phosphorylation of huntingtin reduces the accumulation of its nuclear fragments." Mol Cell Neurosci **40**(2): 121-127.

Warita, H., Y. Itoyama, et al. (1999). "Selective impairment of fast anterograde axonal transport in the peripheral nerves of asymptomatic transgenic mice with a G93A mutant SOD1 gene." Brain Res **819**(1-2): 120-131.

Wexler, N. S., J. Lorimer, et al. (2004). "Venezuelan kindreds reveal that genetic and environmental factors modulate Huntington's disease age of onset." Proc Natl Acad Sci U S A **101**(10): 3498-3503.

Wheeler, V. C., W. Auerbach, et al. (1999). "Length-dependent gametic CAG repeat instability in the Huntington's disease knock-in mouse." Hum Mol Genet **8**(1): 115-122.

White, J. K., W. Auerbach, et al. (1997). "Huntingtin is required for neurogenesis and is not impaired by the Huntington's disease CAG expansion." Nat Genet **17**(4): 404-410.

Wu, L. L., Y. Fan, et al. (2010). "Huntingtin-associated protein-1 interacts with pro-brain-derived neurotrophic factor and mediates its transport and release." J Biol Chem **285**(8): 5614-5623.

Young, A. B., J. T. Greenamyre, et al. (1988). "NMDA receptor losses in putamen from patients with Huntington's disease." Science **241**(4868): 981-983.

Zeitlin, S., J. P. Liu, et al. (1995). "Increased apoptosis and early embryonic lethality in mice nullizygous for the Huntington's disease gene homologue." Nat Genet **11**(2): 155-163.

Zhang, H., Q. Li, et al. (2008). "Full length mutant huntingtin is required for altered Ca2+ signaling and apoptosis of striatal neurons in the YAC mouse model of Huntington's disease." Neurobiol Dis **31**(1): 80-88.

Zhang, S., R. Binari, et al. (2010). "A genomewide RNA interference screen for modifiers of aggregates formation by mutant Huntingtin in Drosophila." Genetics **184**(4): 1165-1179.

Zuccato, C., N. Belyaev, et al. (2007). "Widespread disruption of repressor element-1 silencing transcription factor/neuron-restrictive silencer factor occupancy at its target genes in Huntington's disease." J Neurosci **27**(26): 6972-6983.

Zuccato, C. and E. Cattaneo (2007). "Role of brain-derived neurotrophic factor in Huntington's disease." Prog Neurobiol **81**(5-6): 294-330.

Zuccato, C., A. Ciammola, et al. (2001). "Loss of huntingtin-mediated BDNF gene transcription in Huntington's disease." Science **293**(5529): 493-498.

Zuccato, C., M. Marullo, et al. (2008). "Systematic assessment of BDNF and its receptor levels in human cortices affected by Huntington's disease." <u>Brain Pathol</u> **18**(2): 225-238.

Zuccato, C., M. Tartari, et al. (2003). "Huntingtin interacts with REST/NRSF to modulate the transcription of NRSE-controlled neuronal genes." <u>Nat Genet</u> **35**(1): 76-83.

Chapter 2

Characterization of Aggregation Kinetics and their Pathological Role in a *Drosophila* Huntington's Disease Model

Kurt R. Weiss[*], Yoko Kimura[*,§], Wyan-Ching Mimi Lee[*] and J. Troy Littleton[*,1]

[*]The Picower Institute for Learning and Memory, Department of Biology and Department of Brain and Cognitive Sciences, Massachusetts Institute of Technology, Cambridge, MA 02139

[§]Laboratory of Protein Metabolism, The Tokyo Metropolitan Institute of Medical Science, Kamikitazawa, Setagaya-Ku, Tokyo 156-8506, Japan

Data, text and figures, for figures 1-5 were generated by Wyan Ching Mimi Lee and J Troy Littleton. The deficiency screen was started by Yoko Kimura, who isolated the large Df's in the screen and generated most data for figure 6. All other experiments, figures, and text were done by Kurt Weiss and edited by J. Troy Littleton.

Abstract

Huntington's Disease (HD) is a neurodegenerative disorder resulting from expansion of a polyglutamine tract in the Huntingtin protein (Htt). Mutant Htt forms intracellular aggregates within neurons, though it is unclear if aggregates or more soluble forms of Htt represent the pathogenic species. To examine the link between aggregation and neurodegeneration, we generated *Drosophila melanogaster* transgenic strains expressing fluorescently-tagged human *huntingtin* gene encoding pathogenic (Q138) or non-pathogenic (Q15) proteins, allowing *in vivo* imaging of Htt expression and aggregation in live animals. Neuronal expression of pathogenic Htt leads to pharate adult lethality, accompanied by formation of large aggregates within the cytoplasm of neuronal cell bodies and neurites. Live imaging and FRAP analysis of pathogenic Htt demonstrated new aggregates can form in neurons within 12 hours, while pre-existing aggregates rapidly accumulate new Htt protein within minutes. To examine the role of aggregates in pathology, we conducted haplo-insufficiency suppressor screens for huntingtin-Q138 aggregation or huntingtin-Q138-induced lethality using deficiencies covering ~80% of the *Drosophila* genome. We identified two classes of interacting suppressors in our screen: those that rescue viability while decreasing Htt expression and aggregation, and those that rescue viability independent of effects on Htt aggregation. The identification of dosage-sensitive suppressors of mutant Htt toxicity that reduce lethality without disrupting aggregation suggests that pathways downstream of aggregate formation can be targeted for neuroprotection in Huntington's Disease. The most robust suppressors reduced both soluble and aggregated Huntingtin levels, suggesting toxicity is likely to be associated with both forms of the mutant protein in Huntington's Disease.

Introduction

Huntington's disease (HD) is an autosomal dominant neurodegenerative disorder and one of the first characterized members of a family of neurological diseases that result from expansion of a polyglutamine (polyQ) tract within the causative protein (ORR and ZOGHBI 2007). HD is characterized by neurodegeneration and formation of neuronal intracellular inclusions, primarily in the striatum and cortex, leading to motor impairment, personality disorders, dementia and ultimately death (PORTERA-CAILLIAU *et al.* 1995; VONSATTEL *et al.* 1985). Currently, HD has no known cure and treatments focus on delaying HD-associated symptoms. The causative mutation in HD is expansion of a CAG tract beyond 35 repeats in exon 1 of the *IT15* gene encoding huntingtin (Htt) (HUNTINGTON'S DISEASE RESEARCH COLLABORATION, 1993). Similar to other polyQ-repeat neurological disorders, abnormal protein conformation(s) secondary to polyQ expansion are central to HD pathogenesis (PERSICHETTI *et al.* 1999; SCHERZINGER *et al.* 1997). The expanded polyQ Htt protein can exist in multiple states (HOFFNER *et al.* 2005; NAGAI *et al.* 2007), including aberrantly folded monomeric forms, oligomeric micro-aggregates, fibril states and larger inclusion body aggregates. It is currently unclear which form(s) of mutant Htt are pathogenic and how the abnormally folded protein causes neuronal toxicity.

PolyQ expansion leading to aggregation is a common theme in neurodegenerative disorders. Spinocerebellar ataxias (SCA1 SCA2, SCA3/MJD, SCA6, SCA7, SCA17), spinal bulbar muscular atrophy (SMBA), and dentatorubral pallidoluysian atrophy (DRPLA) all involve polyQ expansion, aggregation, and neurodegeneration (KIMURA *et al.* 2007). Evidence that aggregates are toxic is mostly correlative for these diseases, but several studies support the aggregation-toxicity hypothesis. The threshold of polyQ repeat number required for *in vitro* aggregation threshold is similar to that required for disease manifestation (DAVIES *et al.* 1997; SCHERZINGER

et al. 1999). Longer polyQ tracts have faster *in vitro* aggregation kinetics and result in earlier

disease onset (SCHERZINGER *et al.* 1999). Similarly, treatments that suppress aggregation,

including chaperone overexpression (CARMICHAEL *et al.* 2000) and administration of small

molecule aggregation inhibitors (CHOPRA *et al.* 2007), have been shown to decrease

neurodegeneration. Live imaging also demonstrates that Htt aggregates can sequester and alter

kinetics of trafficked organelles and proteins such as synaptic vesicles (SINADINOS *et al.* 2009)

and transcription factors (CHAI *et al.* 2002). However, there is also evidence that aggregates may

be inert or even neuroprotective. Medium spiny projection neurons of the striatum exhibit fewer

Htt aggregates than striatal interneurons, yet are more vulnerable to neurodegeneration in HD

(KUEMMERLE *et al.* 1999). An HD mouse model known as the 'short stop' model demonstrates

Htt aggregation, but no neuronal dysfunction or degeneration (SLOW *et al.* 2005). Additionally,

several mouse (HODGSON *et al.* 1999) and *Drosophila* (ROMERO *et al.* 2008) HD models

expressing full-length mutant Htt show selective neurodegeneration and behavioral phenotypes

without obvious aggregation. Indeed, neuronal cell death associated with transient expression of

mutant Htt in cultured striatal neurons is inversely proportional to Htt aggregate formation

(ARRASATE *et al.* 2004), suggesting that inclusion body formation may decrease levels of other

toxic forms of Htt and promote neuronal survival. There is also evidence suggesting that

oligomers precede aggregate formation and are the toxic species in HD (LAJOIE and SNAPP 2010;

LAM *et al.* 2008). These contradictory results in different cellular contexts and HD models have

led to confusion over the toxicity of aggregates, and subsequently, over whether therapeutic

approaches in HD should focus on reducing or enhancing aggregate formation.

To further analyze the link between aggregation and toxicity in a model system, we generated

transgenic *Drosophila* that express an N-terminal fragment of the human Htt gene with either a

pathogenic polyQ tract of 138 repeats (HttQ138), corresponding to a juvenile form of HD, or a wild-type non-pathogenic tract of 15 repeats (HttQ15). The Htt transgene used in our analysis is a human Caspase-6 cleavage fragment containing exons 1 to 12 of the larger Htt locus. Proteolysis of Htt at the Caspase-6 site is an important pathogenic event in HD (GRAHAM *et al.* 2006). Given the uncertainty of cleavage of a larger human Htt transgenic protein in Drosophila, the 588 a.a. fragment represents an attractive biologically relevant cleavage product. The constructs were fused to monomeric red fluorescent protein (mRFP) (CAMPBELL *et al.* 2002) or enhanced green fluorescent protein (eGFP) to allow *in vivo* analysis of aggregate formation and localization. Expression of pathogenic Htt leads to the formation of non-nuclear aggregates and causes death during the pupal stage. This model provided a tractable system to analyze Htt aggregation kinetics in live animals and for conducting forward genetic screens for modifiers of HD pathology and/or aggregation, allowing us to examine the link between Htt aggregation and neuronal toxicity.

Materials and Methods

Generation of Htt Constructs: cDNAs for mRFP-HttQ15, mRFP-HttQ138, eGFP-HttQ15 and eGFP-HttQ138 were subcloned into EcoRI (blunt end ligation) and KpnI sites of the pUAST expression vector. cDNA for eGFP-HttQ138-mRFP was subcloned into the XbaI site of the pUAST vector. HttQ15 and HttQ138 cDNAs were kindly provided by Ray Truant (Department of Biochemistry, McMaster University). cDNA for HttQ96-GFP was kindly provided by David Housman (Center for Cancer Research, MIT) and subcloned into the KpnI and XbaI sites of the pUAST vector. Microinjection of constructs and generation of transgenic *Drosophila* were performed by Genetics Services (Cambridge, MA).

S2 Cell Transfection and Analysis: cDNAs for mRFP-HttQ15 and mRFP-HttQ138 were subcloned into the BamH1 and EcoRI (blunt end ligation) sites of the pSR11 S2 transformation vector. To generate constructs expressing mRFP-HttQ15-eGFP and mRFP-HttQ138-eGFP, mRFP-HttQ15 and mRFP-HttQ138 cDNAs were PCR amplified with a forward primer containing an EcoRI restriction site and a reverse primer containing a 3' Sal I site and subcloned into the pPL17 vector. Constructs were transfected with 50 μL cytofectene (BioRad) into *Drosophila* S2 cells using the BioRad Liposome Mediated Transfection Protocol. After 72 hours, 20 μL cell suspensions were fixed with 3.7% formaldehyde in PBT and mounted on slides with 50% glycerol. Images were captured with a Zeiss Pascal laser scanning confocal microscope (Carl Zeiss MicroImaging, Inc.) using the accompanying Zeiss PASCAL software.

Glue Secretion Assay: Pupae reared at 25°C were isolated shortly after pupariation and placed on slides with the ventral side facing up using double-sided tape. Visualization was performed on a Pascal confocal microscope (Zeiss).

***Drosophila* Genetics and Deficiency Screen:** *Drosophila* were maintained on standard medium at 25°C. The deficiency collection used in the screen was obtained from the Bloomington Stock Center. Males from deficiency lines on chromosome II and III were crossed to C155; A37/CyO-GFP or C155; *Df(3)3450*/TM6 virgins, respectively. For the viability screen, F1 C155/y; Df/Balancer males were mated to homozygous mRFP-HttQ138 high expression females and the number of F2 males and females was scored. For the aggregation screen, F1 C155/y; Df/Balancer males were mated to homozygous mRFP-HttQ138 low expression virgins and live wandering 3rd instar larvae expressing mRFP-HttQ138/Df were viewed under a fluorescent stereoscope (Zeiss) to assay changes in aggregation in larval salivary glands. For aggregation formation analysis, the *CCAP*-Gal4 driver was recombined with a *tubulin*-Gal80^{ts} repressor to drive high expression mRFP-HttQ138 in a temporally restricted manner. mRFP-HttQ138 expression was repressed at 19°C until the 2nd instar stage, at which point larvae were moved to 30°C to induce expression.

Adult Viability Analysis: *Drosophila* viability assays were performed on white/C155, HttQ96-GFP/C155, mRFP-HttQ15/C155, mRFP-HttQ138/C155, and mRFP-HttQ138B/C155 flies by daily quantification of lethality for 100 females of each genotype. Flies were aged at 25°C, with 20 flies per vial, and transferred every 2-3 days.

Western Blot Analysis: For HttQ96-GFP Western blots, *Drosophila* were frozen in liquid nitrogen and vortexed. 20 heads for each indicated genotype were isolated and homogenized in sample buffer, and proteins were separated on 10% SDS-PAGE gels and transferred to nitrocellulose. Blots were incubated with rabbit anti-GFP sc8334 (Santa Cruz Biotechnology) at 1:1000. For eGFP-HttQ138/Q15 and mRFP-HttQ138/Q15, five larvae for each genotype were homogenized in sample buffer and proteins were separated on 10% SDS-PAGE gels. Blots were

incubated with mouse anti-Htt MAb2166 (Chemicon) at 1:1000. To assay for cleavage of Htt *in vivo*, we crossed UAS-HttQ138-mRFP and UAS-eGFP-HttQ138-mRFP to C155 GAL4 driver strains and prepared head extracts from F1 progeny expressing Htt. One head extract per lane was loaded and blots were probed with anti-Htt antibodies. Western blots were visualized on a Li-Cor Odyssey infrared imaging system and protein expression quantified with the accompanying software.

Immunostaining: Wandering 3rd instar larvae reared at 25°C were dissected as previously described (RIECKHOF *et al.* 2003), except that fixation was limited to 10 minutes in 4% formaldehyde. Images were captured with a Zeiss Pascal laser scanning confocal microscope (Carl Zeiss MicroImaging, Inc.) using the accompanying Zeiss PASCAL software.

Quantitative RT-PCR: Quantitative RT-PCR was carried out using an Applied Biosystems 7300 Real-Time PCR System. Total RNA was extracted from 10-15 adult flies per sample using an RNeasyMini Kit (Qiagen) and treated with DNase I (Ambion) according to the manufacturers' instructions. Single stranded cDNA was synthesized in a total volume of 20 L from 1 g of total RNA using a High Capacity cDNA Reverse Transcription Kit (Applied Biosystems) according to the manufacturer's protocol. PCR was carried out in triplicate for each of two independent total RNA samples per genotype in optical 96-well plates (Applied Biosystems). The reaction mixtures were as follows: 25 L of 2x QuantiTect SYBR Green PCR Master Mix (Qiagen), 300 nM forward primer, 300 nM reverse primer, and 5 L of single stranded cDNA (see above) in a total volume of 50 L. A final dissociation step was carried out to evaluate product integrity, and reaction samples were run on a 1.2% agarose gel and stained with ethidium bromide. The primer sequences were as follows: Act88F (actin) forward 5'-ACTTCTGCTGGAAGGTGGAC-3' and reverse 5'-ATCCGCAAGGATCTGTATGC-3'.

FRAP and Live Imaging: FRAP analysis was carried out using a Zeiss spinning disk confocal microscope with Perkin Elmer Velocity 4-D imaging software. Animals were anesthetized with Suprane in a custom chamber that allows imaging thru the cuticle of a live 3rd instar larvae (FUGER *et al.* 2007) with a 63x oil objective. Camera settings were adjusted so that the aggregate to be bleached was just below saturation. Aggregates were photobleached using 100% laser power at 488 nm for 2 to 5 iterations through the entire z-plane until they were at 35% of the original fluorescence intensity. Z-stack recovery images were recorded at a rate of one per minute for 60 minutes for FRAP recovery curves at long time scales. An imaging rate of 1 frame per 10 seconds was used for analysis of how individual puncta interact with aggregates and for characterizing aggregate formation events.

Results

A 588 amino acid N-terminal fragment of pathogenic human Htt reduces *Drosophila* lifespan: To explore pathogenic mechanisms in HD, we generated transgenic *Drosophila* that express 588 aa N-terminal fragments of human Htt with either a pathogenic polyQ tract of 138 repeats (HttQ138) or a non-pathogenic tract of 15 repeats (HttQ15). While several models of HD have focused on expression of the polyQ-containing first exon of Htt alone, the 588 amino acid fragment is truncated near a number of well-characterized caspase cleavage sites important in the generation of aggregate-forming Htt fragments (KIM *et al.* 2001; WELLINGTON *et al.* 2002). Additionally, many sites of protein interaction that are lost in exon 1 constructs are conserved in the longer 588 aa fragment, including a region of well-conserved HEAT repeats thought to be involved in Htt binding to interaction partners such as HIP1, HAP1, and HIP14 (HARJES and WANKER 2003). Htt was fluorescently tagged with mRFP or eGFP at the N-terminus, or tagged at both ends with eGFP at the N-terminus and mRFP at the C-terminus (Figure 1A). For

comparison, we generated a transgenic strain expressing exon 1 (81 aa) of the human Htt protein with a pathogenic 96Q repeat, fused to GFP at the C-terminus (HttQ96-GFP). All constructs were expressed using the UAS-GAL4 system, allowing for temporal and tissue-specific control of transgene expression. To confirm transgene expression, strains were crossed to the neuronal driver *elav*-GAL4 (C155), and Htt expression in offspring was assessed through Western blot analysis with anti-human Htt antibodies (Figure 1B). No Htt expression is detected in control *white* strains crossed to C155, while mRFP-Htt, eGFP-Htt, and HttQ96-GFP lines all demonstrate abundant Htt expression. As expected, the product detected in HttQ15 strains lacking the expanded polyQ tract is smaller than that in HttQ138 or HttQ96 strains. These transgenic lines allow imaging of Htt aggregation in live *Drosophila*, providing a resource for following Htt dynamics *in vivo*.

To determine the effects of pathogenic and non-pathogenic Htt expression in *Drosophila*, viability profiles were generated for control and HttQ138-expressing animals. Pan-neuronal expression of mRFP-HttQ138 with C155 causes pharate adult lethality with less than 1% viable adult escapers. Expression of pathogenic Htt with a weaker *elav*-GAL4 driver results in viable adults that appear behaviorally normal at the time of eclosion. However, several days after eclosion, these adults begin to exhibit motor coordination defects and abnormal grooming behaviors, worsening with age and resulting in premature death. Similar defects occur at a later time in a separate mRFP-HttQ138 insertion line (mRFP-HttQ138B) expressing pathogenic Htt at a lower level, as well as in flies expressing the pathogenic HttQ96-GFP exon 1 protein (Figure 1C). These behaviors are not observed in mRFP-HttQ15-expressing or control *Drosophila*. To quantify the reduction in viability of pathogenic Htt-expressing lines, lifespan curves were generated for control adults and adults expressing mRFP-HttQ15, mRFP-HttQ138, mRFP-

HttQ138B or HttQ96-GFP (Figure 1C). The T_{50} (age at which 50% of the culture has died) for mRFP-HttQ138 lines is dramatically decreased by over 70% in comparison to controls. mRFP-HttQ138B expression results in a 30% decrease in T_{50}, indicating that lethality is correlated with the level of expression of the pathogenic protein. HttQ96-GFP lines also demonstrate a decrease in T_{50} of 50%, suggesting that expression of the expanded polyQ-containing first exon of Htt is also toxic. Decreases in T_{50} for all lines expressing fragments of the pathogenic Htt protein, but not the normal protein, indicate that expression of pathogenic Htt results in behavioral dysfunction and reduced lifespan in *Drosophila*.

Pathogenic Htt forms cytoplasmic aggregates in neuronal and non-neuronal cells *in vivo*: A hallmark of HD is the formation of intracellular aggregates immunopositive for the pathogenic Htt protein. Aggregates have been found in the nucleus, cell body and neurites in HD (DiFiglia *et al.* 1997). However, it is unknown whether toxic Htt activity occurs in the nucleus, in the cytoplasm, or in both. To determine the intracellular distribution of our pathogenic and non-pathogenic transgenic Htt fragments, *Drosophila* S2 cells were transiently transfected with the mRFP-HttQ15 or mRFP-HttQ138 constructs and fixed cells were imaged by confocal microscopy. While mRFP-HttQ15 demonstrated diffuse cytoplasmic localization, mRFP-HttQ138 formed large, distinct cytoplasmic aggregates (Figure 2A). Neither protein localized to the nucleus.

To assess whether intracellular aggregates are formed *in vivo* by transgenic Htt proteins in *Drosophila*, UAS-mRFP-Htt strains were crossed to lines expressing the *elav*-GAL4 driver. As observed in S2 cells, the non-pathogenic mRFP-HttQ15 remained diffuse throughout the cytoplasm and neurites of neurons in both the CNS (Figure 2B) and PNS (Figure 2D). In contrast, distinct Htt aggregates were observed throughout the cytoplasm and neurites in lines

69

expressing the pathogenic mRFP-HttQ138 (Figure 2C, E). To observe subcellular localization in other cell types, mRFP-HttQ15 and mRFP-HttQ138 were driven with a ubiquitous GAL4 driver (*tubulin*-GAL4). In non-neuronal cells, including epidermis (Figure 2F) and salivary glands (Figure 2H), mRFP-HttQ15 localized diffusely in the cytoplasm, while mRFP-HttQ138 formed cytoplasmic aggregates (Figure 2G & I). Nuclear aggregates were not observed in any cell type. These results suggest Htt fragments induce pathology without apparent nuclear localization or formation of nuclear aggregates in our *Drosophila* model.

Mutant Htt causes defects in salivary gland glue secretion in *Drosophila*: To determine whether HttQ138 expression might cause defects in non-neuronal tissues, we tested whether Htt expression in larval salivary glands causes cellular dysfunction. We analyzed secretion of the GFP-tagged salivary gland glue protein Sgs3 (BIYASHEVA *et al.* 2001) in controls and animals expressing mRFP-HttQ15 or mRFP-HttQ138 (Figure 3). During normal pupariation, *Drosophila* secretes ecdysteriod-induced glue granules that mediate attachment of the developing pupal case to surfaces. While glue secretion is evident in both control and mRFP-HttQ15-expressing pupae (Figure 3A, B), secretion is decreased in pupae expressing mRFP-HttQ138 (Figure 3C). Normal third instar larval salivary gland cells are filled with glue proteins (Figure 3D) that are depleted during pupariation (Figure 3E). In contrast, the pupal salivary glands of mRFP-HttQ138-expressing larvae retain glue (Figure 3G), suggesting salivary gland dysfunction mediated by the cytoplasmic accumulation of mutant Htt.

The 588 aa fragment of pathogenic human Htt does not produce nuclear cleavage products in *Drosophila*: Mutant forms of Htt have been reported to undergo cleavage by caspases and calpains to generate smaller N-terminal fragments that can be observed in the nucleus and cytoplasm (GAFNI *et al.* 2004; KIM *et al.* 2001; LUNKES *et al.* 2002; WELLINGTON *et al.* 2002).

To determine whether cleavage of the N-terminal 588 aa of Htt occurs in our *Drosophila* model to generate smaller fragments that might localize to the nucleus, S2 cells were transiently transfected with 588 aa Htt constructs labeled with eGFP at the N-terminus and mRFP at the C-terminus. Complete co-localization of the eGFP and mRFP signals is seen for both the normal eGFP-HttQ15-mRFP fragment (Figure 4A), and the pathogenic eGFP-HttQ138-mRFP fragment (Figure 4B), suggesting that cleavage of the proteins does not occur in the context of *Drosophila* S2 cells, or alternatively, that any cleaved N- and C-terminal fragments of Htt remain colocalized in the cytoplasm.

To assess whether cleavage and separation of N- and C-terminal fragments of Htt occur *in vivo*, we generated transgenic strains expressing the double-labeled pathogenic Htt fragment eGFP-HttQ138-mRFP. As observed in the S2 cell model, eGFP and mRFP signals co-localized in all tissues studied, including CNS neurons (Figure 4C), salivary gland cells (Figure 4D), and epidermal cells (Figure 4E), suggesting that the pathogenic Htt protein is unlikely to be cleaved *in vivo* in *Drosophila*. Neither N- nor C- terminal fragments of Htt are observed in the nucleus. To further test if cleavage occurs *in vivo*, we performed western analysis with anti-Htt antibodies to probe for breakdown products that would result from cleavage of the protein. As shown in Figure 4F, no differential cleavage products were observed by western analysis in head extracts prepared from animals expressing HttQ138-mRFP versus eGFP-HttQ138-mRFP animals. Thus, the pathogenic Htt-mediated toxicity seen in our *Drosophila* HD model does not appear to require Htt cleavage or nuclear entry, and reflects an effect of the 588 aa fragment in the cytoplasm.

Exon 1 of pathogenic Htt forms cytoplasmic and neuritic aggregates: Many classic HD models express exon 1 of the mutant protein (DAVIES *et al.* 1997; JACKSON *et al.* 1998;

KROBITSCH and LINDQUIST 2000; TAGAWA *et al.* 2004), which is capable of forming inclusions postulated to play a role in HD pathology (BECHER *et al.* 1998; DAVIES *et al.* 1997). To determine whether the *in vivo* subcellular localization of the 81 aa exon 1 fragment of pathogenic human Htt (HttQ96-GFP) differs from that of the 588 aa pathogenic Htt fragment in our *Drosophila* model, HttQ96-GFP-expressing 3rd instar larvae were imaged using confocal microscopy. In both neuronal and non-neuronal cell types, HttQ96-GFP formed distinct cytoplasmic aggregates similar in appearance and localization to those formed by the 588 aa mRFP-HttQ138 protein. GFP-labeled aggregates are found in the cytoplasm of salivary gland cells (Figure 5B) and CNS (Figure 5D) and PNS (Figure 5G) neurons, while no aggregates are observed with expression of a UAS-GFP construct alone (Figure 5A, C, F). As observed with the 588 aa fragment, the exon 1 fragment also forms aggregates in axons (Figure 5E) and localizes at nerve terminals. The non-nuclear localization of both 588 aa and 81 aa pathogenic Htt fragments indicates that the neurodegenerative effects induced by these toxic Htt forms are independent of Htt nuclear entry in *Drosophila*. In addition, targeting sequences in exon 1 of Htt are sufficient to localize the protein to neurites in our model.

Kinetics of HttQ138 aggregate formation: To examine how aggregates form in our model, we visualized mRFP-HttQ138 dynamics in live larvae. We expressed mRFP-HttQ138 using *CCAP-GAL4* that expresses in a single neuron per hemisegment (PARK *et al.* 2003; VOMEL and WEGENER 2007). This driver allows single cell resolution to determine how HttQ138 interacts with larger aggregates. Time-lapse confocal imaging of photobleached aggregates in 3rd instar larval motor neurons expressing mRFP-HttQ138 demonstrate that these aggregates are immobile over a 1 hour imaging session. FRAP analysis reveals that large HttQ138 positive aggregates continually add new HttQ138 particles, with a 40% recovery of original fluorescence within 50

minutes (Figure 6A, 6C, Supplemental Movie 1). Two general types of recovery were observed. Larger HttQ138 aggregates tended to recover more quickly by trapping Htt particles (right-most aggregate in Supplemental Movie 1). A second class of aggregates recovered more slowly and displayed a more gradual and uniform increase in brightness (left three aggregates in Supplemental Movie 1). To determine if the rapid FRAP in axons was due to increased local concentration of HttQ138 mediated by delivery of new particles by FAT, we compared FRAP rates of aggregates in axons with constant HttQ138 flux to that in neuronal cell bodies aggregates where HttQ138 movement is dictated largely by diffusion. We did not observe a significant difference in aggregation kinetics in these two compartments, indicating axonal aggregation is not strictly dependent on FAT (Figure 6B).

We next examined the kinetics of HttQ138 aggregate formation in our model *in vivo*. During our time-lapse imaging sessions in 3rd instar larvae we did not visualize any new aggregates forming. We attempted to visualize aggregate formation in younger animals, but numerous aggregates were already present at the 1st instar larval stage. It appeared that aggregates formed early in development grew, but that new aggregates rarely formed in the presence of preexisting aggregates. To bypass this problem, we used the temperature-sensitive GAL80 repressor to restrict expression of mRFP-HttQ138 through the 2nd instar stage. Expression of mRFP-HttQ138 with the *CCAP*-GAL4 driver was repressed by GAL80^{ts} at 18°C until the larvae reached the 3rd instar stage. We then turned on HttQ138 expression by shifting animals to the GAL80^{ts} restrictive temperate of 30°C. Two hours after induction of expression, a low level of diffuse mRFP-HttQ138 was observed in the salivary gland. By four hours, small Htt aggregates were observed forming in the salivary gland (Figure 7). After eight hours of expression, diffuse mRFP-HttQ138 was seen in neuronal cell bodies in the ventral nerve cord, as well as in the

proximal regions of axons. By 12 hours, aggregates were seen forming in axons and cell bodies, while salivary gland aggregates increased in size. During the window from 12-24 hours after induction, aggregates became larger and more numerous (Figure 7). Beyond 12 hours post-induction, HttQ138 aggregates began growing in size rather than number. The increase in aggregated mRFP-HttQ138 was accompanied by a decrease in the soluble fraction of the protein. We also examined the effectiveness of reducing aggregation by turning off expression of the mRFP-HttQ138 transgene after aggregates had formed, assaying if cells had the ability to remove aggregates without new HttQ138 expression. After a 24-hour pulse of mRFP-HttQ138 followed by 72 hours of recovery, we observed a reduction in the size and number of aggregates present in all tissues analyzed (data not shown), suggesting reducing pathogenic Htt expression may have beneficial effects in adults. We conclude that new aggregates can form in neurons within a 12-hour time frame, while pre-existing aggregates rapidly accumulate new HttQ138 protein within minutes.

mRFP-HttQ138 induced lethality can be rescued by heterozygous disruption of single loci: To further define the role of aggregation in HD pathology, we performed forward genetic screens for suppressors of HttQ138-induced lethality or suppressors of HttQ138 aggregation. For the first screen to identify lethality suppressors, we employed a dominant suppressor strategy with the *Drosophila* autosomal deficiency (Df) set to identify chromosomal regions containing loci that could dominantly rescue mRFP-HttQ138-induced lethality. We reasoned that loci identified in a haplo-insufficiency screen might represent attractive targets for ameliorating HD pathology, as a 50% decrease in protein activity might be accomplished with fewer side effects and require only partial reduction of the protein's function through pharmacological approaches. We obtained the Df kit for chromosomes II and III from the Bloomington Stock Center, which contains 160 Df

lines that cover ~80% of the *Drosophila* genome. We crossed Df/Balancer males to females carrying the *elav*-GAL4 driver homozygous on the X chromosome (C155) and a marked Balancer, with *CyO* for the 2nd chromosome and *Sb* or *Hu* for the 3rd chromosome. F1 C155/y; Df/Bal offspring were then mated to homozygous mRFP-HttQ138 high expression females. Under normal conditions, expression of mRFP-HttQ138 driven by C155 caused pharate adult lethality. We screened for Dfs that rescued this lethality, comparing the number of adult females expressing mRFP-HttQ138 to males not expressing the HttQ138 transgene. Deficiencies that dominantly increased the ratio of mRFP-HttQ138 expressing females by 10-fold (Female/Male ratio = 0.1) were identified as hits. We identified 11 large Dfs, each removing ~100 genes, which suppressed HttQ138-induced lethality, indicating the presence of multiple potential targets that can modify HttQ138 toxicity in a dominant manner (Figure 8A). Ten out of eleven deletions gave a partial rescue of viability, increasing the number of escapers to ~20-30% of that expected for a full rescue. The viable animals displayed several motor defects, as they were unable to climb the walls of the vials or mate, and most died within several days of eclosion, indicating partial rescue. One of the 11 large deletions, *Df(3L)vin7* showed a near complete rescue of viability at eclosion. C155; *Df(3L)vin7*/mRFP-HttQ138 animals showed less severe motor defects than other rescuing Dfs, but were unable to climb the vial walls and lived ~10 days post-eclosion.

Reduction of HttQ138 expression and aggregation increases viability in mRFP-HttQ138 expressing *Drosophila*: In addition to the viability screen, we conducted a deficiency screen for suppressors of aggregation. The same mating scheme was used in both screens. However the aggregation screen used the lower expression adult-viable mRFP-HttQ138B insert, instead of the

pharate lethal high expression mRFP-HttQ138 line. We reasoned the lower expression line

would represent a more sensitized system to identify potentially weak aggregation suppressors

that might not be found in strong expression strains. Live wandering 3rd instar larvae expressing

mRFP-HttQ138 with C155 and heterozygous for each Df were screened under a fluorescent

microscope for changes in aggregation. We focused on Htt aggregation within the salivary gland,

as these large cells were easily visualized in live animals. We screened for changes in size,

density or brightness of peri-nuclear mRFP-Htt salivary gland aggregates. Four large deletions

(*Df(2R)59AD, Df(2R)AA21, Df(2R)cn9* and *Df(3L)vin7*) caused a reduction in aggregate density

in the salivary gland (Figure 8B-F). Interestingly, each of these aggregation suppressors was

independently identified in the viability screen. Thus, reducing aggregation in our screen was

always associated with increased viability. We did not identify any hits that reduced aggregation

without increasing viability, suggesting that aggregates may represent a toxic species in this

model. While *Df(2R)59AD* reduced the density and size of salivary gland aggregates, *Df(2R)cn9*,

Df(3L)vin7 and *Df(2R)AA21* were most effective in reducing aggregation, with the mRFP-Htt

Q138 pattern appearing as diffuse as the nonpathogenic mRFP-HttQ15. We attempted finer

mapping for each larger Df to define the smallest relevant genetic interval. We were able to map

the *Df(2R)59AD* interval to a region uncovered by *Df(2R)59AB*, which deletes ~ 20 genes. The

larger *Df(2R)cn9* was subdivided to a critical region uncovered by *Df(2R)sple-J1*, which removes

~39 genes.

To determine whether the suppression of aggregation was associated with a change in mRFP-

HttQ138 expression, we quantified western blots of flies expressing mRFP-HttQ138 with C155

in the Df background (Figure 9A, B). As a control for UAS-GAL4 transgene regulation, we also

quantified expression of UAS-CD8-GFP in the Df backgrounds (Figure 9C). All four

deletions that reduced aggregation resulted in reduced mRFP-HttQ138 and CD8-GFP protein

expression. However, two single gene suppressors (*lab*[14], PBc02324 – see below) had no effect

on salivary gland aggregation or transgenic protein expression by Western analysis. To further

characterize the effect the suppressors have on transgene expression, we measured HttQ138

mRNA levels using semi-quantitative RT-PCR. Despite showing vastly different effects on

protein level, all Dfs decreased HttQ138 mRNA levels. These results are consistent with the

observation that Htt aggregation is strongly influenced by the protein expression, and that

toxicity in our model correlates with HttQ138 expression level (Figure 1C).

We next determined whether the reduction in salivary gland HttQ138 aggregates and suppression

of lethality by these Dfs also resulted in alteration in the subcellular distribution or density of Htt

aggregates in peripheral nerves. Htt aggregates in axons have been suggested to cause axonal

transport defects and contribute to HD pathogenesis (GUNAWARDENA *et al.* 2003; LEE *et al.*

2004; LI *et al.* 1999; LI *et al.* 2001). We found a significant ($p < 0.05$) decrease in the number of

mRFP-HttQ138 aggregates >1uM diameter in axons in the *Df(3L)vin7* background, but no

change in the other Dfs (Figure 10). Interestingly, *Df(3L)vin7* had the strongest effect on

suppressing lethality (Supplemental Table 1) and improving motor performance in HttQ138

expressing animals. We also analyzed Syt-1 distribution along axons, which we have previously

observed to co-aggregate with Htt in axonal aggregations (LEE *et al.* 2004), while remaining

diffuse in axons from controls or HttQ15-expressing animals. Abnormal aggregation of Syt-1

was still observed in the rescued animals (Figure 10A-G), indicating that although the Dfs

reduced aggregation in salivary glands and suppressed lethality, they did not display a strong

suppression of axonal transport defects in HttQ138 expressing animals. The differences in

HttQ138 mRNA levels versus HttQ138 aggregates also suggest that subtle changes in transcript

level can have a dramatic effect on the concentration reached within a cell that is required to trigger aggregation.

Mapping of suppressors of HttQ138-induced lethality: To begin identifying loci that underlie suppression of HttQ138-induced phenotypes, we attempted finer mapping of hits from the viability and aggregation screen by testing smaller and overlapping Dfs within these regions using stocks available from the Bloomington stock center. In many cases, coverage across the original Df region was not sufficient to map suppression to individual loci. It is also possible that the ability of some Dfs to suppress toxicity may have resulted from additive effects of haplo-insufficiency for several genes within the deleted region. However, we were able to successfully refine three of the original 11 large deletions to two individual loci. The large Df suppressors *Df(3L)st-f13* and *Df(3L)brm11* overlapped a 43-gene region from 72C1-72D5. *Df(3L)ED220* further refined the area to 72C1-72D4, a 20-gene interval with mutant stocks available for 12 predicted loci (Supplemental Table 2). We tested the 12 lines and observed that stock 10887 was the only one that rescued HttQ138 expressing animals at greater than the 10% expected ratio. Line 10887 (PBc02324) is a *piggyBac* transposable element insertion into the 5' region between two genes, CG5830 and *mRpS31*. RT-PCR of line 10887 revealed that CG5830 is downregulated 2-fold and *mRpS31* is not significantly affected by the insertion. CG5830 is 60% identical to mammalian CTD phosphatases, which function in silencing neuronal gene expression. The repressor element 1/neuron-restrictive silencer element (REST) transcription repressor family is essential for neuronal gene silencing and has been linked to HD (RIGAMONTI *et al.* 2009).

The remaining interval we were able to refine to a single mutation was *Df(3R)Tpl10*, which deletes the 83C1-84B2 region and uncovers 173 genes. Screening other Dfs in this region revealed that *Df(3R)MAP117* and *Df(3R)MAP2* significantly rescued viability of HttQ138

expressing animals. These Dfs overlap the 84A1 to 84A5 interval, which contains 47 genes with 18 stocks available that disrupt loci within. We tested these strains and found that stock 2092 rescued mRFP-HttQ138 induced lethality, increasing the expected adult viability ratio to 24% versus 0% in strains expressing HttQ138 alone. Stock 2092 is an x-ray induced amorphic mutant (lab^{14}) of the *labial* gene. *Labial* is one of eight homeobox genes in the Antennapedia cluster that plays critical developmental roles in anterior-posterior body axis specification (BRODY 1999). To determine if other members of the Antennapedia HOX complex could also suppress HD pathology in our model, we tested mutations in additional members of the Antennapedia cluster for their ability to rescue HttQ138-induced lethality. Haplo-insufficiency for mutations in *Sex combs reduced* (Scr^{CP1} – 22% viability ratio; Scr^6 -24% viability ratio), *proboscopedia* (pr^1 – 22% viability ratio), *Deformed* (Dfd^6 - 15% viability ratio) and *Ultrabithorax* (Ubx^{51} - 12% viability ratio) resulted in a significant rescue of HttQ138-induced lethality, suggesting a link between abnormal homeotic transcription factor activity and HD pathology.

Both aggregated and soluble HttQ138 likely represent toxic species: By comparing the relative contributions of decreased aggregation and decreased soluble HttQ138 measured experimentally to increased lifespan, we observed a general trend whereby decreasing Htt expression causes a decrease in aggregation and increase in viability (Figure 10). However, two suppressors uncovered in the screen show a large increase in viability without a significant change in aggregation in peripheral motor axons (*Df(2R)59AB, Df(2R)sple-j1*, Figure 10). mRFP-HttQ138 expression in these backgrounds is decreased by Western analysis and RT-PCR, but there is no significant change in the number of aggregates in the axon (Figure 8C, E). Additionally, *Pbc020324* and lab^{14} show increased lifespan over controls without a significant change in aggregation in any cell type, though the increase in lifespan is modest. These

suppressor backgrounds demonstrate that increased viability can be achieved independent of decreased aggregated HttQ138. In these lines, the increase in lifespan is correlated with a decrease in soluble HttQ138, arguing that this form of HttQ138 may also be contributing to toxicity in our model.

Discussion

Many neurodegenerative diseases associated with protein misfolding have been modeled in *Drosophila*, including Parkinson's disease (FEANY and BENDER 2000), Alzheimer's disease (WITTMANN *et al.* 2001), spinocerebeller ataxia type 1 (FERNANDEZ-FUNEZ *et al.* 2000) and type 3 (WARRICK *et al.* 1999) and Huntington's disease (GUNAWARDENA *et al.* 2003; JACKSON *et al.* 1998; LEE *et al.* 2004; STEFFAN *et al.* 2001). These models replicate many neuropathological features characteristic of the diseases, such as late onset, progressive neurodegeneration, and formation of inclusions containing the mutant protein. A strength of *Drosophila* disease models is the ability to perform second-site modifier screens to identify molecular pathways that lead to neurodegeneration, facilitating the discovery of new targets for potential therapeutic intervention. Here we describe the generation of a new *Drosophila* HD model in which expression of a 588 aa N-terminal fragment of human Htt containing a 138 polyQ tract results in pharate adult lethality, enabling us to perform large-scale screens for genetic suppressors of the lethal phenotype. By engineering a fluorescent tag on the mutant Htt fragment, we are also able to visualize the location, trafficking and aggregation of Htt in both neuronal and non-neuronal cells in live *Drosophila*. As such, we were able to screen independently for suppressors of Htt aggregation by following HttQ138-mRFP localization in live animals. The screens resulted in the identification of seven large Dfs uncovering genomic regions that are capable of suppressing Htt-induced lethality without altering HttQ138 aggregate formation, and four additional Dfs that suppressed

both Htt-induced lethality and HttQ138 aggregation. Our findings indicate the presence of gene products downstream, or independent, of aggregation that can dominantly reduce HD toxicity. Our results also indicate that expression levels of mutant Htt are critical for disease pathology, as all Dfs we identified that reduced Htt expression levels by ~50% increased viability. As such, targeted approaches that reduce mutant Htt expression by relatively modest amounts may have profound effects on toxicity in HD patients.

The ability to follow Htt dynamics in live animals using our fluorescently-tagged HttQ15 and HttQ138 transgenes has revealed several important aspects of our *Drosophila* HD model. We find that both pathogenic and nonpathogenic versions of Htt are localized specifically to the cytoplasm of all cell types examined. In humans, cleavage of Htt is thought to be important in generation of toxic Htt fragments (QIN and GU 2004), with several studies indicating that small cleaved N-terminal fragments enter the nucleus to form intranuclear inclusions that contribute to pathogenesis (DIFIGLIA *et al.* 1997; SIERADZAN *et al.* 1999). Although evidence suggests that intranuclear aggregates can contribute to HD pathology (BECHER *et al.* 1998; DAVIES *et al.* 1997), several studies indicate that pathogenic Htt aggregates in the cytoplasm and neurites may play a causative role (LI *et al.* 1999; SAPP *et al.* 1999). As such, where toxic Htt fragments responsible for HD pathology reside in neurons remains to be conclusively identified. Using Htt fragments that were tagged at the N-terminus with GFP and at the C-terminus with mRFP, we demonstrate that cleavage of Htt does not occur in *Drosophila*. In addition, expression of a smaller Htt Exon 1 fragment still localizes specifically to the cytoplasm. Pathology in our HD model thus occurs secondary to cytoplasmic polyQ Htt localization, with no evidence for nuclear localization.

To characterize the kinetics of Htt aggregation, we used live imaging of fluorescently tagged mRFP-HttQ138. Several studies indicate mutant Htt can disrupt FAT (GUNAWARDENA *et al.* 2003; LEE *et al.* 2004; SZEBENYI *et al.* 2003), but the mechanism by which defects occur is unclear. Since Htt is selectively toxic to neurons, an attractive model is that disrupted FAT may confer toxicity due to transport defects. Our FRAP data suggests that while large immobile aggregates do acquire new HttQ138 puncta, they may not represent a complete block in transport, as some particles were observed to bypass aggregates. We determined the rate of FRAP recovery within aggregates was the same in both axons and the cell body, suggesting that aggregation kinetics are not dependent on the higher local concentrations of Htt induced by FAT. We took advantage of the Gal80^{ts} repressor to view early events in aggregate formation and visualize the aggregation progression. We observed that soluble HttQ138 forms aggregates that grow in size over a 12-hour window, decreasing the amount of soluble Htt present in the cell. Incorporation of HttQ138 into pre-existing aggregates was much faster, suggesting once aggregates are formed, they represent an active sink for accumulating new Htt protein.

A key question in the HD field is whether Htt aggregates are toxic, neuro-protective or simply byproducts of the disease process. This issue is of critical importance for therapeutic considerations, as many current efforts are aimed at reducing Htt aggregation, assuming that this will decrease toxicity. Our previous observations that Htt aggregates accumulate in axons and impede axonal transport (LEE *et al.* 2004) support a model in which axonally localized aggregates are neurotoxic. Whether aggregates in other cellular compartments cause toxicity is still an open question. The ability of drugs like Congo Red (HEISER *et al.* 2000; SANCHEZ *et al.* 2003), minocycline (CHEN *et al.* 2000; SMITH *et al.* 2003), and the transglutaminase inhibitor cystamine (DEDEOGLU *et al.* 2002) to block Htt aggregation and reduce behavioral phenotypes in

R6/2 Htt polyQ mice is suggestive of aggregate toxicity as well. Molecular (CUMMINGS *et al.* 2001; FERNANDEZ-FUNEZ *et al.* 2000; JANA *et al.* 2000; VACHER *et al.* 2005; WARRICK *et al.* 1999) and chemical (YOSHIDA *et al.* 2002) chaperones that reduce aggregate formation have been shown to reduce cytotoxicity in several polyQ disease models. Likewise, intracellular antibodies (COLBY *et al.* 2004; KHOSHNAN *et al.* 2002; LECERF *et al.* 2001; WOLFGANG *et al.* 2005) that bind mutant Htt epitopes and suppress aggregate formation provide some neuroprotection in animal models. Our genetic screens support a model where aggregate formation and soluble Htt (monomers or oligomers) contribute to toxicity, as every Df which reduced aggregation and/or soluble Htt levels showed an increase in viability. The observation that we did not identify any haplo-insufficient loci capable of reducing aggregation without altering Htt expression levels suggests that aggregation inhibition may require more potent pharmacological effects than can be achieved with only a 50% reduction in activity of a single protein. In contrast, the finding that *Df(2R)spleJ1* and *Df(2R)59AB* increase viability without changes in aggregation suggests that HttQ138 toxicity can be reduced without altering Htt aggregation.

Although neuronal toxicity associated with Htt polyQ expansion has been the emphasis of most HD studies, the Htt protein is expressed in many nonneuronal tissues, including testes, liver, heart, lungs, and pancreatic islets (CATTANEO *et al.* 2005; FERRANTE *et al.* 1997). HD patients have been shown to have a higher risk of diabetes (LALIC *et al.* 2008), and mouse HD models show pancreatic pathology (MARTIN *et al.* 2008) indicating that Htt polyQ expansion may also cause defects in non-neuronal cells. We found that HttQ138 expression in Drosophila salivary glands results in defective glue secretion (Figure 3), suggesting that non-neuronal defects from HttQ138 expression exist in our model as well. The ease with which the Sgs3-GFP glue secretion

assay can be performed opens up the possibility of additional screens for second-site suppressors that alleviate salivary gland dysfunction in HttQ138 expressing animals. It is currently unclear whether salivary cell Htt aggregates induce pathology, or whether they are secondary to other defective secretion mechanisms. Htt is associated with numerous organelles, including the Golgi, ER, clathrin-coated vesicles, synaptic vesicles and endosomal vesicles (HOFFNER *et al.* 2002; KEGEL *et al.* 2002; VELIER *et al.* 1998). In addition, Htt interacts with numerous vesicle trafficking proteins, including dynamin, huntingtin-interacting protein 1 (HIP1), and huntingtin-associated protein1 (HAP1), which binds the p150glued subunit of dynactin (LI *et al.* 1998). Potential defects in vesicle trafficking or fusion may thus account for the defects observed in glue secretion.

The results from our haplo-insufficiency screen provide several clues regarding the role of soluble and aggregated forms of Htt and their contribution to toxicity, but no clear information about cellular pathways disrupted by HD. We mapped the suppression mediated by three large Dfs down to two single genes. One of our hits was a *piggyBac* insertion in strain PBc020324 in the small 5' interval between CG5830 and *mRpS3,* which reduces CG5830 expression. CG5830 encodes a phosphatase with sequence homology to small CTD phosphatases that function in silencing neuronal gene expression (YEO *et al.* 2005). Disruption of neurotrophic factor expression, especially BDNF through aberrant function of its transcriptional repressor REST/NRSF, has been implicated in HD (ZUCCATO *et al.* 2001; ZUCCATO *et al.* 2003). Increased REST/NFSF activity is also evident in postmortem HD human brains (ZUCCATO and CATTANEO 2007). It will be important to test whether previously identified *Drosophila* neurotrophic proteins (ZHU *et al.* 2008) are disregulated in mRFP-HttQ138 expressing animals, and whether haplo-insufficiency of CG5830 reduces this effect. Although Pbc020324 is likely rescuing toxicity in

part by reducing Htt transgene expression, we did not observe any decrease in HttQ138 protein levels by Western blot, or any decrease in HttQ138 aggregation in tissues. This discrepancy between the reduced transcription and actual Htt protein levels suggests CG5830 may have other neuroprotective effects as well.

The other single gene we mapped, *Labial* is a member of the ANTP complex, and has been linked to neural stem cell survival during postembryonic neurogenesis in *Drosophila* (BELLO *et al.* 2007). Mutant Htt has been implicated in transcriptional dysregulation of a broad range of genes, reducing levels of highly pleiotropic proteins like RNA polymerase II (LUTHI-CARTER *et al.* 2002), and facilitating expression in mice of polycomb repressive complex 2, which specifically regulates HOX gene expression (SEONG *et al.*). Htt has also been linked to HOX gene regulation through the polyQ and polyproline regions shared between Htt and several transcriptional regulators, including *Sex combs reduced* (GERBER *et al.* 1994). Similar to Pbc020324, this mutation decreases Htt transgene transcription, but has no effect on aggregation. An intriguing hypothesis suggested by microarray analysis from Htt-polyQ expressing brains in *Drosophila* (Lee and Littleton, unpublished data) is that ANTP genes are upregulated in HD and contribute to neuropathology. Several Hox genes, including *labial*, *proboscipedia,* and *Sex combs reduced* were increased in Htt-polyQ brains, suggesting that haplo-insufficiency for these loci might function to reduce Htt expression to a less toxic level. Further studies will be needed to dissect this link between the homeotic genes and HD pathology.

Examining the pattern by which suppressor mutations interact with HttQ138 provides insight into the role of aggregates in toxicity. The weakest suppressors had no alteration in aggregation or HttQ138 expression, suggesting some minor rescue is possible without disrupting aggregation.
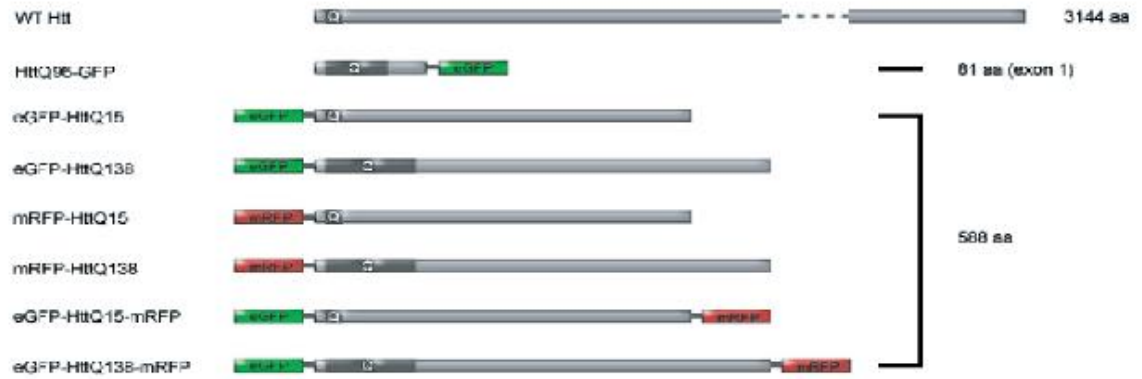
A larger increase in viability occurs with decreased expression of HttQ138, but little to no change in aggregated Htt, suggesting that soluble HttQ138 is a toxic species in these cases. The final group of suppressors increased viability even more, while decreasing both soluble and aggregated Htt. In summary, we have generated a new HD model in *Drosophila* that allows for *in vivo* analysis of pathogenic Htt localization, aggregation and dynamics. Using this model, we identified several genetic suppressors that can reduce HttQ138-mediated toxicity. The most robust suppressors reduced both soluble and aggregated Htt levels, suggesting toxicity is likely to be associated with both forms of the mutant protein.

Acknowledgments

Figure 1

A

WT Htt	3144 aa
HttQ96-GFP	81 aa (exon 1)
eGFP-HttQ15	
eGFP-HttQ138	
mRFP-HttQ15	588 aa
mRFP-HttQ138	
eGFP-HttQ15-mRFP	
eGFP-HttQ138-mRFP	

B

150 kD •
100 kD •
75 kD •

HttQ138
HttQ15

WT, eGFP-HttQ15, eGFP-HttQ138, mRFP-HttQ15, mRFP-HttQ138

90 kD •
50.7 kD •

HttQ96
Loading Control

WT, HttQ96-GFP

C

— white
— mRFP-HttQ15
— mRFP-HttQ138
— mRFP-HttQ138B
— HttQ96-GFP

% Viable
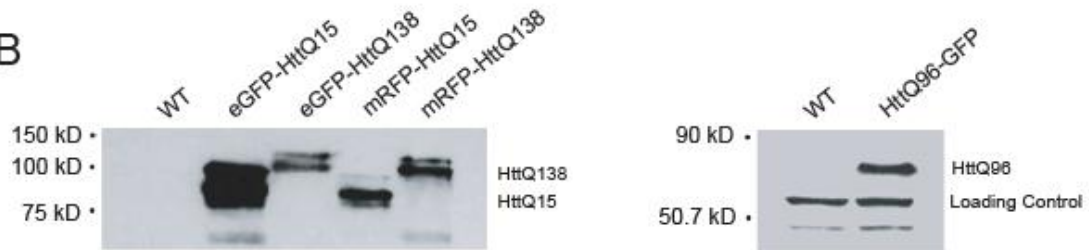
Days at 29°C

Figure 1. Generation of *Drosophila* transgenic models of HD. (A) The N-terminal fragments of human Htt used for transgenic construction are shown. PolyQ tracts and fluorescent tags (mRFP, eGFP) are indicated. The full-sized Htt protein is depicted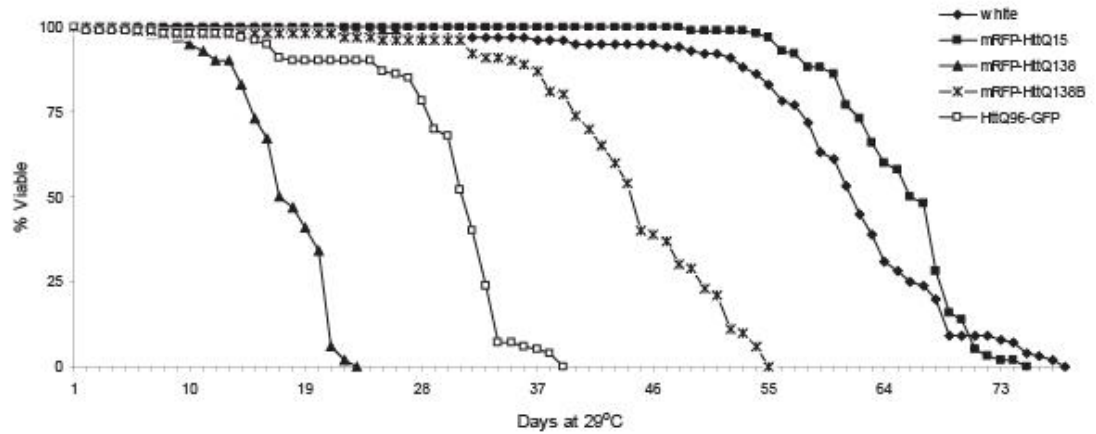 for comparison. (B) Expression of Htt in control, mRFP-Htt, eGFP-Htt, and HttQ96-GFP strains with transgene expression driven by C155. Western blotting was performed with an antibody to the N-terminus of human Htt (mRFP-Htt and eGFP-Htt blot – left panel) or an antibody to GFP (HttQ96-GFP blot – right panel). (C) Reduced viability of transgenic strains expressing mutant Htt with a weaker *elav*-GAL4 driver. T_{50} is decreased by over 70% in strains expressing mRFP-HttQ138, 30% in strains expressing mRFP-HttQ138B (a lower expression strain), and 50% in strains expressing HttQ96-GFP, in comparison to control white flies crossed to the same driver.
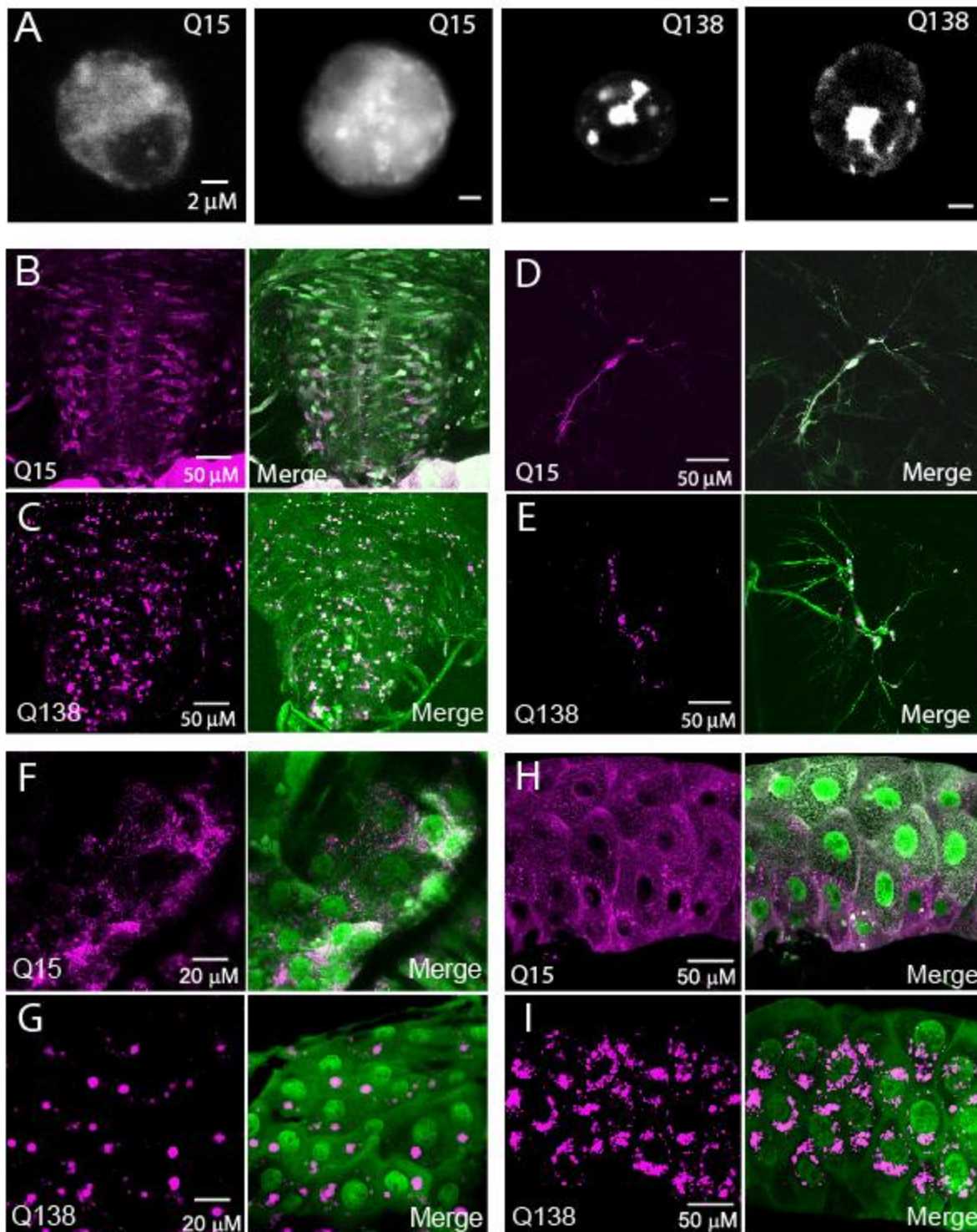
Figure 2

Figure 2. Cytoplasmic aggregation of mRFP-HttQ138 in neuronal and non-neuronal tissues. (A) Htt localization in *Drosophila* S2 cells transiently transfected with mRFP-HttQ15 or mRFP-HttQ138. mRFP-HttQ15 is found diffusely throughout the cytoplasm, while mRFP-HttQ138 forms cytoplasmic aggregates. The scale bar is 2 μm for each panel. (B) Visualization of mRFP-HttQ15 (magenta) and GFP with a nuclear localization signal (nls) (green) in 3rd instar larvae with transgene expression driven by the C155. mRFP-HttQ15 is diffusely localized in the cytoplasm of CNS neurons in the ventral nerve cord. (C) Visualization of mRFP-HttQ138 (magenta) and GFP-nls (green) in CNS neurons of 3rd instar larvae with transgene expression driven by C155. Unlike mRFP-HttQ15, mRFP-HttQ138 forms cytoplasmic aggregates throughout the cell bodies of ventral nerve cord neurons. (D, E) Visualization of mRFP-Htt in peripheral MD neurons. While mRFP-HttQ15 exhibits diffuse cytoplasmic localization, mRFP-HttQ138 is found in cytoplasmic aggregates throughout the cell body and neurites. (F-I) Expression of mRFP-Htt (magenta) and GFP-nls (green) driven by the *tubP*-GAL4 driver in the epidermis (F, G) and salivary gland (H, I). In all cases, mRFP-HttQ15 is diffuse throughout the cytoplasm, while mRFP-HttQ138 forms cytoplasmic aggregates.
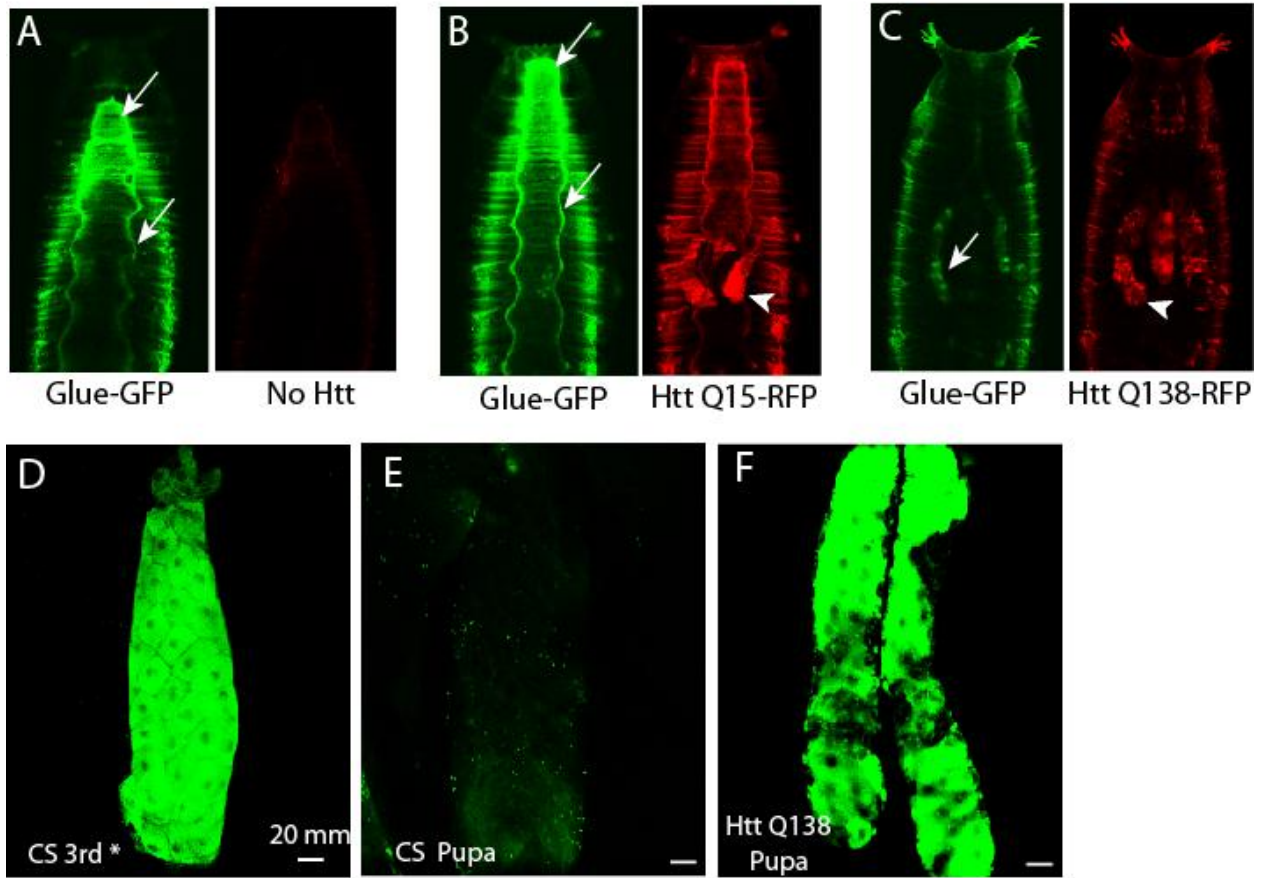
Figure 3

Glue-GFP   No Htt   Glue-GFP   Htt Q15-RFP   Glue-GFP   Htt Q138-RFP

Figure 3. Salivary gland glue secretion is defective in *Drosophila* expressing mRFP-HttQ138. (A) Pupa were removed from vials of CS (A), Htt-Q15 (B) or HttQ138 (C) animals expressing the Sgs3 GFP-tagged glue protein. Confocal images of Sgs3-GFP fluorescence is shown in the left panels and mRFP-Htt fluorescence in the right panel. (A) The Sgs3-GFP glue protein can be readily seen in the left panel lining the exterior surface of the pupal case (arrows) following secretion from salivary glands. CS animals do not express Htt-mRFP, with only minor autofluorescence visible in the red channel (right panel). (B) Glue secretion (arrows) is not disrupted in pupae that express mRFP-HttQ15, which localizes diffusely in the salivary gland (arrowhead). (C) Glue secretion is decreased in pupae expressing mRFP-HttQ138, with the Sgs3-GFP protein largely retained in salivary glands (arrows). Aggregation of mRFP-HttQ138 in the pupal salivary glands is noted by the arrowhead in the right panel. (D) Sgs3-GFP is abundant in CS third instar larval salivary glands before pupation, and depleted from salivary glands following secretion during pupation (E). (F) Sgs3-GFP is retained in pupal salivary glands of mRFP-HttQ138-expressing animals. Scale bar is 20 μm in each panel.

Figure 4
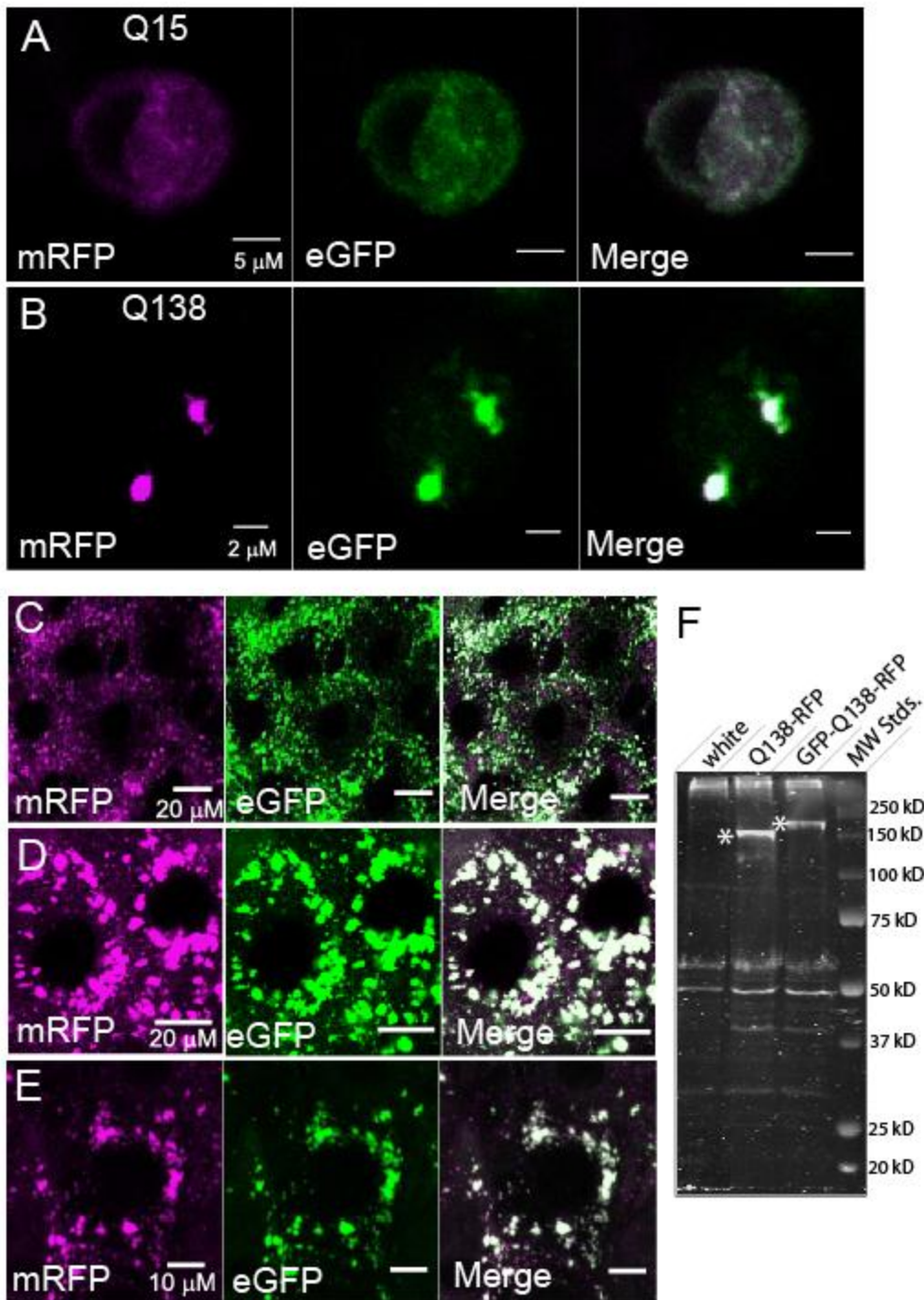
Figure 4. The 588 aa fragment of mutant human Htt does not undergo cleavage in *Drosophila*. (A, B) Transient transfection of *Drosophila* S2 cells with eGFP-HttQ15-mRFP (A) or eGFP-HttQ138-mRFP (B) demonstrates no separation of eGFP (green) and mRFP (magenta) signals, suggesting that the mutant Htt protein does not undergo cleavage in S2 cells. (C-E) Visualization of signal localization in 3rd instar larvae with expression of eGFP-HttQ138-mRFP driven by the C155 shows no separation of eGFP (green) and mRFP (magenta) signals CNS neurons (C), salivary gland cells (D), or epidermal cells (E). (F) Western analysis of brain extracts from control *white* animals, and animals expressing Q138-mRFP or eGFP-Q138-mRFP, showing expression of the Htt protein (asterisk). Immunoblotting with anti-Htt antibodies reveals no breakdown products in the double-labeled strain compared to single-labeled lines or control animals that do not express Htt.

Figure 5
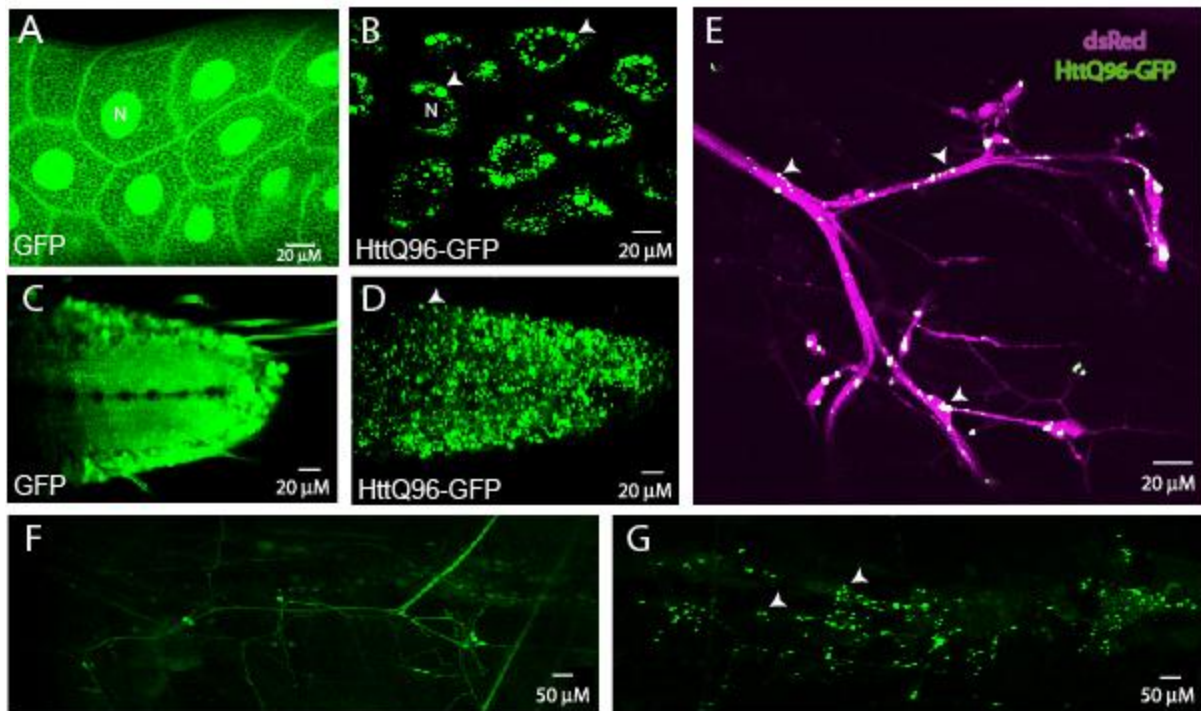
Figure 5. Cytoplasmic aggregation of HttQ96-GFP in neuronal and non-neuronal tissues. (A) Visualization of UAS-GFP (green) expression alone in the salivary gland shows localization to the cytoplasm and nucleus (indicated by N). (B) Visualization of HttQ96-GFP (green) in the salivary gland. Unlike GFP, HttQ96-GFP forms cytoplasmic aggregates in the salivary gland. The nucleus is indicated by N, with aggregates indicated by arrowheads. (C, D) Visualization of GFP alone or HttQ96-GFP in CNS neurons of the ventral nerve cord. GFP is diffusely localized in CNS neurons, while HttQ96-GFP forms aggregates. Several Htt aggregates are denoted by arrowheads. (E) HttQ96-GFP aggregates (green, indicated by arrowheads) are found in axons labeled expressing dsRed (magenta) in C155, UAS-dsRed, UAS-HttQ96-GFP larvae. (F) In peripheral axons and synapses of C155, UAS-GFP larvae, GFP (green) is diffuse in the cytoplasm. (G) In contrast, HttQ96-GFP (green) is found in cytoplasmic aggregates (indicated by arrows) in peripheral axons and synapses in C155, UAS-HttQ96-GFP larvae.

Figure 6

A

B

C
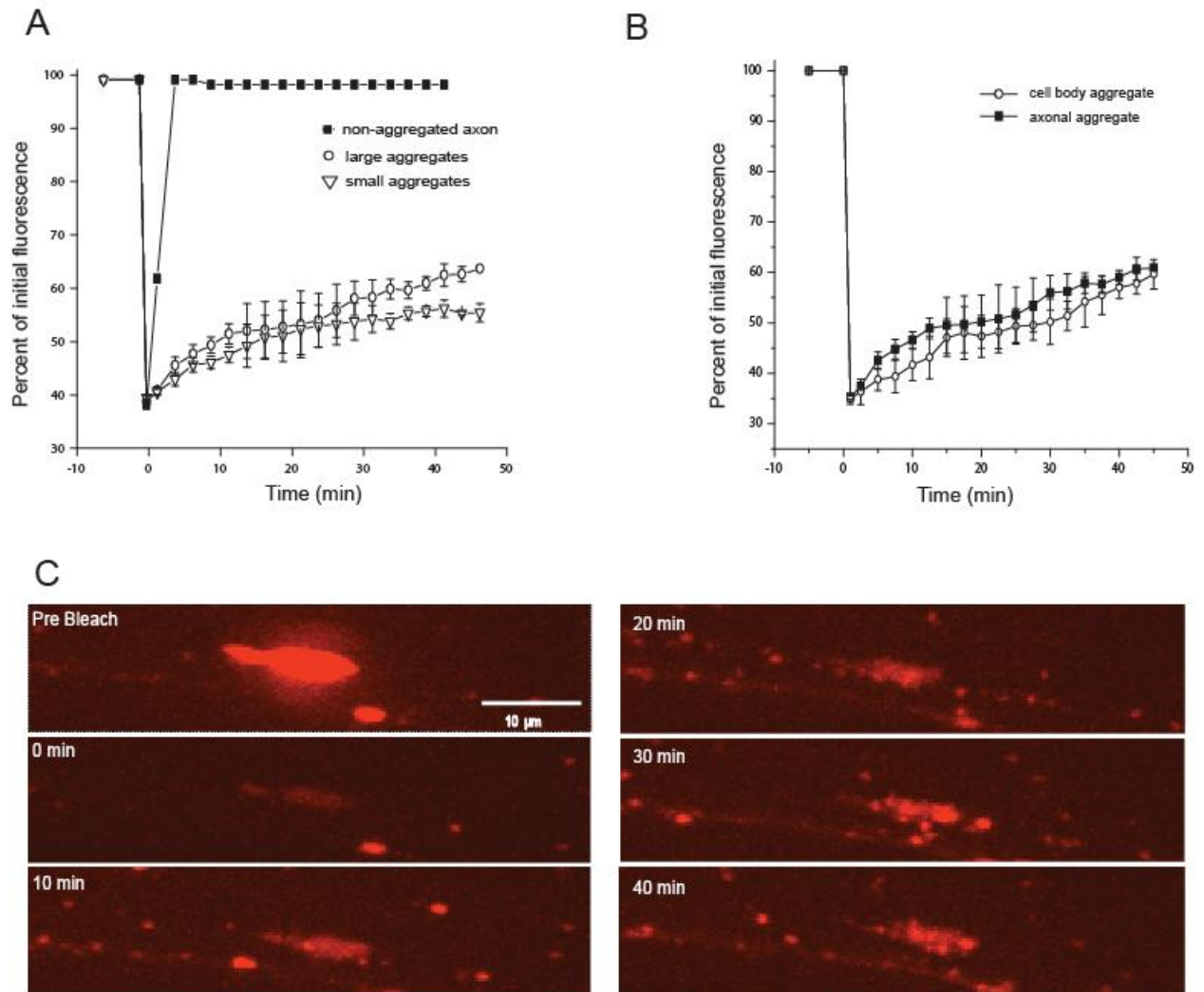
Figure 6. FRAP microscopy shows mRFP-HttQ138 aggregates continue to accumulate HttQ138 in live anesthetized 3rd instar larval axons. (A) Averaged traces comparing FRAP rates of regions of axons with no aggregates, large aggregates that equal or exceed the diameter of the axon, and smaller aggregates less than the diameter of the axon. While regions without aggregates recover quickly due to fast axonal transport, large and small HttQ138 aggregates recover at a slower rate but to a greater level. The graph shows percent of initial fluorescence, not total fluorescence. Larger aggregates recover at a greater rate than smaller ones. (B) HttQ138 aggregation kinetics demonstrated by FRAP in different regions of the motor neuron. (C) Time-lapse images of a FRAP experiment showing recovery of an aggregate over 40 minutes in a live anesthetized 3rd instar larval motor neuron axon.

Figure 7

	Salivary Gland	Ventral Nerve Cord	Axons
2 Hours		No expression	No expression
4 Hours	100 µm	50 µm	20 µm
8 Hours			
12 Hours			
18 Hours			
24 Hours			
72 hours of recovery after 24 hours of expression			

Time post-induction of expression of Gal80^{ts} CCAP-HttQ138-RFP
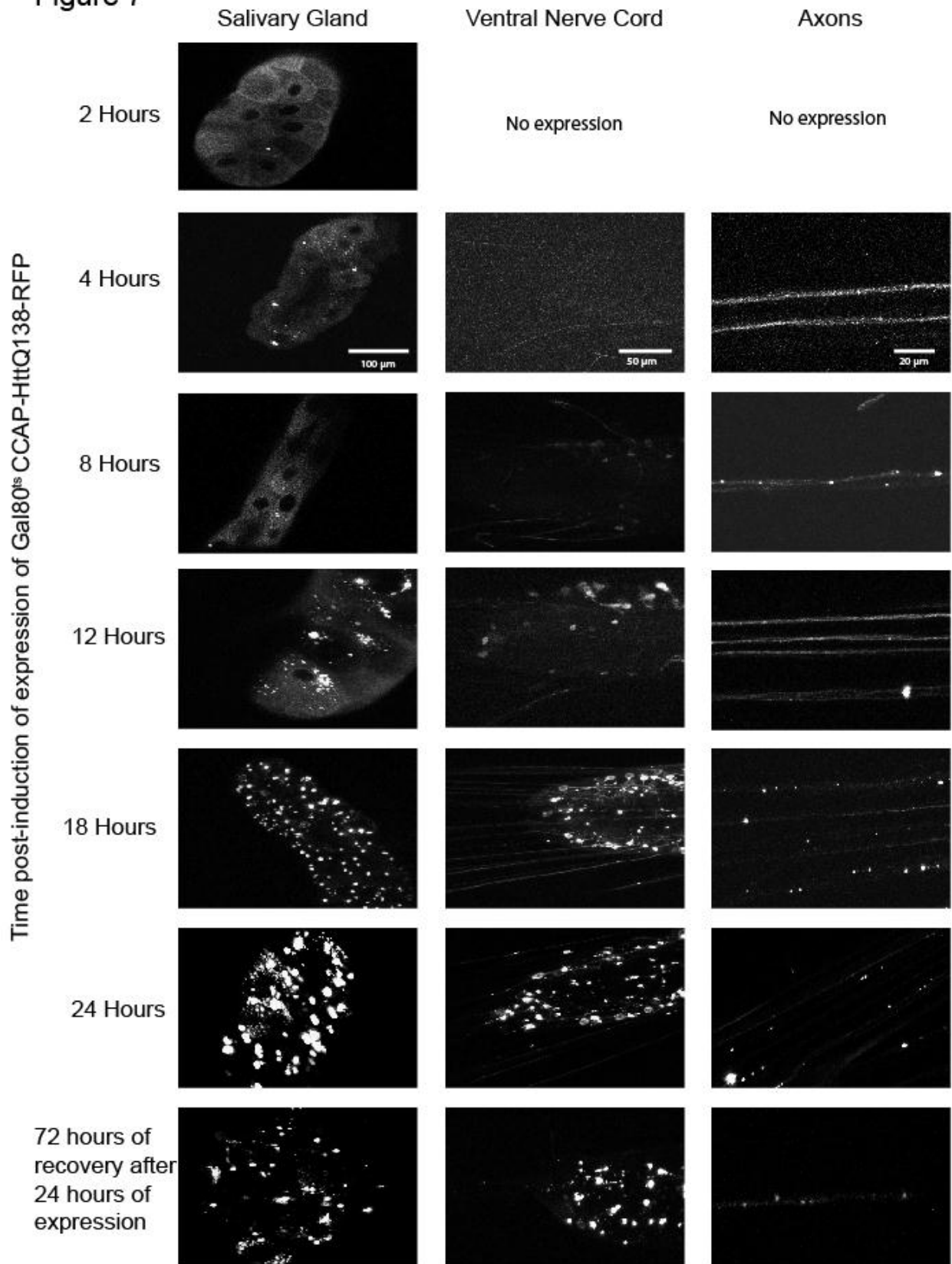
Figure 7. Acute induction of mRFP-HttQ138 expression by *CCAP*-GAL4 shows the pattern of aggregate formation in salivary glands, ventral nerve cord, and axons over 24 hours. Expression of UAS-HttQ138 was repressed using *tubulin*-Gal80^{ts} at 19°C during early development. Animals were moved to 30°C for the designated time, dissected, and imaged immediately to avoid fixation artifacts.

Figure 8
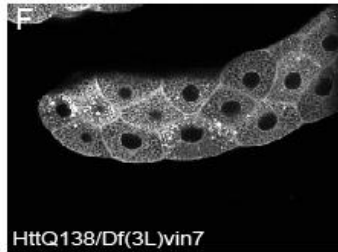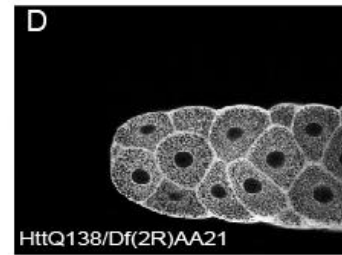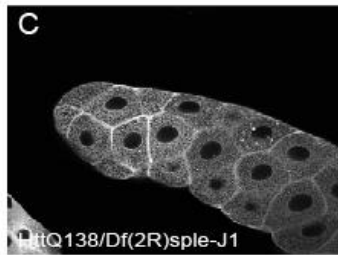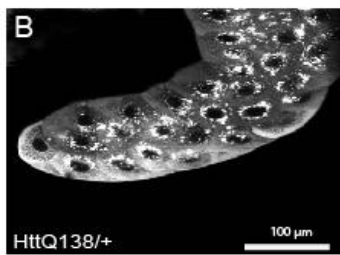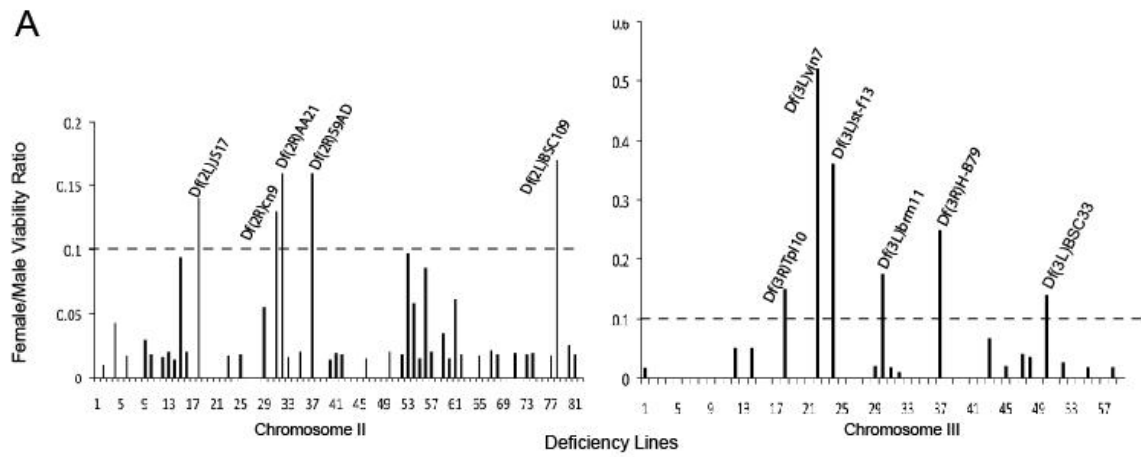
Figure 8. Suppression of lethality by Df haploinsufficiency screen. (A) Male/female viability ratio of mRFP-HttQ138 expressing Df lines. Homozygous mRFP-HttQ138 females were crossed to C155/y; Df/Bal males for 81 Df lines on chromosome II and 60 Df lines on chromosome III. Few female escapers expressing mRFP-HttQ138 are ever seen in control crosses (male/female ratio = 0.01). All Dfs with a viability ratio greater than 0.1 were identified as hits. (B-F) Confocal images of mRFP-HttQ138 aggregates in the salivary glands of 3rd instar larvae from controls (B) and animals heterozygous for *Df(3L)vin7* (C), *Df(2R)sple-J1* (D), *Df(2R)AA21* (E) and *Df(2R)59AB* (F). The scale bar is 100 μm in all panels.

Figure 9
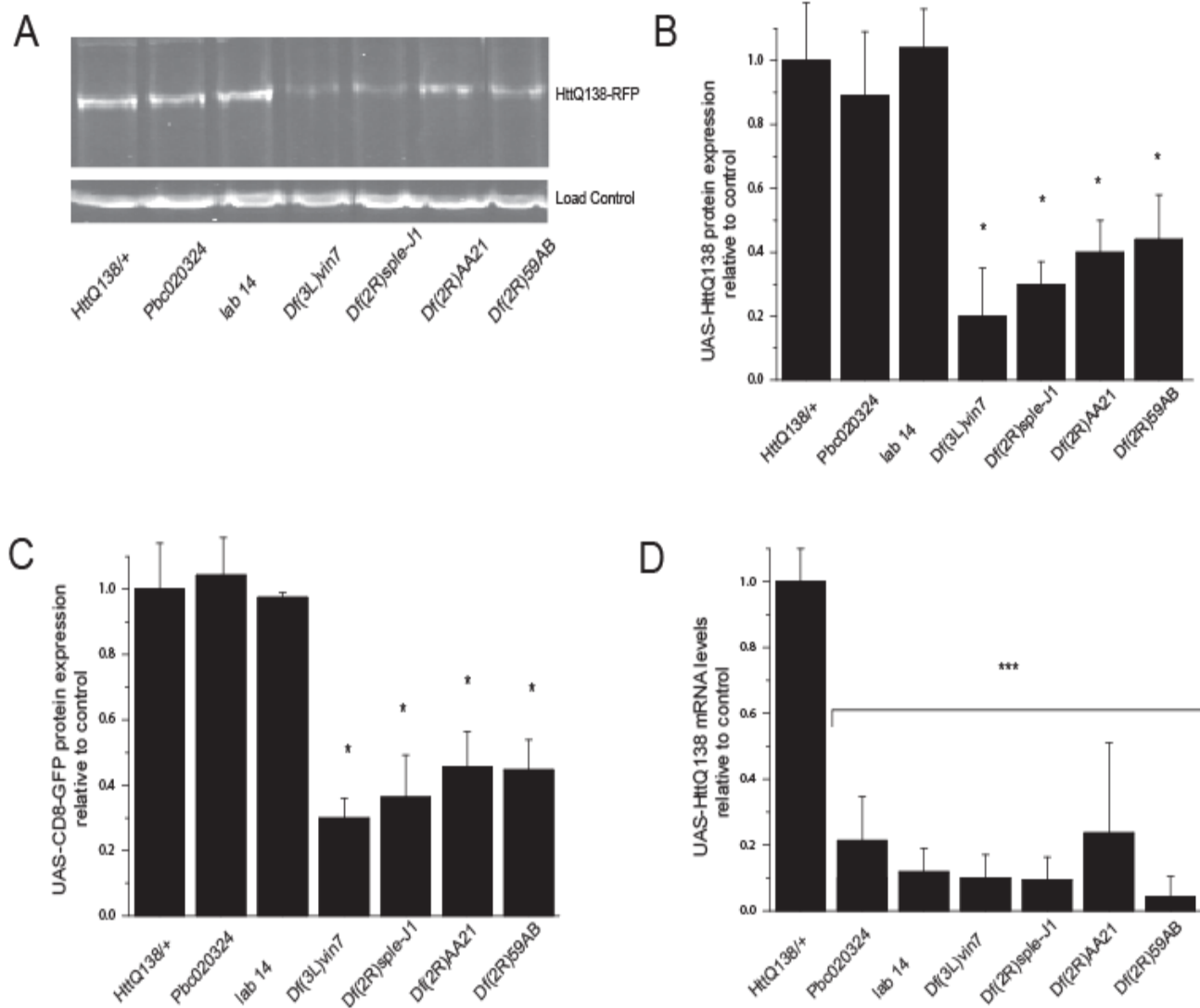
Figure 9. Quantification of transgenic Htt expression. (A) Western blot with C155-driven HttQ138 expression in control (white) and the indicated genotypes from pupal head extracts probed with anti-Htt antibodies and control XXX antibodies. (B) Quantification of C155-driven HttQ138 protein expression in control (white) and the indicated genotypes from pupal head extracts. The control containing C155; UAS-mRFP-HttQ138 was normalized to one for the genotypic comparisons. (C) Quantification of C155-driven GFP-CD8 expression in control (white) and the indicated genotypes from adult head extracts by western blot analysis with anti-GFP antibodies. (D) HttQ138 mRNA levels were measured in pupal head extracts by quantitative RT-PCR and normalized to control (white) expression. Error bars indicate SEM. * indicates $p<0.05$, *** indicates $p<0.001$ by Student's t-test.

Figure 10
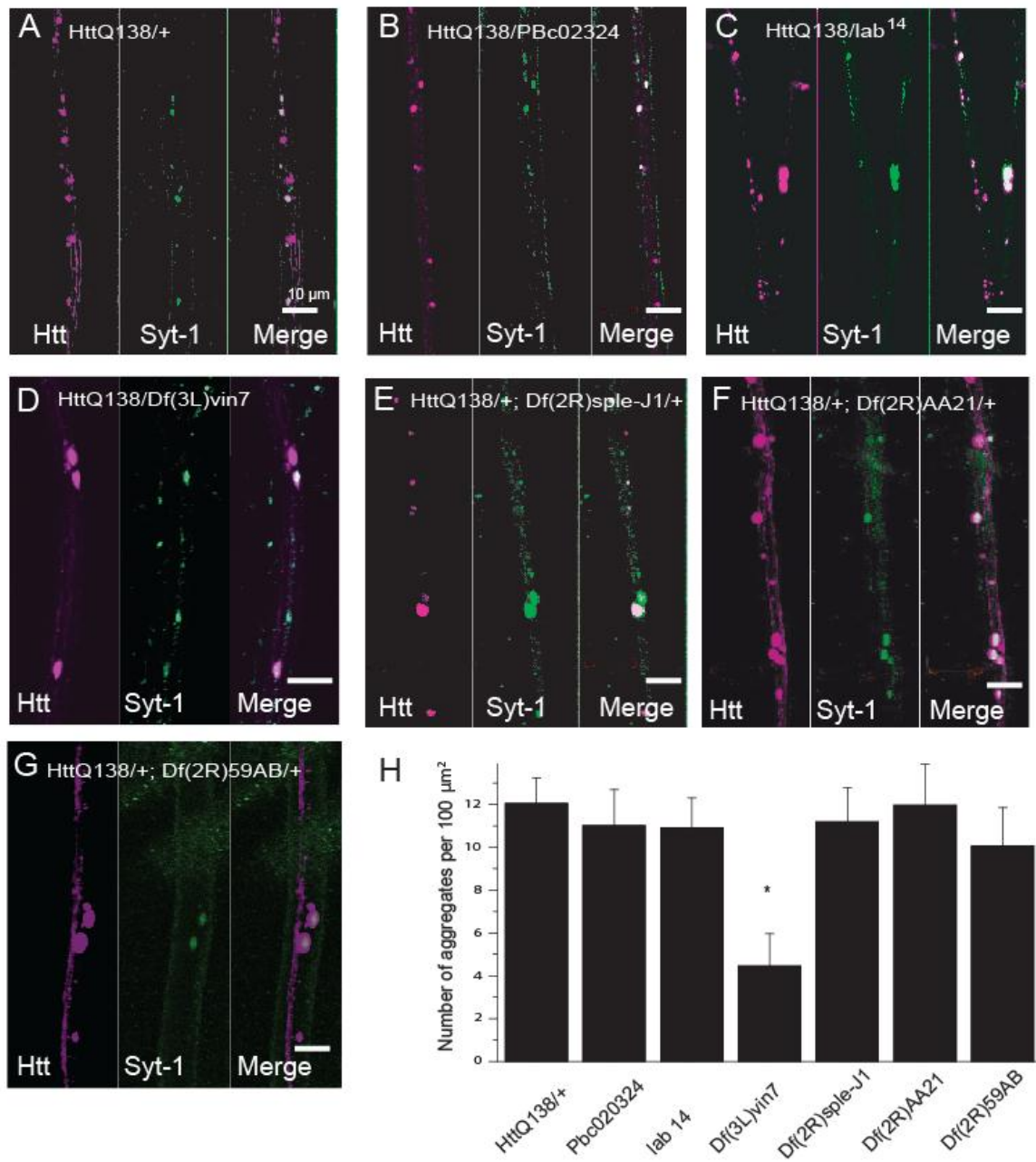
Figure 10. HttQ138 and Synaptotagmin aggregation in peripheral axons. Confocal images of 3rd instar larval peripheral nerves expressing mRFP-HttQ138 (red-left panel) and immunostained with anti-synaptotagmin I antibodies (green- middle panel) from controls (A) and animals heterozygous for PBc02324 (B), *lab*^{14} (C), *Df(3L)vin7* (D), *Df(2R)sple-J1* (E), *Df(2R)AA21* (F) and *Df(2R)59AB* (G). The scale bar is 10 μm for all panels. (H) Quantification of HttQ138 aggregate number for 100 μm axon segments for 25 segments (n= 5 larvae) of the indicated genotypes. Aggregates > 0.5 μm were counted using the 'find 2D nucleus' function of the Velocity version 5.4 software (Perkin Elmer). Error bars indicate SEM, with * denoting $p<0.05$ using Student's t-test.

Figure 11
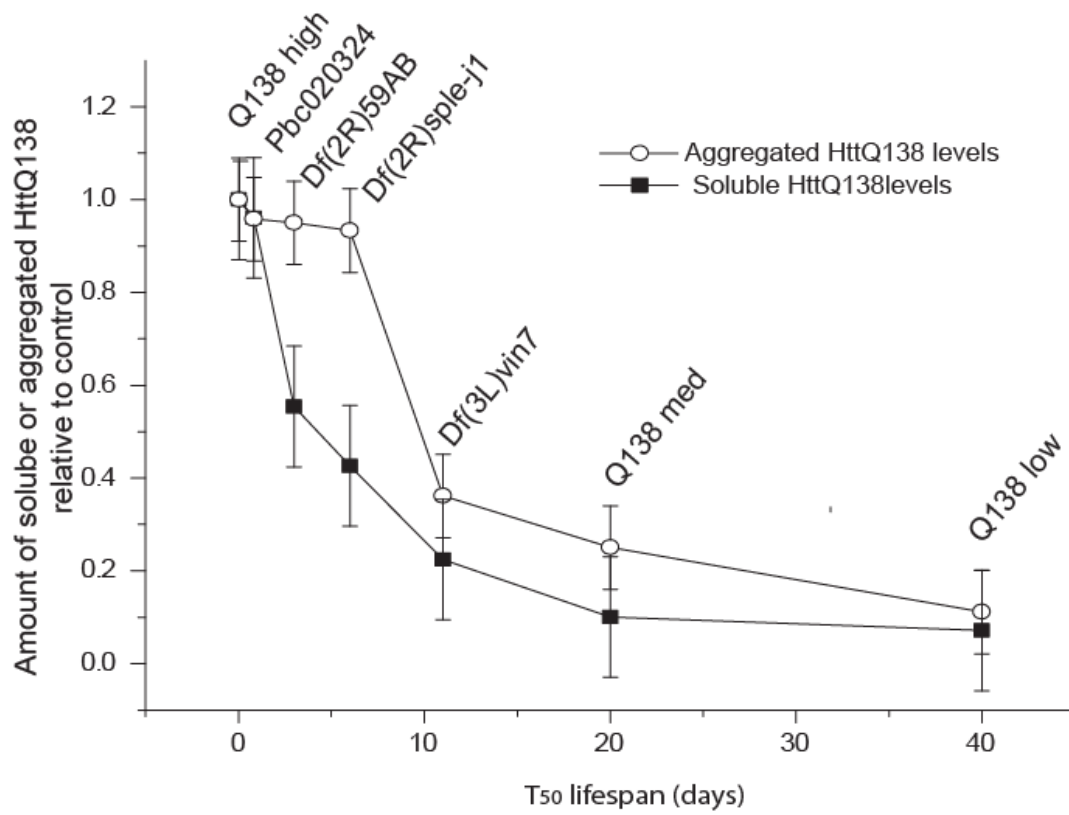
Figure 11. Graph of lifespan versus soluble HttQ138 (measured by western blot) or axonal aggregates (quantified per 100 μm section of larval axon) for identified suppressors. Htt expression and aggregation are tightly linked and correlate with increased toxicity. *Df(2R)sple-J1* has reduced toxicity that is correlated with decreased soluble Htt only.

References

ARRASATE, M., S. MITRA, E. S. SCHWEITZER, M. R. SEGAL and S. FINKBEINER, 2004 Inclusion body formation reduces levels of mutant huntingtin and the risk of neuronal death. Nature **431:** 805-810.

BECHER, M. W., J. A. KOTZUK, A. H. SHARP, S. W. DAVIES, G. P. BATES *et al.*, 1998 Intranuclear neuronal inclusions in Huntington's disease and dentatorubral and pallidoluysian atrophy: correlation between the density of inclusions and IT15 CAG triplet repeat length. Neurobiology of disease **4:** 387-397.

BELLO, B., N. HOLBRO and H. REICHERT, 2007 Polycomb group genes are required for neural stem cell survival in postembryonic neurogenesis of Drosophila. Development **134:** 1091-1099.

BIYASHEVA, A., T. V. DO, Y. LU, M. VASKOVA and A. J. ANDRES, 2001 Glue secretion in the Drosophila salivary gland: a model for steroid-regulated exocytosis. Developmental biology **231:** 234-251.

BRODY, T., 1999 The Interactive Fly: gene networks, development and the Internet. Trends in genetics : TIG **15:** 333-334.

CAMPBELL, R. E., O. TOUR, A. E. PALMER, P. A. STEINBACH, G. S. BAIRD *et al.*, 2002 A monomeric red fluorescent protein. Proceedings of the National Academy of Sciences of the United States of America **99:** 7877-7882.

CARMICHAEL, J., J. CHATELLIER, A. WOOLFSON, C. MILSTEIN, A. R. FERSHT *et al.*, 2000 Bacterial and yeast chaperones reduce both aggregate formation and cell death in mammalian cell models of Huntington's disease. Proceedings of the National Academy of Sciences of the United States of America **97:** 9701-9705.

CATTANEO, E., C. ZUCCATO and M. TARTARI, 2005 Normal huntingtin function: an alternative approach to Huntington's disease. Nature reviews. Neuroscience **6:** 919-930.

CHAI, Y., J. SHAO, V. M. MILLER, A. WILLIAMS and H. L. PAULSON, 2002 Live-cell imaging reveals divergent intracellular dynamics of polyglutamine disease proteins and supports a sequestration model of pathogenesis. Proceedings of the National Academy of Sciences of the United States of America **99:** 9310-9315.

CHEN, M., V. O. ONA, M. LI, R. J. FERRANTE, K. B. FINK *et al.*, 2000 Minocycline inhibits caspase-1 and caspase-3 expression and delays mortality in a transgenic mouse model of Huntington disease. Nature medicine **6:** 797-801.

CHOPRA, V., J. H. FOX, G. LIEBERMAN, K. DORSEY, W. MATSON *et al.*, 2007 A small-molecule therapeutic lead for Huntington's disease: preclinical pharmacology and efficacy of C2-8 in the R6/2 transgenic mouse. Proceedings of the National Academy of Sciences of the United States of America **104:** 16685-16689.

COLBY, D. W., Y. CHU, J. P. CASSADY, M. DUENNWALD, H. ZAZULAK *et al.*, 2004 Potent inhibition of huntingtin aggregation and cytotoxicity by a disulfide bond-free single-domain intracellular antibody. Proceedings of the National Academy of Sciences of the United States of America **101:** 17616-17621.

CUMMINGS, C. J., Y. SUN, P. OPAL, B. ANTALFFY, R. MESTRIL *et al.*, 2001 Over-expression of inducible HSP70 chaperone suppresses neuropathology and improves motor function in SCA1 mice. Human Molecular Genetics **10:** 1511-1518.

DAVIES, S. W., M. TURMAINE, B. A. COZENS, M. DIFIGLIA, A. H. SHARP *et al.*, 1997 Formation of neuronal intranuclear inclusions underlies the neurological dysfunction in mice transgenic for the HD mutation. Cell **90:** 537-548.

DEDEOGLU, A., J. K. KUBILUS, T. M. JEITNER, S. A. MATSON, M. BOGDANOV *et al.*, 2002 Therapeutic effects of cystamine in a murine model of Huntington's disease. The Journal of neuroscience : the official journal of the Society for Neuroscience **22:** 8942-8950.

DIFIGLIA, M., E. SAPP, K. O. CHASE, S. W. DAVIES, G. P. BATES *et al.*, 1997 Aggregation of huntingtin in neuronal intranuclear inclusions and dystrophic neurites in brain. Science **277:** 1990-1993.

FEANY, M. B., and W. W. BENDER, 2000 A Drosophila model of Parkinson's disease. Nature **404:** 394-398.

FERNANDEZ-FUNEZ, P., M. L. NINO-ROSALES, B. DE GOUYON, W. C. SHE, J. M. LUCHAK *et al.*, 2000 Identification of genes that modify ataxin-1-induced neurodegeneration. Nature **408:** 101-106.

FERRANTE, R. J., C. A. GUTEKUNST, F. PERSICHETTI, S. M. MCNEIL, N. W. KOWALL *et al.*, 1997 Heterogeneous topographic and cellular distribution of huntingtin expression in the normal human neostriatum. The Journal of neuroscience : the official journal of the Society for Neuroscience **17:** 3052-3063.

FUGER, P., L. B. BEHRENDS, S. MERTEL, S. J. SIGRIST and T. M. RASSE, 2007 Live imaging of synapse development and measuring protein dynamics using two-color fluorescence recovery after photo-bleaching at Drosophila synapses. Nature protocols **2:** 3285-3298.

GAFNI, J., E. HERMEL, J. E. YOUNG, C. L. WELLINGTON, M. R. HAYDEN *et al.*, 2004 Inhibition of calpain cleavage of huntingtin reduces toxicity: accumulation of calpain/caspase fragments in the nucleus. The Journal of biological chemistry **279:** 20211-20220.

GERBER, H. P., K. SEIPEL, O. GEORGIEV, M. HOFFERER, M. HUG *et al.*, 1994 Transcriptional activation modulated by homopolymeric glutamine and proline stretches. Science **263:** 808-811.

GRAHAM, R. K., Y. DENG, E. J. SLOW, B. HAIGH, N. BISSADA *et al.*, 2006 Cleavage at the caspase-6 site is required for neuronal dysfunction and degeneration due to mutant huntingtin. Cell **125:** 1179-1191.

GUNAWARDENA, S., L. S. HER, R. G. BRUSCH, R. A. LAYMON, I. R. NIESMAN *et al.*, 2003 Disruption of axonal transport by loss of huntingtin or expression of pathogenic polyQ proteins in Drosophila. Neuron **40:** 25-40.

HARJES, P., and E. E. WANKER, 2003 The hunt for huntingtin function: interaction partners tell many different stories. Trends in biochemical sciences **28:** 425-433.

HEISER, V., E. SCHERZINGER, A. BOEDDRICH, E. NORDHOFF, R. LURZ *et al.*, 2000 Inhibition of huntingtin fibrillogenesis by specific antibodies and small molecules: implications for Huntington's disease therapy. Proceedings of the National Academy of Sciences of the United States of America **97:** 6739-6744.

HODGSON, J. G., N. AGOPYAN, C. A. GUTEKUNST, B. R. LEAVITT, F. LEPIANE *et al.*, 1999 A YAC mouse model for Huntington's disease with full-length mutant huntingtin, cytoplasmic toxicity, and selective striatal neurodegeneration. Neuron **23:** 181-192.

HOFFNER, G., M. L. ISLAND and P. DJIAN, 2005 Purification of neuronal inclusions of patients with Huntington's disease reveals a broad range of N-terminal fragments of expanded huntingtin and insoluble polymers. Journal of neurochemistry **95:** 125-136.

HOFFNER, G., P. KAHLEM and P. DJIAN, 2002 Perinuclear localization of huntingtin as a consequence of its binding to microtubules through an interaction with beta-tubulin: relevance to Huntington's disease. Journal of Cell Science **115:** 941-948.

JACKSON, G. R., I. SALECKER, X. DONG, X. YAO, N. ARNHEIM *et al.*, 1998 Polyglutamine-expanded human huntingtin transgenes induce degeneration of Drosophila photoreceptor neurons. Neuron **21:** 633-642.

JANA, N. R., M. TANAKA, G. WANG and N. NUKINA, 2000 Polyglutamine length-dependent interaction of Hsp40 and Hsp70 family chaperones with truncated N-terminal huntingtin: their role in suppression of aggregation and cellular toxicity. Human Molecular Genetics **9:** 2009-2018.

KEGEL, K. B., A. R. MELONI, Y. YI, Y. J. KIM, E. DOYLE *et al.*, 2002 Huntingtin is present in the nucleus, interacts with the transcriptional corepressor C-terminal binding protein, and represses transcription. The Journal of biological chemistry **277:** 7466-7476.

KHOSHNAN, A., J. KO and P. H. PATTERSON, 2002 Effects of intracellular expression of anti-huntingtin antibodies of various specificities on mutant huntingtin aggregation and toxicity. Proceedings of the National Academy of Sciences of the United States of America **99:** 1002-1007.

KIM, Y. J., Y. YI, E. SAPP, Y. WANG, B. CUIFFO *et al.*, 2001 Caspase 3-cleaved N-terminal fragments of wild-type and mutant huntingtin are present in normal and Huntington's disease brains, associate with membranes, and undergo calpain-dependent proteolysis. Proceedings of the National Academy of Sciences of the United States of America **98:** 12784-12789.

KIMURA, Y., W. C. LEE and J. T. LITTLETON, 2007 Therapeutic prospects for the prevention of neurodegeneration in Huntington's disease and the polyglutamine repeat disorders. Mini reviews in medicinal chemistry **7:** 99-106.

KROBITSCH, S., and S. LINDQUIST, 2000 Aggregation of huntingtin in yeast varies with the length of the polyglutamine expansion and the expression of chaperone proteins. Proceedings of the National Academy of Sciences of the United States of America **97:** 1589-1594.

KUEMMERLE, S., C. A. GUTEKUNST, A. M. KLEIN, X. J. LI, S. H. LI *et al.*, 1999 Huntington aggregates may not predict neuronal death in Huntington's disease. Annals of neurology **46:** 842-849.

LAJOIE, P., and E. L. SNAPP, 2010 Formation and toxicity of soluble polyglutamine oligomers in living cells. PLoS One **5:** e15245.

LALIC, N. M., J. MARIC, M. SVETEL, A. JOTIC, E. STEFANOVA *et al.*, 2008 Glucose homeostasis in Huntington disease: abnormalities in insulin sensitivity and early-phase insulin secretion. Archives of neurology **65:** 476-480.

LAM, W., W. M. CHAN, T. W. LO, A. K. WONG, C. C. WU *et al.*, 2008 Human receptor for activated protein kinase C1 associates with polyglutamine aggregates and modulates polyglutamine toxicity. Biochemical and biophysical research communications **377:** 714-719.

LECERF, J. M., T. L. SHIRLEY, Q. ZHU, A. KAZANTSEV, P. AMERSDORFER *et al.*, 2001 Human single-chain Fv intrabodies counteract in situ huntingtin aggregation in cellular models of Huntington's disease. Proceedings of the National Academy of Sciences of the United States of America **98:** 4764-4769.

LEE, W. C., M. YOSHIHARA and J. T. LITTLETON, 2004 Cytoplasmic aggregates trap polyglutamine-containing proteins and block axonal transport in a Drosophila model of Huntington's disease. Proceedings of the National Academy of Sciences of the United States of America **101:** 3224-3229.

LI, H., S. H. LI, A. L. CHENG, L. MANGIARINI, G. P. BATES *et al.*, 1999 Ultrastructural localization and progressive formation of neuropil aggregates in Huntington's disease transgenic mice. Human molecular genetics **8:** 1227-1236.

LI, H., S. H. LI, Z. X. YU, P. SHELBOURNE and X. J. LI, 2001 Huntingtin aggregate-associated axonal degeneration is an early pathological event in Huntington's disease mice. The Journal of neuroscience : the official journal of the Society for Neuroscience **21:** 8473-8481.

LI, S. H., C. A. GUTEKUNST, S. M. HERSCH and X. J. LI, 1998 Interaction of huntingtin-associated protein with dynactin P150Glued. The Journal of neuroscience : the official journal of the Society for Neuroscience **18:** 1261-1269.

LUNKES, A., K. S. LINDENBERG, L. BEN-HAIEM, C. WEBER, D. DEVYS *et al.*, 2002 Proteases acting on mutant huntingtin generate cleaved products that differentially build up cytoplasmic and nuclear inclusions. Molecular cell **10:** 259-269.

LUTHI-CARTER, R., S. A. HANSON, A. D. STRAND, D. A. BERGSTROM, W. CHUN *et al.*, 2002 Dysregulation of gene expression in the R6/2 model of polyglutamine disease: parallel changes in muscle and brain. Human molecular genetics **11:** 1911-1926.

MARTIN, B., E. GOLDEN, A. KESELMAN, M. STONE, M. P. MATTSON *et al.*, 2008 Therapeutic perspectives for the treatment of Huntington's disease: treating the whole body. Histology and histopathology **23:** 237-250.

NAGAI, Y., T. INUI, H. A. POPIEL, N. FUJIKAKE, K. HASEGAWA *et al.*, 2007 A toxic monomeric conformer of the polyglutamine protein. Nature structural & molecular biology **14:** 332-340.

ORR, H. T., and H. Y. ZOGHBI, 2007 Trinucleotide repeat disorders. Annual review of neuroscience **30:** 575-621.

PARK, J. H., A. J. SCHROEDER, C. HELFRICH-FORSTER, F. R. JACKSON and J. EWER, 2003 Targeted ablation of CCAP neuropeptide-containing neurons of Drosophila causes specific defects in execution and circadian timing of ecdysis behavior. Development **130:** 2645-2656.

PERSICHETTI, F., F. TRETTEL, C. C. HUANG, C. FRAEFEL, H. T. TIMMERS *et al.*, 1999 Mutant huntingtin forms in vivo complexes with distinct context-dependent conformations of the polyglutamine segment. Neurobiology of disease **6:** 364-375.

PORTERA-CAILLIAU, C., J. C. HEDREEN, D. L. PRICE and V. E. KOLIATSOS, 1995 Evidence for apoptotic cell death in Huntington disease and excitotoxic animal models. The Journal of neuroscience : the official journal of the Society for Neuroscience **15:** 3775-3787.

QIN, Z. H., and Z. L. GU, 2004 Huntingtin processing in pathogenesis of Huntington disease. Acta pharmacologica Sinica **25:** 1243-1249.

RIECKHOF, G. E., M. YOSHIHARA, Z. GUAN and J. T. LITTLETON, 2003 Presynaptic N-type calcium channels regulate synaptic growth. The Journal of biological chemistry **278:** 41099-41108.

RIGAMONTI, D., C. MUTTI, C. ZUCCATO, E. CATTANEO and A. CONTINI, 2009 Turning REST/NRSF dysfunction in Huntington's disease into a pharmaceutical target. Current pharmaceutical design **15:** 3958-3967.

ROMERO, E., G. H. CHA, P. VERSTREKEN, C. V. LY, R. E. HUGHES *et al.*, 2008 Suppression of neurodegeneration and increased neurotransmission caused by expanded full-length huntingtin accumulating in the cytoplasm. Neuron **57:** 27-40.

SANCHEZ, I., C. MAHLKE and J. YUAN, 2003 Pivotal role of oligomerization in expanded polyglutamine neurodegenerative disorders. Nature **421:** 373-379.

SAPP, E., J. PENNEY, A. YOUNG, N. ARONIN, J. P. VONSATTEL *et al.*, 1999 Axonal transport of N-terminal huntingtin suggests early pathology of corticostriatal projections in Huntington disease. Journal of neuropathology and experimental neurology **58:** 165-173.

SCHERZINGER, E., R. LURZ, M. TURMAINE, L. MANGIARINI, B. HOLLENBACH *et al.*, 1997 Huntingtin-encoded polyglutamine expansions form amyloid-like protein aggregates in vitro and in vivo. Cell **90:** 549-558.

SCHERZINGER, E., A. SITTLER, K. SCHWEIGER, V. HEISER, R. LURZ *et al.*, 1999 Self-assembly of polyglutamine-containing huntingtin fragments into amyloid-like fibrils: implications for Huntington's disease pathology. Proceedings of the National Academy of Sciences of the United States of America **96:** 4604-4609.

SEONG, I. S., J. M. WODA, J. J. SONG, A. LLORET, P. D. ABEYRATHNE *et al.*, 2010 Huntingtin facilitates polycomb repressive complex 2. Human molecular genetics **19:** 573-583.

SIERADZAN, K. A., A. O. MECHAN, L. JONES, E. E. WANKER, N. NUKINA *et al.*, 1999 Huntington's disease intranuclear inclusions contain truncated, ubiquitinated huntingtin protein. Experimental neurology **156:** 92-99.

SINADINOS, C., T. BURBIDGE-KING, D. SOH, L. M. THOMPSON, J. L. MARSH *et al.*, 2009 Live axonal transport disruption by mutant huntingtin fragments in Drosophila motor neuron axons. Neurobiology of disease **34:** 389-395.

SLOW, E. J., R. K. GRAHAM, A. P. OSMAND, R. S. DEVON, G. LU *et al.*, 2005 Absence of behavioral abnormalities and neurodegeneration in vivo despite widespread neuronal huntingtin inclusions. Proc Natl Acad Sci U S A **102:** 11402-11407.

SMITH, D. L., B. WOODMAN, A. MAHAL, K. SATHASIVAM, S. GHAZI-NOORI *et al.*, 2003 Minocycline and doxycycline are not beneficial in a model of Huntington's disease. Annals of neurology **54:** 186-196.

STEFFAN, J. S., L. BODAI, J. PALLOS, M. POELMAN, A. MCCAMPBELL *et al.*, 2001 Histone deacetylase inhibitors arrest polyglutamine-dependent neurodegeneration in Drosophila. Nature **413:** 739-743.

SZEBENYI, G., G. A. MORFINI, A. BABCOCK, M. GOULD, K. SELKOE *et al.*, 2003 Neuropathogenic forms of huntingtin and androgen receptor inhibit fast axonal transport. Neuron **40:** 41-52.

TAGAWA, K., M. HOSHINO, T. OKUDA, H. UEDA, H. HAYASHI *et al.*, 2004 Distinct aggregation and cell death patterns among different types of primary neurons induced by mutant huntingtin protein. Journal of neurochemistry **89:** 974-987.

VACHER, C., L. GARCIA-OROZ and D. C. RUBINSZTEIN, 2005 Overexpression of yeast hsp104 reduces polyglutamine aggregation and prolongs survival of a transgenic mouse model of Huntington's disease. Human Molecular Genetics **14:** 3425-3433.

VELIER, J., M. KIM, C. SCHWARZ, T. W. KIM, E. SAPP *et al.*, 1998 Wild-type and mutant huntingtins function in vesicle trafficking in the secretory and endocytic pathways. Experimental neurology **152:** 34-40.

VOMEL, M., and C. WEGENER, 2007 Neurotransmitter-induced changes in the intracellular calcium concentration suggest a differential central modulation of CCAP neuron subsets in Drosophila. Developmental neurobiology **67:** 792-808.

VONSATTEL, J. P., R. H. MYERS, T. J. STEVENS, R. J. FERRANTE, E. D. BIRD *et al.*, 1985 Neuropathological classification of Huntington's disease. Journal of neuropathology and experimental neurology **44:** 559-577.

WARRICK, J. M., H. Y. CHAN, G. L. GRAY-BOARD, Y. CHAI, H. L. PAULSON *et al.*, 1999 Suppression of polyglutamine-mediated neurodegeneration in Drosophila by the molecular chaperone HSP70. Nature genetics **23:** 425-428.

WELLINGTON, C. L., L. M. ELLERBY, C. A. GUTEKUNST, D. ROGERS, S. WARBY *et al.*, 2002 Caspase cleavage of mutant huntingtin precedes neurodegeneration in Huntington's disease. The Journal of neuroscience : the official journal of the Society for Neuroscience **22:** 7862-7872.

WITTMANN, C. W., M. F. WSZOLEK, J. M. SHULMAN, P. M. SALVATERRA, J. LEWIS *et al.*, 2001 Tauopathy in Drosophila: neurodegeneration without neurofibrillary tangles. Science **293:** 711-714.

WOLFGANG, W. J., T. W. MILLER, J. M. WEBSTER, J. S. HUSTON, L. M. THOMPSON *et al.*, 2005 Suppression of Huntington's disease pathology in Drosophila by human single-chain Fv antibodies. Proceedings of the National Academy of Sciences of the United States of America **102:** 11563-11568.

YEO, M., S. K. LEE, B. LEE, E. C. RUIZ, S. L. PFAFF *et al.*, 2005 Small CTD phosphatases function in silencing neuronal gene expression. Science **307:** 596-600.

YOSHIDA, H., T. YOSHIZAWA, F. SHIBASAKI, S. SHOJI and I. KANAZAWA, 2002 Chemical chaperones reduce aggregate formation and cell death caused by the truncated Machado-Joseph disease gene product with an expanded polyglutamine stretch. Neurobiology of disease **10:** 88-99.

ZHU, B., J. A. PENNACK, P. MCQUILTON, M. G. FORERO, K. MIZUGUCHI *et al.*, 2008 Drosophila neurotrophins reveal a common mechanism for nervous system formation. PLoS biology **6:** e284.

ZUCCATO, C., and E. CATTANEO, 2007 Role of brain-derived neurotrophic factor in Huntington's disease. Progress in neurobiology **81:** 294-330.

ZUCCATO, C., A. CIAMMOLA, D. RIGAMONTI, B. R. LEAVITT, D. GOFFREDO *et al.*, 2001 Loss of huntingtin-mediated BDNF gene transcription in Huntington's disease. Science **293:** 493-498.

ZUCCATO, C., M. TARTARI, A. CROTTI, D. GOFFREDO, M. VALENZA *et al.*, 2003 Huntingtin interacts with REST/NRSF to modulate the transcription of NRSE-controlled neuronal genes. Nature genetics **35:** 76-83.

Chapter 3

The *Drosophila* Huntingtin protein mediates cargo processivity of mitochondria and synaptic vesicles in fast axonal transport

Kurt R. Weiss and J. Troy Littleton

Department of Biology and The Picower Institute for Learning and Memory, MIT, Cambridge, MA 02139

Abstract

Huntingtin (Htt) is ubiquitously expressed and conserved from *Drosophila* to humans, yet its biological role is unknown. Polyglutamine (polyQ) expansion within Htt is responsible for Huntington's Disease (HD), though the underlying mechanism for toxicity is unclear. We have recently identified functions for wild-type *Drosophila* Htt (dHtt) in fast axonal transport (FAT), as well as defects in axonal transport in animals overexpressing pathogenic Htt proteins (HttQ138). We generated a UAS–dHtt-mRFP N-terminal dHtt fragment and found it co-localizes with mitochondria and synaptic vesicles undergoing FAT. Htt is not a ubiquitous component of the transport machinery, as it is excluded from certain cargos, including dense-core vesicles and those labeled by APLIP1-GFP. We analyzed FAT of GFP-tagged cargo in motor axons of live anesthetized and freshly dissected larvae lacking the *Drosophila huntingtin* locus. Mitochondria and synaptic vesicles show a decrease in the distance and duration of axonal transport, an increase in the number of pauses, and an increase in the ratio of retrograde to anterograde flux. ANF-GFP containing dense core vesicles did not display defects in processivity, but did display altered flux. Since dHtt shows a high degree of co-localization with mitochondria and synaptic vesicles, but does not co-localize with dense core vesicles, our data suggest a role for dHtt acting locally to regulate cargo processivity in FAT. We also observed an increase in dynein heavy chain expression in aged adults, suggesting a broad effect on transport that may account for the global changes in cargo flux. To investigate the molecular interactions between Htt and motor-cargo complexes, we expressed dHtt-RFP in a *milton* (HAP1) mutant background and found that dHtt does not require mitochondria or functional HAP1 to localize to axons.

Introduction

A growing body of evidence has implicated Huntingtin (Htt) as having a role in intracellular transport, specifically fast axonal transport (FAT). Late onset degeneration in Huntington's Disease is specific to neurons, which are highly dependent on FAT to move synaptic building blocks and signaling molecules in the anterograde direction, and neurotrophic factors in the retrograde direction. One model of HD pathology suggests that certain fast axonal transport defects may cause continual insult to the neuron over the life of the cell and confer the specificity and late onset symptoms in HD. Knowing the specific role of Htt in FAT is essential to evaluate this model.

The endogenous role of *htt* has been previously investigated by knocking out or reducing endogenous *htt* expression in mouse and *Drosophila* models. Genetic knockouts of *htt* in mice leads to early embryonic lethality (Duyao, Auerbach et al. 1995; Nasir, Floresco et al. 1995; Zeitlin, Liu et al. 1995). The lethality is rescued by wild-type extraembyronic tissue expression, and data suggests a role for Htt in transport of essential ferric ions to the embryo (Dragatsis, Efstratiadis et al. 1998). Conditional knockouts in the CNS and testis of adult mice leads to late-onset neurodegeneration (O'Kusky, Nasir et al. 1999; Dragatsis, Levine et al. 2000). Murine neuronal culture experiments with reduced Htt expression showed reduced axonal transport of mitochondria and vesicles (Trushina, Dyer et al. 2004). In *Drosophila*, RNAi has been utilized to reduce dHtt expression, resulting in axonal swellings and accumulation of synaptic vesicles (Gunawardena, Her et al. 2003).

The *Drosophila huntingtin* homolog shows ~ 49 percent similarity and 24 percent identity in amino acid sequence with human *huntingtin*, and both contain three large regions of high homology, including the N-terminal region of the protein used in many HD models. The

Drosophila huntingtin locus does not contain a polyglutamine or polyproline tract, as found in vertebrate *huntingtin*. However, *dhtt* does contain the repeating HEAT (huntingtin, elongation factor 3, PR65/A subunit of protein phosphatase 2a and mTor) domain present in all known homologs (Li, Karlovich et al. 1999). HEAT repeats are roughly 40 amino acid domains that repeat several times within a protein and are involved in mediating protein-protein interactions (Andrade, Petosa et al. 2001). These domains are commonly found in proteins involved in axonal transport, chromosome segregation, and entry/exit from the nuclear pore complex (Neuwald and Hirano 2000; Andrade, Perez-Iratxeta et al. 2001).

Yeast two-hybrid experiments have implicated Htt in binding HAP1 (Li, Li et al. 1995), which is implicated in FAT via its interaction with kinesin (McGuire, Rong et al. 2006) and dynein (Engelender, Sharp et al. 1997; Rong, Li et al. 2007), and HIP-1 and HIP-14, which have roles in endocytosis, suggesting a role for Htt in various aspects of microtubule based intracellular transport (Kalchman, Koide et al. 1997; Wanker, Rovira et al. 1997). Additionally, the N-terminal 17 amino acids of Htt have been shown to confer membrane binding and specificity of Htt to mitochondria, vesicles, and other membrane bound organelles, and can alter the aggregation and toxicity of expanded polyQ Htt (Rockabrand, Slepko et al. 2007).

In addition to biochemical experiments, the interaction between Htt and the dynein/dynactin complex has been demonstrated functionally in cell culture experiments which show that loss of Htt can alter dynein mediated Golgi organization, and antibodies against Htt reduce dynein mediated vesicle movement *in situ* (Caviston, Ross et al. 2007; Caviston, Zajac et al. 2011). Experiments done in striatal and embryonic murine cell culture show that loss of Htt alters mitochondrial transport, with an increase in pauses and decrease in distance and velocity

(Trushina, Dyer et al. 2004). This data suggests Htt is present in a complex involving kinesin, dynein/dynactin, and membrane bound organelles.

Mitochondria are transported in larval motor axons in the anterograde direction by kinesin-1, and in the retrograde direction by dynein (Pilling, Horiuchi et al. 2006). The *Drosophila* larval PNS has been well established as a system for analysis of fast axonal transport of cargos, such as vesicles and mitochondria (Hurd and Saxton 1996; Hollenbeck and Saxton 2005). We used this system to investigate the role of dHtt in FAT of several membrane bound organelles. We find that dHtt functions to regulate processivity of mitochondria and synaptic vesicles, but not dense core vesicles, likely by regulating the coordination of microtubule motors associated with these organelles.

Materials and Methods

Generation of Htt constructs: cDNAs for mRFP-HttQ15 and mRFP-HttQ138 were subcloned into EcoRI (blunt end ligation) and KpnI sites of the pUAST expression vector. cDNA for eGFP-HttQ138-mRFP was subcloned into the XbaI site of the pUAST vector. HttQ15 and HttQ138 cDNAs were kindly provided by Ray Truant (Department of Biochemistry, McMaster University). A cDNA encoding the N-terminal 2kb of dHtt was cloned using the Gateway cloning system (Invitrogen). The N-terminal 2kb of dHtt was PCR-amplified from a cDNA library using primers 5'CACCATGGACAAATCCAGGTCCAGT 3' and 5' GGACTTAGAGCCGCTTGATTGACGAAAGAG 3'. The PCR product was subcloned into the pENTR-dTOPO vector and recombined into the pTWR destination vector with a C-terminal mRFP tag and UAS promoter for expression under the GAL4-UAS system (Brand and Perrimon 1993). The microinjection of constructs and generation of transgenic *Drosophila* were performed by Genetics Services (Cambridge, MA).

Drosophila Stocks and Genetics: The C380-GAL4 driver was chosen due to its high expression levels in all motor axons, as well as expression in the ventral ganglion, salivary gland, and in some body wall sensory neurons (Sanyal 2009). C380-GAL4, Mito-GFP, ANF-GFP and Syt-1-GFP were all obtained from the Bloomington Fly Stock Center, Bloomington, IN. All crosses were maintained at 25ºC on standard medium.

Live Imaging: Data on mitochondrial runs, pauses, and velocities was collected from freshly dissected larvae pinned to a Sylgard covered slide immersed in HL3 with 0.2 mM Ca^{2+} with a Zeiss upright scanning confocal microscope. Data on cargo flux and long term transport analysis was collected using third instar larvae anesthetized under suprane in a custom chamber that allowed imaging of fluorescently tagged constructs through the cuticle for up to 3 hours (Fuger, Behrends et al. 2007). For both imaging protocols images were collected at one frame per second for mitochondria and three per second for synaptic and dense core vesicles over six minutes across a bleached 50 µm region of motor neuron axon with a 60x objective. The faster, smaller vesicles required a faster frame rate to resolve movement from one image to the next so images were taken with a Zeiss spinning disk. Imaging was done in the distal 200 µm of axons innervating muscle 12/13 at section A3 to minimize possible contamination by sensory neurons that may be expressing under the C380 driver.

Transport analysis and Statistics: Individual mitochondria moving into the bleached region were marked with a mouse cursor in the ImageJ plugin MtrackJ (NIH) to indicate x,y,t coordinates. The leading edge of each mitochondrion was used to mark the location as a fluorescent maximum was variable from frame to frame. For each time series a stationary mitochondria outside the bleached region was marked at each time-point and used to correct for drift or other unwanted movements. Coordinates were imported into a Microsoft Excel

spreadsheet which calculated movement parameters such as direction, run length, velocity, stop number, and percent of time in each of a three state motion paradigm, anterograde runs, retrograde runs, and stops (Louie 2008). For automated analysis on mitochondrial flux, Individual mitochondria could be reliably tracked for 10-20 seconds with the Volocity Imaging software by Perkin Elmer to obtain bearing and instantaneous velocity measurements for individual mitochondrial tracks. Short and inaccurate tracks were filtered out by sorting data by time-tracked and direction-moved. After filtering, approximately 100 tracks per animal were sorted by bearing to determine the retrograde to anterograde flux measurement. Tracks obtained by automatic tracking were used to evaluate flux as bearing can be accurately determined with very few time-points. Manual tracking was done for a minimum of 60 seconds per mitochondria. Due to large variance within an animal for all transport parameters, data was not averaged per animal, but rather means for individual organelles were aggregated within a genotype. This gave a normal distribution of values to compare between genotypes. Student's T-Test for significance was used with a 95% confidence interval, equal variances were not assumed. Statistical values were calculated using Microsoft Excel (Microsoft, Redmond, WA) and Origin Graphing Software (Northhampton, MA).

Western Blot Analysis: For kinesin and dynein heavy chain Western blots, aged *Drosophila* were frozen in liquid nitrogen and vortexed. 10 heads for each indicated genotype were isolated and homogenized in sample buffer in triplicate, and proteins were separated on 7% SDS-PAGE gels at a concentration of one head per lane and transferred to nitrocellulose. Blots were incubated with monoclonal anti-kinesin heavy chain (SUK4) and anti-dynein heavy chain (2C-11) at 1:100 (Developmental Studies Hybridoma Bank). Blots were visualized on a Li-Cor

Odyssey infrared imaging system and protein expression was quantified with the accompanying software.

Immunohistochemistry: For HRP staining, wandering 3rd instar larvae expressing mito-GFP or Syt-1-GFP under the C380-GAL4 driver were reared at 25oC and dissected inHL3. Images were captured with a Zeiss Pascal laser scanning confocal microscope (Carl Zeiss MicroImaging, Inc.) using the accompanying Zeiss PASCAL software. Area and number of puncta were measured using ImageJ channel area measurement functions and the ICTN counter plugin.

Results

dHtt and human Q15Htt both localize to a subset of axonal cargos: To validate dHtt as a human Htt homolog and characterize the co-localization pattern of dHtt undergoing FAT in axons, we co-expressed mRFP-tagged N-terminal fragments of dHtt or human Htt along with GFP-tagged cargos in motor neurons. We find that dHtt and Q15Htt show a high degree of co-localization with mitochondria, a medium degree of co-localization with synaptic vesicles (about half of synaptic vesicles co-localize with Htt), and little to no co-localization with dense core vesicles or cargos marked by the JIP-1 like protein APLIP-1 (Horiuchi, Barkus et al. 2005) (Figure 1, left and middle panels). The co-localization data suggests that dHtt and human Htt may play a homologous role in FAT. Since dHtt only co-localizes with a subset of cargos, a role for dHtt in transport is likely to be specific to certain cargos.

We also characterized the co-localization of these cargos with HttQ138-RFP to determine if misregulation of these cargos may occur in HD (Figure 1, right panels). Indeed we observe that Q138Htt-RFP shows less association with mitochondria, resulting in fewer mitochondria present in the axons of Q138Htt-RFP expressing axons (Figure 1).

dHtt null Drosophila larvae display defects in fast axonal transport of mitochondria and synaptic vesicles: To differentiate between models where dHtt is playing an active or passive role in FAT, we used a *huntingtin* null *Drosophila* line to look for defects in FAT (Zhang, Feany et al. 2009). dHtt RNAi has been shown to disrupt axonal transport and cause axonal 'traffic jams', consisting of concentrated regions of synaptic vesicles and regions of axonal swellings (Gunawardena, Her et al. 2003). Our *huntingtin* null model did not display cargo accumulation along axons, suggesting off-target effects for *dhtt* RNAi. Stains for synaptic vesicles did not reveal cargo accumulations. All cargos analyzed in the null mutant, including mitochondria, synaptic vesicles, endosomes, and dense core vesicles were observed to move bi-directionally through the axon without accumulation during live imaging.

To determine if specific defects in transport are associated with loss of dHtt, mitochondria and dense core vesicles were tracked manually in ImageJ (National Institutes of Health) and using the object tracking function in the Volocity 4-D imaging software package (Perkin Elmer). *huntingtin* null larvae show an alteration in the ratio of anterograde to retrograde moving mitochondria as is represented in kymographs of mitochondrial movement over a 50 μm region of axon imaged over 300 seconds (Figure 2A). This alteration of flux stems from an overall decrease in anterograde flux, and an increase in retrograde flux. The flux phenotype was used to assay the ability of several Htt fragments to rescue *huntingtin* null transport defects since automated tracking could be used to calculate the flux ratio (Figure 2B). The phenotype was rescued by a full-length Q16Htt Human transgene (Romero, Cha et al. 2008), indicating that dHtt and human Htt share a conserved function in FAT. An N-terminal 670 amino acid fragment of dHtt expressing also rescued the flux phenotype, suggesting that the activity required to regulate mitochondrial flux resides in the N-terminal highly conserved domain of Htt. The flux phenotype

was not rescued by an N-terminal 588 amino-acid human Htt with 138 repeats, suggesting a loss-of-function associated with the expanded polyglutamine tract in the Htt protein.

The change in mitochondrial flux does not alter distribution or concentration of mitochondria: An increase in retrograde flux and decrease in anterograde flux of mitochondria in dHtt mutants would predict that mitochondria may be depleted from the synapse. To test this hypothesis, C380-GAL4;UASmito-GFP;dHtt$^{-/-}$ and control third instar larvae were stained with HRP to label neuromuscular junctions, and the number of mitochondria per NMJ area was found to be similar for both genotypes (Figure 3A, C). Changes in flux could also alter the total number of motile mitochondria moving through the axon. Recovery of mitochondria in a bleached region of axon six minutes after photobleaching shows that null motor neurons lacking dHtt have the same number of motile mitochondria as control (Figure 3B, C).

Htt has been implicated in mitochondrial fission and fusion which is postulated to have effects on transport (Knott and Bossy-Wetzel 2008; Song, Chen et al. 2011). To assay for changes in fission/fusion, the average size and shape of mitochondria, and the distribution of sizes was measured at the synapse and along the axon. Both parameters were similar in control and null animals suggesting the loss of dHtt does not alter mitochondrial fission or fusion.

Since having more retrograde than anterograde transport is not sustainable without depletion from the synapse or increased fission, it would seem that altered mitochondrial flux may vary during development, or the third instar stage is too early for accumulation of significant differences in mitochondrial number.

Run analysis of mitochondrial movements suggests a role for dHtt in mitochondrial processivity: To more accurately assay for effects of dHtt on axonal transport, individual

mitochondria were tracked manually in each frame of time-lapse image series to determine changes in run distance, run duration, and velocity (Figure 4). Similar manual tracking analyses of mitochondria have been described previously and revealed defects in transport in various mutant genotypes in *Drosophila* (Barkus, Klyachko et al. 2008; Colin, Zala et al. 2008; Russo, Louie et al. 2009).

Loss of dHtt results in decreased run distance and duration for both anterograde and retrograde mitochondrial movements with a slightly greater decrease in anterograde run distance and duration (Figure 4 A, B), suggesting that either the motor or the cargo processivity is decreased.

Loss of dHtt also results in increased run velocity, which is an average of instantaneous velocity measurements while a mitochondrion is in motion (Figure 4 C, D). Under normal conditions, mitochondria move at a variety of speeds with a normal distribution from -1.0 µm/s to 1.0 µm/s, with the mode occurring at 0 µm/s, as about 40% of mitochondria in motor axons are stationary. In dhtt null animals, the distribution is widened, resulting in an increase in the percentage of the fastest moving mitochondria and a decrease in the percentage of slowest moving mitochondria (Figure 4D). However, the maximum and minimum velocities for mitochondria and thus kinesin or dynein are not significantly altered. These data make it unlikely that dHtt is altering properties of kinesin and dynein motors, but rather the poorly understood mechanisms of cargo attachment or motor coordination. These results argue that Htt regulates mitochondrial processivity by either (a) acting as a cargo adapter, (b) regulating the attachment of motile mitochondria to motors, (c) regulating the coordination of kinesin and dynein motor movements, or (d) as a modifier of motor velocity.

We next analyzed the kinetics of transport for synaptic vesicle and dense core vesicles in dhtt null larvae to evaluate cargo specificity. Synaptic vesicles co-localize with dHtt and show altered

kinetics in dhtt null animals similar to mitochondria, while dense core vesicles do not co-localize with dHtt and do not show altered transport kinetics (Table 1). Since dHtt shows co-localization with synaptic vesicles and mitochondria, and has similar effects on cargo processivity, we would expect dHtt to similarly affect their velocity if it were acting by altering motor kinetics. However, we do not see global changes in organelle velocity, nor do we see anterograde (kinesin) or retrograde (dynein) specific defects. This suggests that dHtt is likely altering cargo attachment, rather than motor velocity.

Track analysis of mitochondrial kinetics reveals defects in cargo attachment and motor coordination: Previous measurements on run kinetics focused only on mitochondria in motion, while track analysis looks at the entire track of an individual mitochondrion from the time it enters the bleached area until it leaves the opposite side. This includes measurements of all runs, stops, and reversals and provides a measure for motor processivity and coordination over a 50 µm range. All mitochondria are imprinted with a specific directionality, either primarily retrograde or anterograde, while occasionally they pause or move in the opposite direction in short movements called reversals (Morris and Hollenbeck 1993). Using track analysis, we find an increase in the number of stops (Figure 5A), suggesting a defect in cargo processivity. We also see an increase in reversals (Figure 5B) suggesting a defect in motor coordination. We observe these effects for mitochondria and synaptic vesicles but not dense core vesicles (Figure 5 and Table 1).

Track analysis also yields the displacement rate, which is the total distance over total time an individual mitochondria moved over $t \geq 60s$. By averaging the increased velocity and increased stops over an entire track we observe a compensatory effect where these values offset one another, such that the displacement rate is not altered in anterograde moving mitochondria, but

slightly increased in retrograde moving mitochondria (Figure 5C). By defining the duty cycles of mitochondrial movement, we calculated the percentage of time spent moving in the imprinted direction, the amount of time in the reverse direction, and the amount of time stopped. We observe an increase in the amount of time spent stopped and going in the reverse direction for both anterograde and retrograde imprinted mitochondria, though only the increases in the anterograde direction were statistically significant (Figure 5D).

Dense core vesicles display a retrograde to anterograde shift in flux, suggesting broader effects on transport: We have shown that dHtt can alter the flux and velocity of mitochondria, a FAT cargo with which it co-localizes. To determine if Htt plays a more global role in regulating trafficking, we also assayed for changes in flux of ANF-tagged dense core vesicles, which show a low degree of co-localization with dHtt (Table 1). Velocity, run lengths, stops and reversals were normal for dense core vesicles, suggesting that the effects dhtt has on cargo processivity are local and mediated by direct interactions between dHtt, cargos, motors, and other adapters.

Contrary to the model that dHtt seems to exert its effects on transport locally, dense core vesicles also show a similar flux phenotype as mitochondria, with a nearly twofold increase in the ratio of retrograde to anterograde moving particles (Table 1). This effect was seen for all organelles studied, and may reflect more global changes in transport related to dHtt function. A possible explanation for this result is that dynein heavy chain levels are increased in dHtt null aged adults. Western blots for dynein heavy chain show an increase in expression in 20 day old aged adults (Figure 6 A, B). Altered dynein levels are also seen to a lesser extent in 10 day aged adults, but not seen in larval preparations (data not shown). Western blots on larval preparations contain a relatively small amount of motor neuron matter compared to adults, so it is possible the assay

was not sensitive enough to detect statistical significance. The data suggests a potential

mechanism whereby loss of dHtt may cause increased dynein levels that increase the retrograde

to anterograde flux of all FAT cargos dependent on dynein-mediated retrograde transport. This

data correlates well with the dHtt adult locomotion phenotype previously described, showing that

dhtt null adults appear normal at 1-5 days old, but develop moderately decreased movement at 10

days, and severely decreased movement at 20 days (Zhang, Feany et al. 2009). Kinesin levels

remain unchanged in dhtt null aged adults (Figure 6 C, D).

HAP1 is not required for dHtt localization to axons: To begin mapping the physical

interactions required for Htt-motor-cargo complex formation we sought to determine if the

interaction between dHtt and HAP1 or mitochondria was necessary for dHtt localization to the

axons. The *Drosophila* homolog of HAP1 is Milton, which is required for proper localization of

mitochondria to axons (Figure 7A) (Stowers, Megeath et al. 2002). In *milton* LOF mutants

($milt^{92}$), mitochondria are concentrated in the cell body and do not enter the axons. Despite the

lack of HAP1 (Milton) or mitochondria in the axon, both dHtt and Q15Htt are found within

axons (Figure 7B, C). Both human and *Drosophila* N-terminal fragments tested are competent to

bind HAP1, as the HAP1 binding domain of Htt was identified as being within the first 230

amino acids of the Htt protein (Li, Li et al. 1995). These findings suggest dHtt is transported

along axons independent of HAP1 or mitochondrial interactions.

Discussion

Given the specific co-localization pattern between Htt and FAT cargos, and the ability of full-

length human Htt to rescue dhtt null defects in mitochondrial flux, our data indicate that dHtt is

likely a functional homolog of human Htt. Functional redundancy has also been shown in

another context where dHtt can rescue human Htt defects in mitotic spindle orientation (Godin,

Colombo et al. 2010). Rescue experiments on the flux phenotype reveal that while an N-terminal region of dHtt can rescue altered mitochondrial flux, an N-terminal human Htt fragment of similar size with expanded polyQ cannot, suggesting a possible loss of function due to expanded polyQ in Htt (Fig 2B).

We also identify axonal transport properties that are altered when expanded polyQ Q138Htt is expressed, suggesting a potential role for defective axonal transport in HD pathology. The reduced interaction between Q138Htt and mitochondria demonstrates a loss of function phenotype that results in fewer mitochondria in the axon, while dense core vesicles display a gain-of-function, whereby they become associated with Q138Htt aggregates. All cargo become susceptible to blockage of transport by large Q138 aggregates in a bi-directional manner in motor axons (Figure 1).

A caveat to our co-localization studies is that co-localization is based on overlaps with Htt puncta. Endogenous Htt is expressed at relatively low levels in human and mouse brains (Bhide, Day et al. 1996) and low level expression of our transgenes results in a diffuse expression pattern without visible puncta. While Htt puncta only co-localize with a subset of cargos, it is possible that diffuse soluble Htt molecules not directly visible by fluorescent light microscopy may co-localize with additional cargos.

We demonstrate for the first time *in vivo* that loss of dHtt causes defects in axonal transport. Our results indicate that dHtt functions as a positive regulator of fast axonal transport of mitochondria and synaptic vesicles, as loss of dHtt results in increased stops and shortened runs for these organelles (Fig 4, 5, table 1). Specifically, this data suggests a role of dHtt in regulating processivity of these cargos. dHtt exerts this effect locally, as we only see this phenotype for organelles which co-localize with dHtt. Since our results indicate endogenous dHtt is

simultaneously playing a negative regulatory role in velocity and a positive role in processivity, it suggests dHtt is acting as a scaffold to coordinate both positive and negative regulators of organelle movement as has been suggested previously (Harjes and Wanker 2003). Further analysis is required to evaluate the state of stationary mitochondria, the microtubule network and mitochondrial health, though preliminary results indicate these are normal.

While we observe velocity changes in both directions the greatest increase in velocity was measured in retrograde moving mitochondria. In contrast, the greatest decrease in run processivity was in anterograde movements. Thus, the net effect observed was reduced anterograde flux and increased retrograde flux. These results agree with those presented by Colin et al 2008, suggesting Htt functions as a 'molecular switch' in controlling anterograde and retrograde transport of BDNF and APP. These experiments in cell culture demonstrated when ser421 of Htt is phosphorylated, anterograde transport was favored, when ser421 was not phosphorylated, retrograde transport is favored (Colin, Zala et al. 2008). Our mutant might represent a similar situation as the unphosphorylated version of Htt in the experiments by Colin et al, increasing retrograde transport, and while we did not confirm the phosphorylation state of dHtt, we also see functional Htt acting as a positive regulator of anterograde transport.

Changes in mitochondria velocity induced by loss of dHtt may reflect a compensatory mechanism by which mitochondria move faster in each run to make up for the increased stops and decreased run lengths. By comparing individual mitochondrial run lengths with their corresponding velocities there is a weak negative correlation whereby shorter runs tend to have faster velocities, though this is not always the case (data not shown). The increase in velocity is also correlated with increased dynein motor expression. The exact mechanisms regulating motor velocity are not well understood, but motor movement has been shown to be cooperative,

allowing increased force and velocity with increasing concentration (Gagliano, Walb et al. 2010). Motor velocity is also known to be affected by load (Svoboda and Block 1994) and the presence of microtubule-associated proteins, such as the p150Glued subunit of dynactin which binds dynein (Culver-Hanlon, Lex et al. 2006), as well as the efficiency of ATP hydrolysis (De Vos, Chapman et al. 2007). Any of these could represent mechanisms whereby Htt could regulate mitochondrial velocity by mediating interactions between mitochondria and regulatory proteins.

We observe loss of dHtt is associated with an increase in dynein expression. It is possible that the increase in dynein is simply a compensatory mechanism for a defect in normal retrograde transport specific neurotrophic factors, although the role of neurotrophic factors in invertebrate systems is not well characterized (Zhu, Pennack et al. 2008). This hypothesis would predict that dHtt null motor neurons exhibit a decrease in retrograde transport of some specific neurotrophic-like factor, and that the increase in retrograde transport of mitochondria, synaptic vesicles, and dense core vesicles is a side-effect of increased dynein to boost retrograde neurotrophin transport. Htt has a well-established role in brain derived neurotrophic factor (BDNF) transport in mammalian systems (Reilly 2001; Zuccato and Cattaneo 2007; Pardo, Molina-Calavita et al. 2010).

Transport kinetics in our Htt mutant are altered for both anterograde and retrograde moving organelles, suggesting dHtt is interacting with both kinesin and dynein motors. In general, it appears that dHtt has more cargo specific effects than motor specific effects, but the question of whether Htt regulates processivity and motor coordination by regulating the attachment of motors to the microtubule track, or the attachment of motors to cargo, is still not clear.

We observe an increase in the number of stops for mitochondria and synaptic vesicles, suggesting that dHtt functions to control attachment of cargos to motors, or motors to microtubules, to regulate movement between anterograde, retrograde, and paused states of motion. While the exact mechanisms that control organelle movement and distribution are not clear, it has been suggested that adapter molecules are necessary to regulate the movement of organelles such as mitochondria (Hollenbeck and Saxton 2005). Several adapter molecules have been identified for mitochondria, including Milton (HAP1), which is required for mitochondrial localization to the axon (Stowers, Megeath et al. 2002), and Miro, which has been demonstrated to control mitochondrial responses to calcium (Russo, Louie et al. 2009). While HAP1 controls binding of mitochondria to the motor, Miro has been shown to control binding of the motor to the microtubule track. It is not clear if dHtt is controlling motor-microtubule interactions or cargo-motor interactions to regulate organelle processivity, as both models have been established (Rice and Gelfand 2006). Biochemical experiments probing motor-cargo and motor-microtubule interactions in the absence of Htt will shed light on this question. One study on the effects of mutant Htt on axonal transport suggests that Htt may regulate the interaction between motors and microtubules. Overexpression of pathogenic Htt with an expanded poly-glutamine tract was found to activate a neuron-specific cJun N-terminal kinase (JNK3), which phosphorylates kinesin-1 and reduces its binding to microtubules, suggesting that wild-type Htt may also facilitate motor-microtubule interactions (Morfini, You et al. 2009).

Htt may function in motor coordination, in addition to cargo-motor binding. Evidence against a specific role in cargo-motor binding comes from the observation that we do not see a decrease in the number of mitochondria or synaptic vesicles in axons or nerve terminals lacking dHtt, as would be expected with defective cargo binding (Figure 3). We also do see significant effects on

reversals, which would imply altered motor switching. Bidirectional transport mechanisms are not well defined, but the ability to coordinate anterograde and retrograde movement of motors on a particular organelle is essential as organelles must alternate between anterograde and retrograde movement for proper localization within the neuron. Evidence suggests that kinesin and dynein motors are both present on several organelles. Mitochondria extracted from a neuroblastoma cell line and used in transport assays were able to move in both anterograde and retrograde directions and contain both kinesin and dynein (De Vos, Sable et al. 2003). A subset of the vesicle population in cultured mammalian neurons was also determined to be bound by both kinesin and dynein motors and direct interactions between kinesin and dynein have shown by yeast two-hybrid and pull down assays (Ligon, Tokito et al. 2004). Thus, the coordination between motors is an essential aspect of bidirectional transport that is not well understood, and may be mediated in part through Htt dependent interactions.

Another important question is whether Htt localization is specific to distinct cargos or motors. While we see cargo specificity for Htt (Fig1), Htt may also display motor specificity. In this model, Htt may be altering motor activity or attachment of specific kinesin and dynein variants. KIF5 (conventional kinesin-1) and KIF1-B are known to be responsible for anterograde mitochondrial transport (Pilling, Horiuchi et al. 2006), while KIF1-A (*Drosophila* UNC-104) is the primary motor for anterograde transport of dense core vesicles and synaptic vesicles (Pack-Chung, Kurshan et al. 2007; Barkus, Klyachko et al. 2008). Together with our results, this data demonstrates that dHtt can associate with different kinesins and different cargos, but cargo association seems primary to motor association since dHtt does not associate with all KIF1-A cargos. However, these motor assignments are not absolute, while 'primary motors' can often be assigned to a specific cargo, the extent of functional redundancy and overlap between them is not

known. There likely 15 -30 unique members of the kinesin family which may yield even greater protein variety considering splice isoforms (Endow and Hatsumi 1991).

Mapping Htt binding partners and its physical location in the motor-cargo complex is essential to understanding Htt function. Htt has been shown to interact indirectly with the molecular motors kinesin (McGuire, Rong et al. 2006) and dynein/dynactin (Engelender, Sharp et al. 1997) via its interaction with HAP1. We find that dHtt and Q15Htt are able to localize within axons without functional HAP1, suggesting that the interaction between HAP1 and Htt is not necessary to physically link Htt to the fast axonal transport machinery (Figure 7). HEAT repeats located throughout the Htt protein provide many potential sites of interaction to directly or indirectly bind motor complexes. For example, amino acids 600-698 of Htt are predicted to be the binding domain of dynein intermediate chain, which may link Htt directly to the dynein motor complex (Caviston, Ross et al. 2007).   Htt is also known to interact with membrane bound organelles through its N-terminal 17 amino acids (Rockabrand, Slepko et al. 2007) . Together, these results suggest the Htt protein may couple to both molecular motors and membrane bound organelles, coordinating signaling and attachment to regulate bi-directional transport. Mitochondrial transport and energy metabolism defects are especially interesting in HD pathology as defects in oxidative phosphorylation has been demonstrated to be especially detrimental to the striatum compared to the cortex or hippocampus, suggesting relevance to the cell specific neurodegeneration seen in HD (Pickrell, Fukui et al. 2011). Since the loss of Htt phenotype is relatively modest and generally results in late-onset neurodegeneration, it is likely that other proteins play redundant functions in transport. Future double mutant analysis to generate synthetic transport phenotypes should provide insight into redundancy with other transport mechanisms.

Acknowledgements
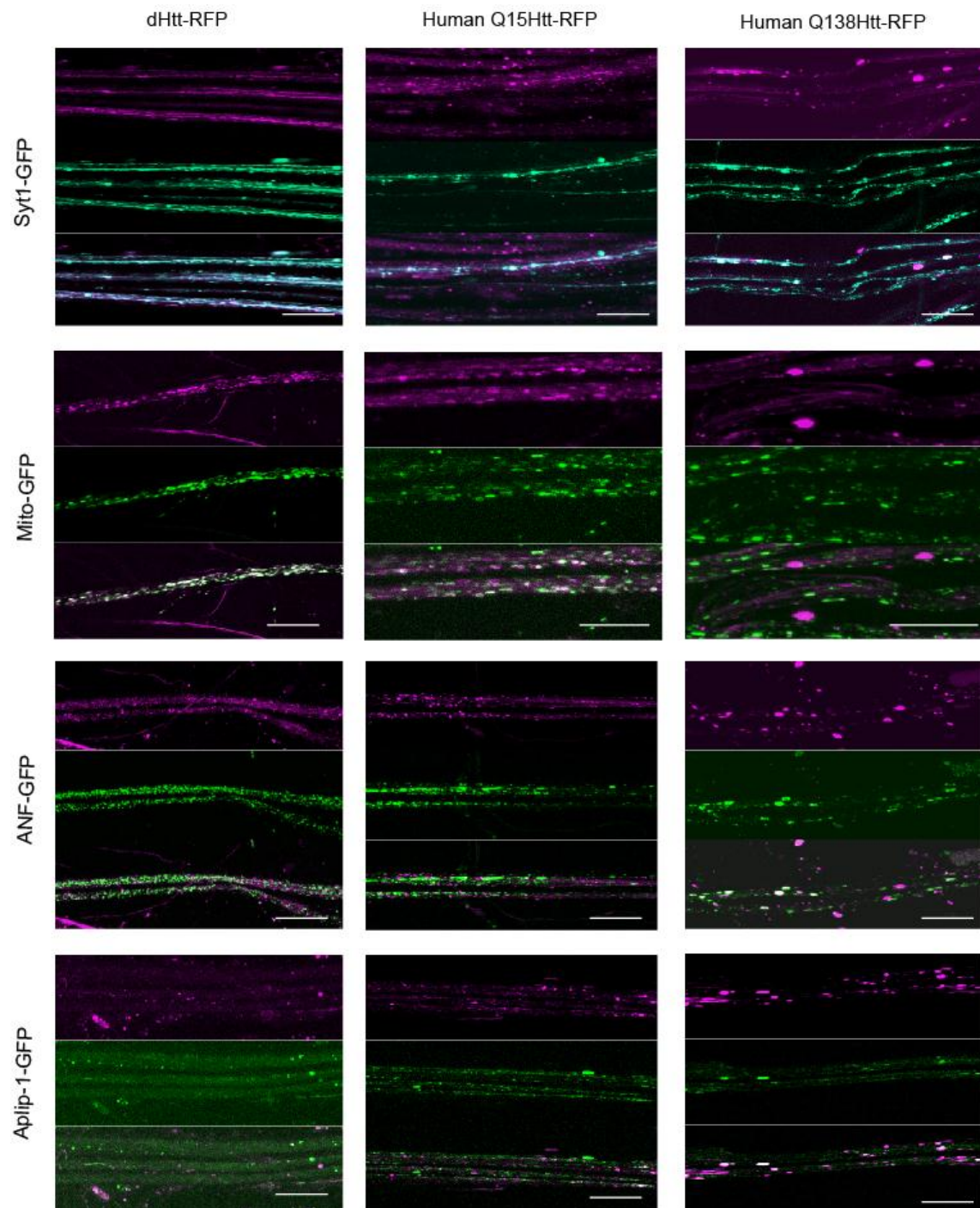
Figure 1

Figure 1. *Drosophila* and human huntingtin show similar co-localization patterns. Co-expression of an N-terminal 665 amino acid fragment of *Drosophila* huntingtin or an N-terminal 588 amino acid fragment of normal (Q15) or disease (Q138) human huntingtin with several fast axonal transport cargos tagged with GFP and driven by the C380-GAL4 motor neuron driver are shown. Synaptic vesicles and mitochondria show a high degree of co-localization, while dense-core vesicles and APLIP-1 show little to no co-localization. Q138Htt shows a decreased association with mitochondria and increased association with dense core vesicles and APLIP-1 at sites of aggregation. Scale bar = 20 µm.
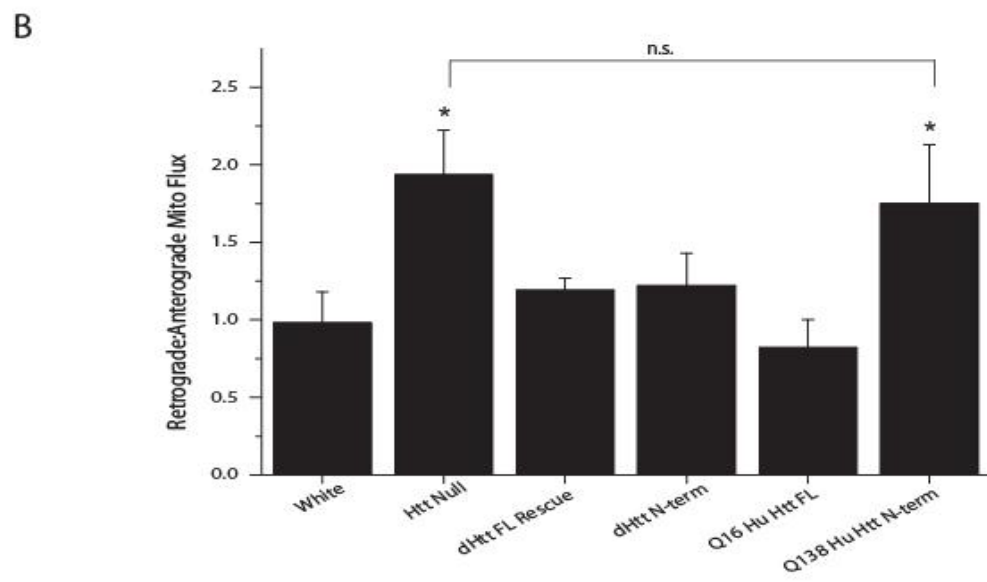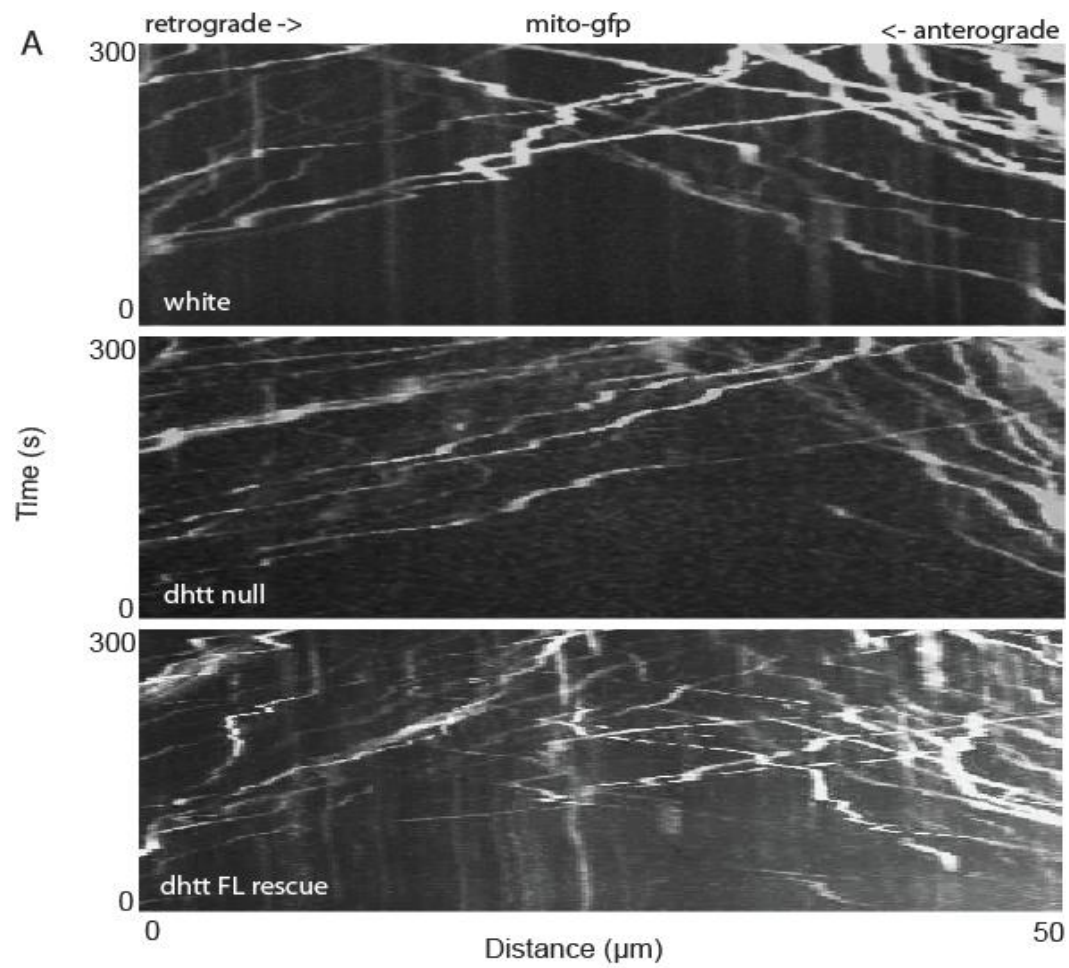
Figure 2

Figure 2. Kymographs made from time-lapse images of mitochondrial movement (mito-gfp) in third instar motor neurons show an increase in the number of retrograde moving mitochondria and a decrease in the number of anterograde moving mitochondria in dHtt null larvae versus control or rescue (A). Quantification of the number of mitochondria moving retrograde divided by the number of mitochondria moving anterograde yields the retrograde: anterograde flux measurement, which was used to assess the ability of several *Drosophila* and human Htt constructs to rescue the Htt null phenotype (B). Error bars represent SEM, * indicates $p<.05$ compared to control with a Student's t-test.

Figure 3

A   Control   Htt Null

B   Control

Htt Null

C
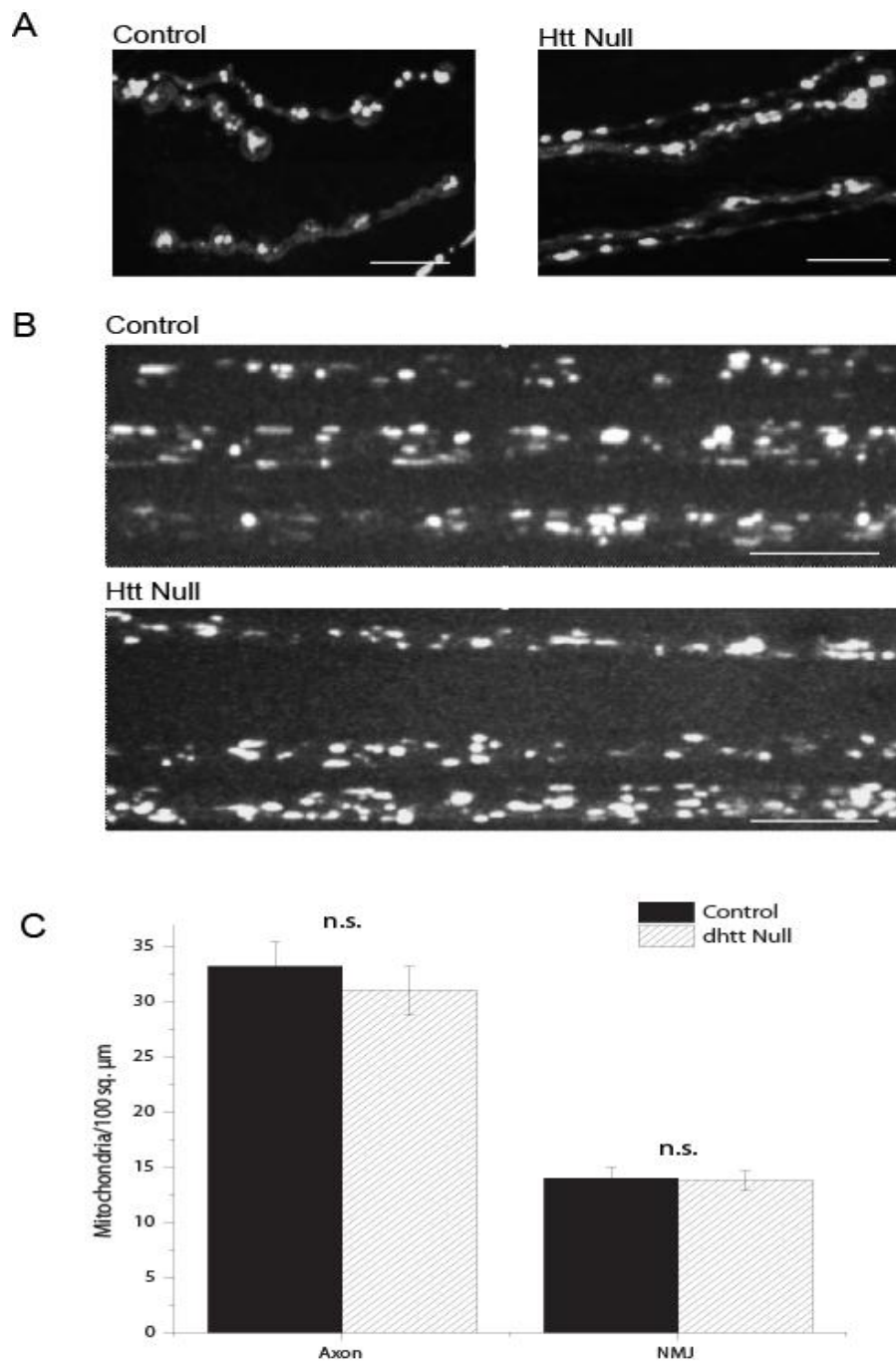
Figure 3. Mito-GFP expressed under the C380-GAL4 motor neuron driver shows mitochondria at nerve terminals stained with HRP-RFP (A) or in axons (B). dhtt null larvae do not display an altered concentration of mitochondria at the nerve terminus or along the axon (C). Scale bar = 10 μm. Error bars represent SEM.

Figure 4
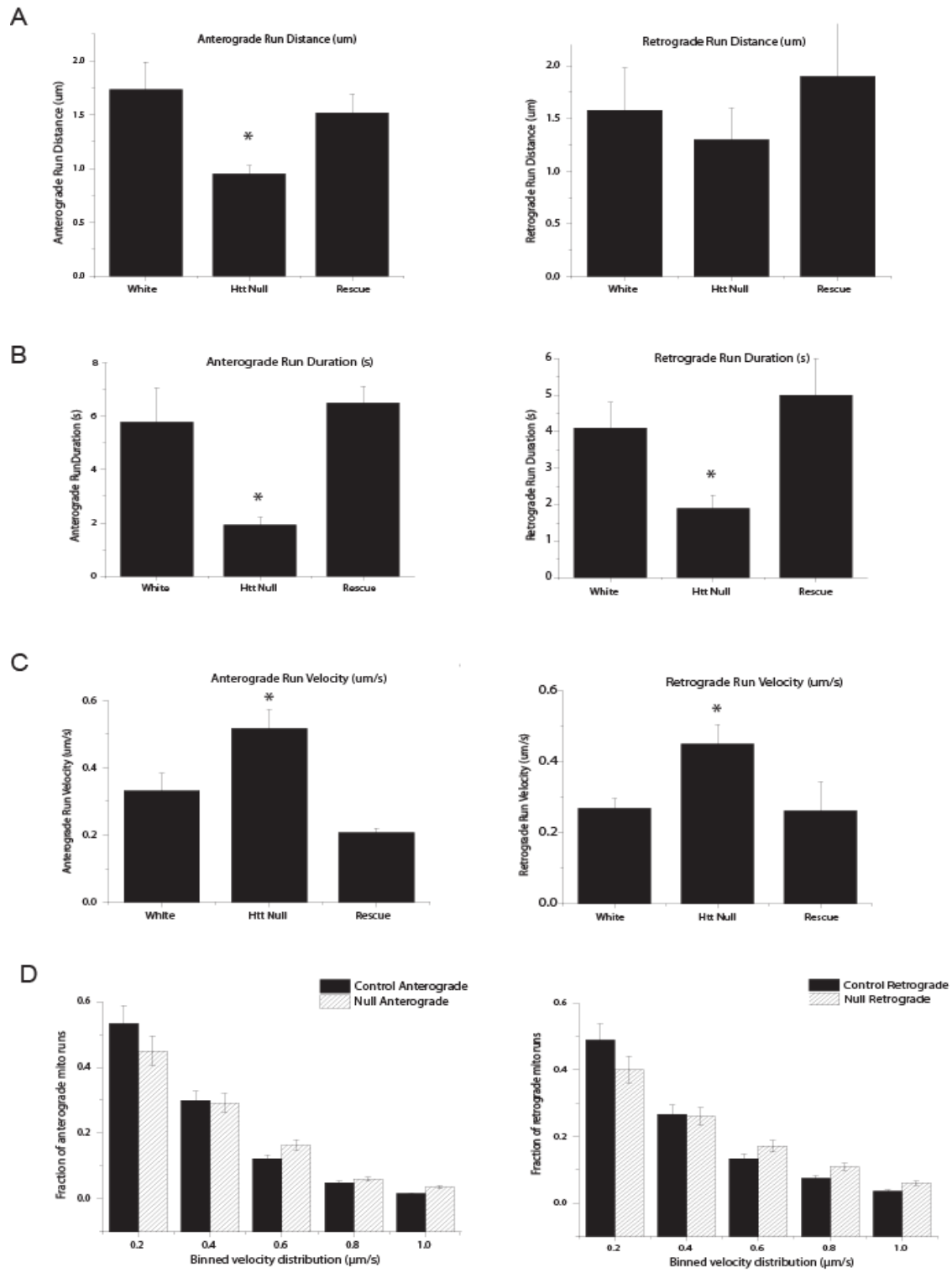
Figure 4. Run data was collected from individual mitochondria tracked in each one second frame of a 300 image confocal time series for at least 60 time points from third instar motor neuron axons. The tracks were then used to calculate run distance, duration, and velocity for white, dHtt null, and a dHtt full-length rescue construct with the endogenous *huntingtin* promoter. dHtt null larvae showed a decrease in run distance (A) and duration (B) and an increase in velocity (C). The increase in average velocity was the result of a shift in the velocity distribution of all moving mitochondria (D). The N=10 larvae per genotype and 12 mitochondria per larvae. Error bars represent SEM, * indicates $p < .05$ for a Student's t-test.

Table 1

	Anterograde			Retrograde		
	control	dhtt null	dhtt rescue	control	dhtt null	dhtt rescue
Synaptic Vesicles						
Flux (particles/min)	16 ± 4.0	12* ± 3.2	17 ± 3.7	6.1 ± 1.5	8.3* ± 1.0	6.2 ± 1.6
Run Distance (μm)	14.1 ± 2.1	10.2* ± 1.8	15.7 ± 2.5	7.6 ± 1.2	7.8 ± 1.1	7.9 ± 1.9
Run Duration (s)	12.7 ± 1.1	7.8* ± 1.0	11.5 ± 1.9	9.1 ± 0.6	8.0 ± 1.0	8.6 ± 1.7
Velocity (μm/s)	0.85 ± 0.09	0.82 ± 0.08	0.86 ± 0.08	0.70 ± 0.08	0.74 ± .07	0.66 ± 0.07
Stops (per min)	5.1 ± 1.1	8.0* ± 1	4.1 ± 0.9	6.5 ± 0.9	8.2 ± 0.9	7.0 ± 0.9
Reversals (per min)	2.3 ± 0.9	2.3 ± 0.8	2.2 ± 0.8	8.2 ± 2.1	8.3 ± 1.9	7.9 ± 1.7
Dense Core Vesicles						
Flux (particles/min)	22 ± 1.8	18* ± 1.7	21 ± 2.2	8.1 ± 1.0	11* ± 2.1	7.6 ± 1.3
Run Distance (μm)	12 ± 1.7	11 ± 1.2	11 ± 1.4	10 ± 1.1	11 ± 1.4	9.8 ± 1.2
Run Duration (s)	8.1 ± 1.0	7.1 ± 0.9	8.7 ± 1.4	7.2 ± 1.5	6.3 ± 0.9	6.1 ± 1.4
Velocity (μm/s)	0.75 ± 0.08	0.77 ± 0.08	0.72 ± 0.1	0.69 ± .07	0.72 ± .07	0.64 ± .07
Stops (per min)	6.1 ± 0.4	6.0 ± 0.3	7.0 ± 0.5	7.2 ± 0.5	6.5 ± 0.4	7.0 ± 0.5
Reversals (per min)	2.2 ± 0.8	2.3 ± 0.	2.5 ± 0.7	5.5 ± 0.5	5.1 ± 0.5	5.9 ± 0.5

Table 1. Summary of transport kinetics for live tracking of synaptic vesicles (Syt-1-GFP) and

dense core vesicles (ANF-GFP) expressed with the CCAP-GAL4 driver. Similar to

mitochondrial transport analysis, a region of bleached axon was allowed to recover for 60

seconds and GFP-tagged organelles were tracked manually as they entered the bleached region.

N=100 particles for each genotype. * indicates $p \leq .05$. Error given as ±SEM.

Figure 5
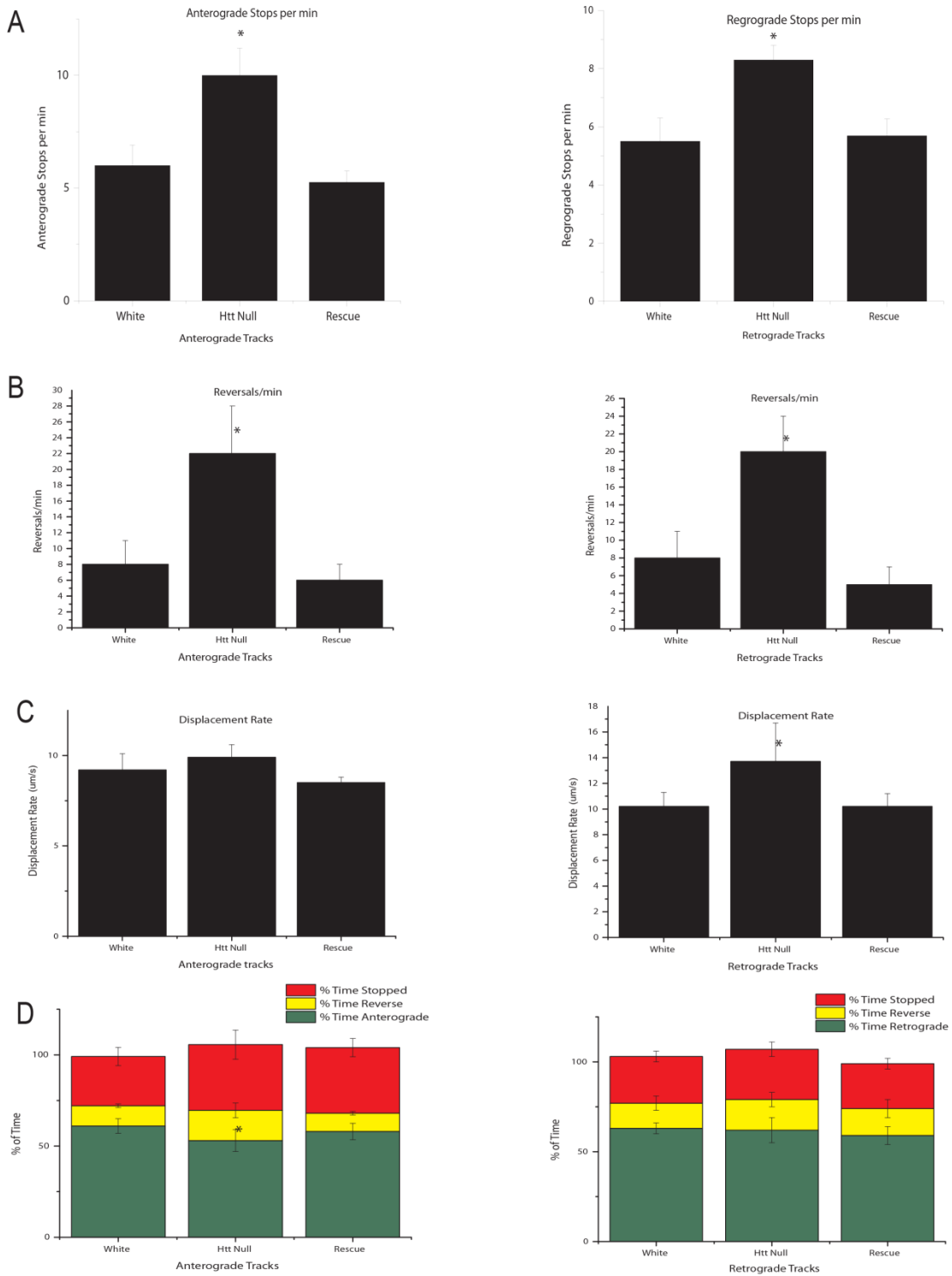
Figure 5. Track analysis for anterograde and retrograde moving mitochondria. Tracks represent three states of mitochondrial movement for individual mitochondria tracked over its entire track length, including movement in the primary direction, reverse direction, and stops. Loss of dHtt results in an increase in stops, which suggests a defect in processivity (A), and an increase in reversals, which suggests a defect in motor coordination (B). The displacement rate, or total track distance over time is increased for retrograde moving mitochondria (C). The percentage of time the average mitochondria spent in each of the three states of motion was calculated, revealing an increase in time stopped and reversals for dhtt null animals (D). Since these stops and reversals were short lived (generally one to two seconds), the percentage of time spent in these states did not change as drastically as the absolute number of events (compare D to A and B). N=100 particles for each genotype. * denotes $p \leq .05$. Error given as ±SEM.

Figure 6
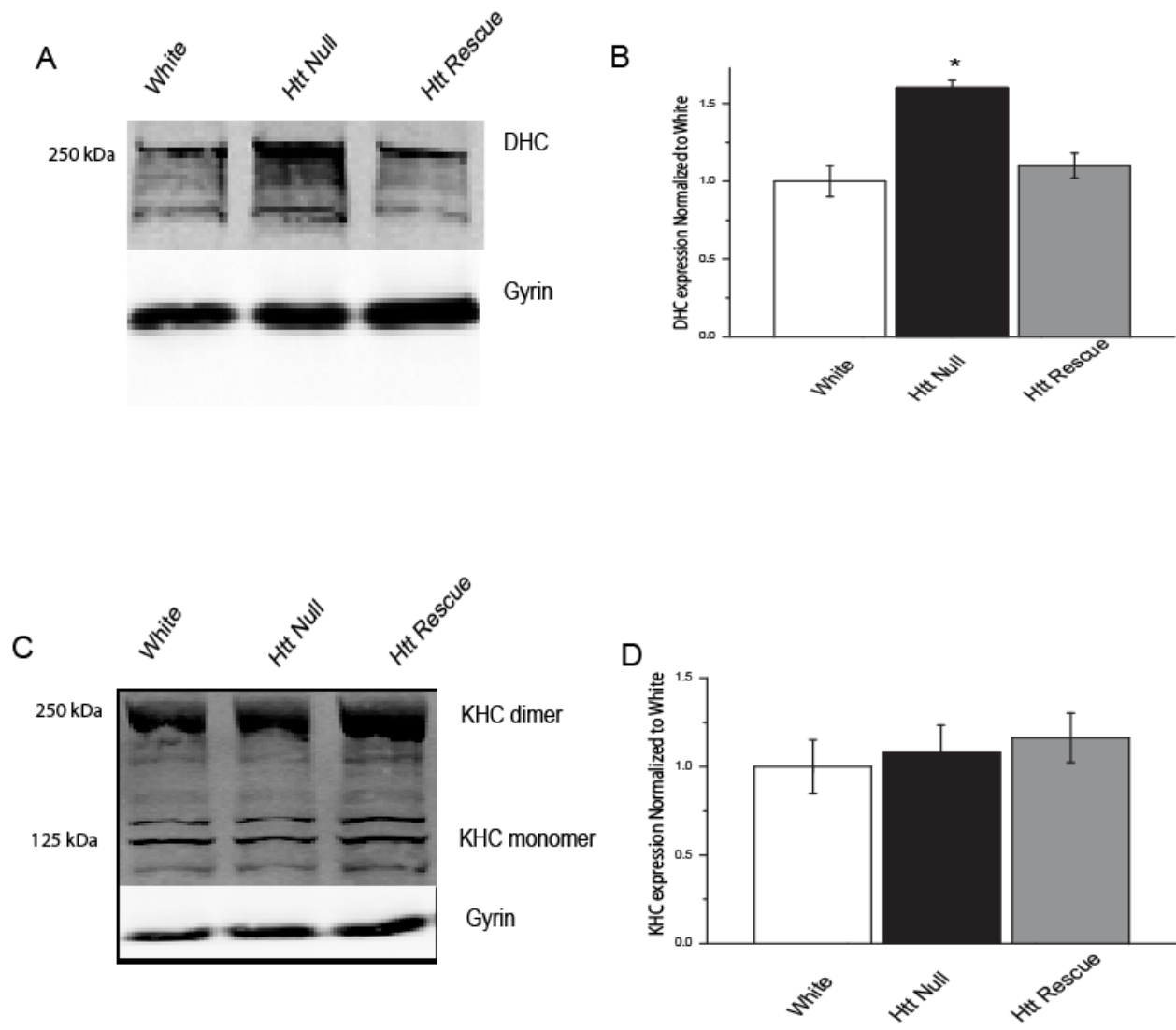
Figure 6. Dynein heavy chain levels are increased in Htt null aged adult. Adult heads from 20 day old flies were processed by Western blot and blotted for dynein heavy chain (A). Quantification of five separate western blot measurements normalized to white (B). Levels of kinesin heavy chain monomer and dimer were not changed in dHtt null aged adults (C, D).

Figure 7
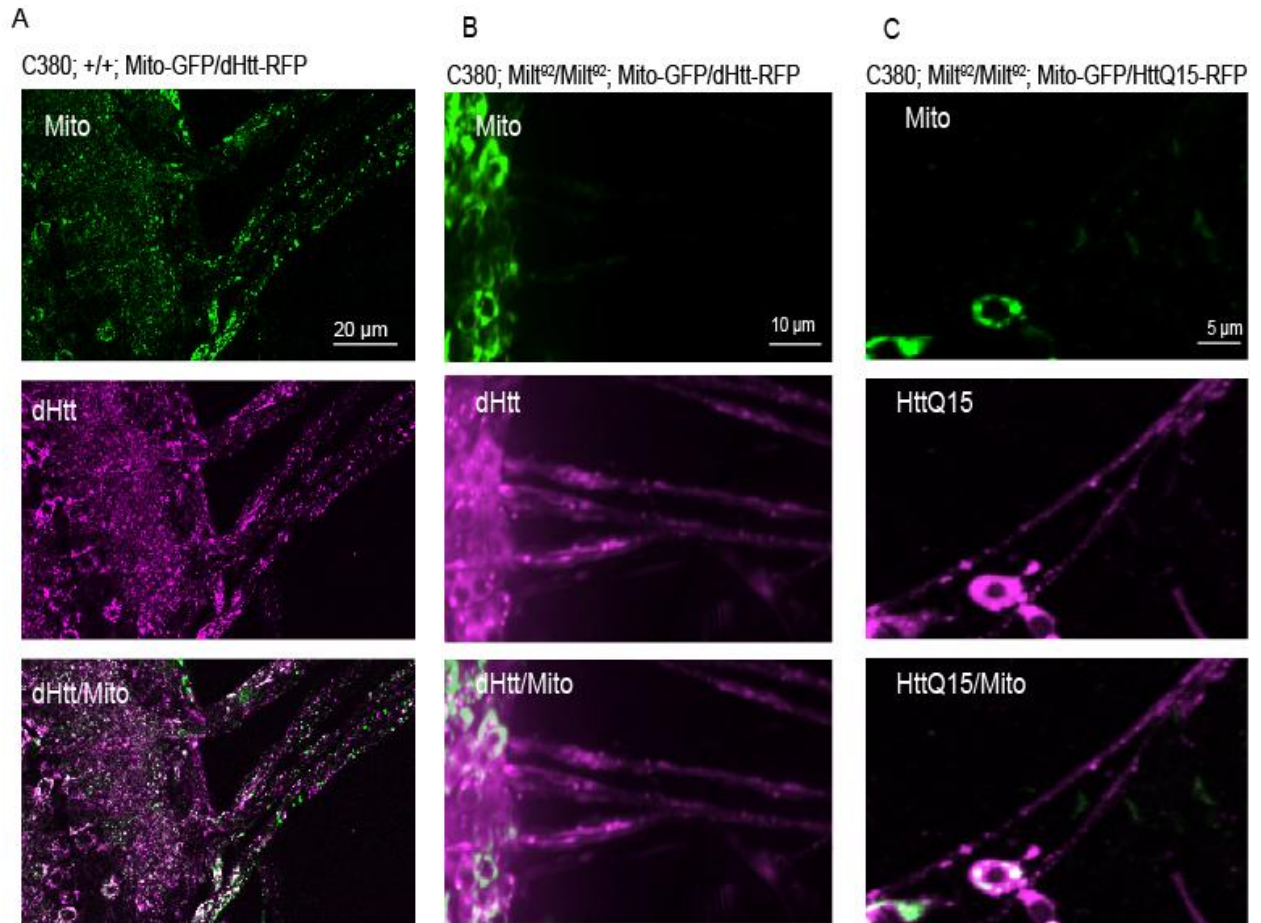
Figure 7. Neither mitochondria nor HAP1 is required for dHtt or Q15Htt localization to axons. Expression of Mito-GFP in motor neurons in a wild-type background shows an even distribution of mitochondria throughout the cell body and axon (A). In a *milt*^{92} background without functional Milton (HAP1) present, mitochondria are seen localized cell body while both dHtt (B) and human Q15Htt (C) are seen properly localized throughout the cell body and axonal processes.

References

Andrade, M. A., C. Perez-Iratxeta, et al. (2001). "Protein repeats: structures, functions, and evolution." <u>J Struct Biol</u> **134**(2-3): 117-131.

Andrade, M. A., C. Petosa, et al. (2001). "Comparison of ARM and HEAT protein repeats." <u>J Mol Biol</u> **309**(1): 1-18.

Barkus, R. V., O. Klyachko, et al. (2008). "Identification of an axonal kinesin-3 motor for fast anterograde vesicle transport that facilitates retrograde transport of neuropeptides." <u>Mol Biol Cell</u> **19**(1): 274-283.

Bhide, P. G., M. Day, et al. (1996). "Expression of normal and mutant huntingtin in the developing brain." <u>J Neurosci</u> **16**(17): 5523-5535.

Brand, A. H. and N. Perrimon (1993). "Targeted gene expression as a means of altering cell fates and generating dominant phenotypes." <u>Development</u> **118**(2): 401-415.

Caviston, J. P., J. L. Ross, et al. (2007). "Huntingtin facilitates dynein/dynactin-mediated vesicle transport." <u>Proc Natl Acad Sci U S A</u> **104**(24): 10045-10050.

Caviston, J. P., A. L. Zajac, et al. (2011). "Huntingtin coordinates the dynein-mediated dynamic positioning of endosomes and lysosomes." <u>Mol Biol Cell</u> **22**(4): 478-492.

Colin, E., D. Zala, et al. (2008). "Huntingtin phosphorylation acts as a molecular switch for anterograde/retrograde transport in neurons." <u>EMBO J</u> **27**(15): 2124-2134.

Culver-Hanlon, T. L., S. A. Lex, et al. (2006). "A microtubule-binding domain in dynactin increases dynein processivity by skating along microtubules." <u>Nat Cell Biol</u> **8**(3): 264-270.

De Vos, K. J., A. L. Chapman, et al. (2007). "Familial amyotrophic lateral sclerosis-linked SOD1 mutants perturb fast axonal transport to reduce axonal mitochondria content." <u>Hum Mol Genet</u> **16**(22): 2720-2728.

De Vos, K. J., J. Sable, et al. (2003). "Expression of phosphatidylinositol (4,5) bisphosphate-specific pleckstrin homology domains alters direction but not the level of axonal transport of mitochondria." <u>Mol Biol Cell</u> **14**(9): 3636-3649.

Dragatsis, I., A. Efstratiadis, et al. (1998). "Mouse mutant embryos lacking huntingtin are rescued from lethality by wild-type extraembryonic tissues." <u>Development</u> **125**(8): 1529-1539.

Dragatsis, I., M. S. Levine, et al. (2000). "Inactivation of Hdh in the brain and testis results in progressive neurodegeneration and sterility in mice." <u>Nat Genet</u> **26**(3): 300-306.

Duyao, M. P., A. B. Auerbach, et al. (1995). "Inactivation of the mouse Huntington's disease gene homolog Hdh." <u>Science</u> **269**(5222): 407-410.

Endow, S. A. and M. Hatsumi (1991). "A multimember kinesin gene family in Drosophila." <u>Proc Natl Acad Sci U S A</u> **88**(10): 4424-4427.

Engelender, S., A. H. Sharp, et al. (1997). "Huntingtin-associated protein 1 (HAP1) interacts with the p150Glued subunit of dynactin." <u>Hum Mol Genet</u> **6**(13): 2205-2212.

Fuger, P., L. B. Behrends, et al. (2007). "Live imaging of synapse development and measuring protein dynamics using two-color fluorescence recovery after photo-bleaching at Drosophila synapses." <u>Nat Protoc</u> **2**(12): 3285-3298.

Gagliano, J., M. Walb, et al. (2010). "Kinesin velocity increases with the number of motors pulling against viscoelastic drag." <u>Eur Biophys J</u> **39**(5): 801-813.

Godin, J. D., K. Colombo, et al. (2010). "Huntingtin is required for mitotic spindle orientation and mammalian neurogenesis." <u>Neuron</u> **67**(3): 392-406.

Gunawardena, S., L. S. Her, et al. (2003). "Disruption of axonal transport by loss of huntingtin or expression of pathogenic polyQ proteins in Drosophila." Neuron **40**(1): 25-40.

Harjes, P. and E. E. Wanker (2003). "The hunt for huntingtin function: interaction partners tell many different stories." Trends Biochem Sci **28**(8): 425-433.

Hollenbeck, P. J. and W. M. Saxton (2005). "The axonal transport of mitochondria." J Cell Sci **118**(Pt 23): 5411-5419.

Horiuchi, D., R. V. Barkus, et al. (2005). "APLIP1, a kinesin binding JIP-1/JNK scaffold protein, influences the axonal transport of both vesicles and mitochondria in Drosophila." Curr Biol **15**(23): 2137-2141.

Hurd, D. D. and W. M. Saxton (1996). "Kinesin mutations cause motor neuron disease phenotypes by disrupting fast axonal transport in Drosophila." Genetics **144**(3): 1075-1085.

Kalchman, M. A., H. B. Koide, et al. (1997). "HIP1, a human homologue of S. cerevisiae Sla2p, interacts with membrane-associated huntingtin in the brain." Nat Genet **16**(1): 44-53.

Knott, A. B. and E. Bossy-Wetzel (2008). "Impairing the mitochondrial fission and fusion balance: a new mechanism of neurodegeneration." Ann N Y Acad Sci **1147**: 283-292.

Li, X. J., S. H. Li, et al. (1995). "A huntingtin-associated protein enriched in brain with implications for pathology." Nature **378**(6555): 398-402.

Li, Z., C. A. Karlovich, et al. (1999). "A putative Drosophila homolog of the Huntington's disease gene." Hum Mol Genet **8**(9): 1807-1815.

Ligon, L. A., M. Tokito, et al. (2004). "A direct interaction between cytoplasmic dynein and kinesin I may coordinate motor activity." Journal of Biological Chemistry **279**(18): 19201-19208.

McGuire, J. R., J. Rong, et al. (2006). "Interaction of Huntingtin-associated protein-1 with kinesin light chain: implications in intracellular trafficking in neurons." J Biol Chem **281**(6): 3552-3559.

Morfini, G. A., Y. M. You, et al. (2009). "Pathogenic huntingtin inhibits fast axonal transport by activating JNK3 and phosphorylating kinesin." Nat Neurosci **12**(7): 864-871.

Morris, R. L. and P. J. Hollenbeck (1993). "The regulation of bidirectional mitochondrial transport is coordinated with axonal outgrowth." J Cell Sci **104 (Pt 3)**: 917-927.

Nasir, J., S. B. Floresco, et al. (1995). "Targeted disruption of the Huntington's disease gene results in embryonic lethality and behavioral and morphological changes in heterozygotes." Cell **81**(5): 811-823.

Neuwald, A. F. and T. Hirano (2000). "HEAT repeats associated with condensins, cohesins, and other complexes involved in chromosome-related functions." Genome Res **10**(10): 1445-1452.

O'Kusky, J. R., J. Nasir, et al. (1999). "Neuronal degeneration in the basal ganglia and loss of pallido-subthalamic synapses in mice with targeted disruption of the Huntington's disease gene." Brain Res **818**(2): 468-479.

Pack-Chung, E., P. T. Kurshan, et al. (2007). "A Drosophila kinesin required for synaptic bouton formation and synaptic vesicle transport." Nat Neurosci **10**(8): 980-989.

Pardo, R., M. Molina-Calavita, et al. (2010). "pARIS-htt: an optimised expression platform to study huntingtin reveals functional domains required for vesicular trafficking." Mol Brain **3**: 17.

Pickrell, A. M., H. Fukui, et al. (2011). "The striatum is highly susceptible to mitochondrial oxidative phosphorylation dysfunctions." J Neurosci **31**(27): 9895-9904.

Pilling, A. D., D. Horiuchi, et al. (2006). "Kinesin-1 and Dynein are the primary motors for fast transport of mitochondria in Drosophila motor axons." Mol Biol Cell **17**(4): 2057-2068.

Reilly, C. E. (2001). "Wild-type huntingtin up-regulates BDNF transcription in Huntington's disease." J Neurol **248**(10): 920-922.

Rice, S. E. and V. I. Gelfand (2006). "Paradigm lost: milton connects kinesin heavy chain to miro on mitochondria." J Cell Biol **173**(4): 459-461.

Rockabrand, E., N. Slepko, et al. (2007). "The first 17 amino acids of Huntingtin modulate its sub-cellular localization, aggregation and effects on calcium homeostasis." Hum Mol Genet **16**(1): 61-77.

Romero, E., G. H. Cha, et al. (2008). "Suppression of neurodegeneration and increased neurotransmission caused by expanded full-length huntingtin accumulating in the cytoplasm." Neuron **57**(1): 27-40.

Rong, J., S. H. Li, et al. (2007). "Regulation of intracellular HAP1 trafficking." J Neurosci Res **85**(14): 3025-3029.

Russo, G. J., K. Louie, et al. (2009). "Drosophila Miro is required for both anterograde and retrograde axonal mitochondrial transport." J Neurosci **29**(17): 5443-5455.

Sanyal, S. (2009). "Genomic mapping and expression patterns of C380, OK6 and D42 enhancer trap lines in the larval nervous system of Drosophila." Gene Expr Patterns **9**(5): 371-380.

Song, W., J. Chen, et al. (2011). "Mutant huntingtin binds the mitochondrial fission GTPase dynamin-related protein-1 and increases its enzymatic activity." Nat Med **17**(3): 377-382.

Stowers, R. S., L. J. Megeath, et al. (2002). "Axonal transport of mitochondria to synapses depends on milton, a novel Drosophila protein." Neuron **36**(6): 1063-1077.

Svoboda, K. and S. M. Block (1994). "Force and velocity measured for single kinesin molecules." Cell **77**(5): 773-784.

Trushina, E., R. B. Dyer, et al. (2004). "Mutant huntingtin impairs axonal trafficking in mammalian neurons in vivo and in vitro." Mol Cell Biol **24**(18): 8195-8209.

Wanker, E. E., C. Rovira, et al. (1997). "HIP-I: a huntingtin interacting protein isolated by the yeast two-hybrid system." Hum Mol Genet **6**(3): 487-495.

Zeitlin, S., J. P. Liu, et al. (1995). "Increased apoptosis and early embryonic lethality in mice nullizygous for the Huntington's disease gene homologue." Nat Genet **11**(2): 155-163.

Zhang, S., M. B. Feany, et al. (2009). "Inactivation of Drosophila Huntingtin affects long-term adult functioning and the pathogenesis of a Huntington's disease model." Dis Model Mech **2**(5-6): 247-266.

Zhu, B., J. A. Pennack, et al. (2008). "Drosophila neurotrophins reveal a common mechanism for nervous system formation." PLoS Biol **6**(11): e284.

Zuccato, C. and E. Cattaneo (2007). "Role of brain-derived neurotrophic factor in Huntington's disease." Prog Neurobiol **81**(5-6): 294-330.

Chapter 4

Inhibition of fast axonal transport by expanded polyQ-Huntingtin

Kurt R. Weiss and J. Troy Littleton

Department of Biology and The Picower Institute for Learning and Memory, MIT,

Cambridge, MA 02139

Abstract

Over expression of an N-terminal 588 amino acid human Htt fragment with an mRFP C-terminal tag and a non-pathogenic 15 glutamine repeat (Q15Htt-RFP) or pathogenic138 glutamine repeat (Q138Htt-RFP) results in aggregate formation in neuronal cell bodies and axonal projections. Cytoplasmic aggregates are also seen in neurons of human patients with Huntington's disease (HD), though the role of aggregates in cytotoxicity is debated. We used a *Drosophila* model of HD to analyze the effects aggregates have on fast axonal transport of mitochondria, synaptic vesicles and dense core vesicles. Expression of Q138Htt-RFP results in decreased processivity, velocity, and flux of mitochondrial transport compared to Q15Htt-RFP. Large Q138Htt-RFP aggregates trap all membrane bound organelles we analyzed in axons and cell bodies. We find that aggregates can incorporate Syt-1-GFP and ANF-GFP tagged cargos, while mitochondria fail to accumulate within aggregates, and can be found at the periphery. EM data also suggests that mitochondria do not incorporate within aggregates, while vesicle-like structures do. For all cargos analyzed, roughly 90% of the cargo flux is capable of bypassing axonal aggregates, arguing that most aggregates are not complete blockages of transport. We observe a subset, but not all moving cargos co-localize with soluble (non-aggregated) Q138Htt-RFP while moving in the axon. We tested whether there was any correlation between a motile cargo having soluble Q138 Htt associated and its susceptibility to becoming trapped in aggregates. We find that aggregation-dependent blockage of cargo transport does not depend on the presence of soluble Q138Htt molecules on that specific cargo. While Q138Htt aggregates show an accumulation of cargos, they do not show significant accumulation of dynein or kinesin motor proteins.

Introduction

Huntington's Disease (HD) is an autosomal dominant, neurodegenerative disorder that occurs when an expansion in the polyglutamine (polyQ) tract in the *huntingtin* gene expands to greater than ~35 glutamine residues (HUNTINGTON'S DISEASE RESEARCH COLLABORATION, 1993). Abnormal protein aggregation resulting from Htt polyQ expansion (polyQex-Htt) is central to pathogenesis of HD and other polyglutamine expansion diseases (Scherzinger, Lurz et al. 1997; Persichetti, Trettel et al. 1999). The polyQex-Htt protein can exist in multiple states (Hoffner, Island et al. 2005; Nagai, Inui et al. 2007), including aberrantly folded monomeric forms, micro-aggregates, fibril states, and larger inclusion body aggregates. It is currently unclear which form(s) of mutant Htt are pathogenic and how the abnormally folded protein causes neuronal toxicity.

Despite ubiquitous expression of the Htt protein, HD only manifests in a subset of neurons (Sieradzan, Mann et al. 1997; Sieradzan and Mann 2001). Neurons are highly dependent on anterograde axonal transport to deliver cargo to the synapse, and retrograde transport to return neurotrophic factors. As such, axonal transport defects may contribute neuron specificity to HD pathology. In addition to steric blocks to transport caused by aggregated polyQex-Htt, soluble polyQex-Htt is also postulated to function in axonal transport given wild-type Htt likely regulates fast axonal transport (FAT) (Velier, Kim et al. 1998; Gunawardena, Her et al. 2003; Trushina, Dyer et al. 2004; Wu, Fan et al. 2010). FAT defects have been demonstrated in several neurodegenerative diseases including Alzheimer's Disease (Gunawardena and Goldstein 2001), ALS (Warita, Itoyama et al. 1999), and Hereditary spastic paraplegias (Salinas, Proukakis et al. 2008). Mutations in kinesin and dynein motors also cause neurodegenerative disease-like phenotypes as a result of defective FAT (Hurd and Saxton 1996).

PolyQex-Htt expression has been shown to alter axonal transport of mitochondria (Lee, Yoshihara et al. 2004; Sinadinos, Burbidge-King et al. 2009), synaptic vesicles (Lee, Yoshihara et al. 2004), neurotrophic factors (Gauthier et al, 2004), and other organelles (Chang, Rintoul et al. 2006). However, the specific details of cargo accumulation have not been characterized. Understanding various cargos' susceptibility to FAT defects caused by polyQex-Htt may provide insight into the cell-type specificity of HD and other neurodegenerative disorders. Additionally, understanding the role of aggregate-dependent and -independent mechanisms of transport defects is important for designing treatments for HD.

Materials and Methods

Generation of Htt constructs: cDNAs for mRFP-HttQ15 and mRFP-HttQ138 were subcloned into EcoRI (blunt end ligation) and KpnI sites of the pUAST expression vector. cDNA for eGFP-HttQ138-mRFP was subcloned into the XbaI site of the pUAST vector. HttQ15 and HttQ138 cDNAs were kindly provided by Ray Truant (Department of Biochemistry, McMaster University). The UAS-KHC-GFP line was obtained from the Bloomington Stock Center (Bloomington, IN).

Time-lapse aggregation image acquisition: To allow long term imaging of aggregation kinetics and to minimize artifacts from staining, all images were acquired through the cuticle in live intact larvae under suprane anesthesia as previously described (Fuger, Behrends et al. 2007). FRAP analysis was carried out using a Zeiss spinning disk confocal microscope with Perkin Elmer Velocity 4-D imaging software. Aggregates were photobleached using 100% laser power at 488 nm for 2 to 5 iterations through the entire z-plane. Z-stack recovery images were recorded at a rate of one per minute for 120 minutes for long-term cargo recovery or one frame per second

for analysis of how individual puncta interact with aggregates. The Z-stacks were taken in 10 planes 0.6 μm apart to image entirely through large 6 μm aggregates.

Transport analysis and statistics: For mitochondrial tracking analysis, suprane anesthetized larvae had 50 μm regions of motor axons bleached, and individual mitochondria moving into the bleached region were marked with a mouse cursor in the ImageJ plugin MtrackJ (NIH) to indicate x,y,t coordinates. The leading edge of each mitochondrion was used to mark the location because a fluorescent maximum was variable from frame to frame. For each time series a stationary mitochondria outside the bleached region was marked at each time-point and used to correct for drift or other unwanted movements. Coordinates were imported into a Microsoft Excel spreadsheet which calculated movement parameters such as direction, run length, velocity, stop number, and percent of time in each of a three state motion paradigm, anterograde runs, retrograde runs, and stops (Louie 2008). Manual tracking was done for a minimum of 60 seconds per mitochondria. Due to large variance within an animal for all transport parameters, data was not averaged per animal, but rather means for individual organelles were aggregated within a genotype. This gave a normal distribution of values to compare between genotypes. Student's T-Test for significance was used with a 95% confidence interval, equal variances were not assumed. Statistical values were calculated using Microsoft Excel (Microsoft, Redmond, WA) and Origin Graphing Software (Northhampton, MA).

Immunohistochemistry: For DHC and KHC staining, wandering 3rd instar larvae expressing UAS-Q138Htt-mRFP or UAS-KHC-GFP under the CCAP-GAL4 driver were reared at 25°C and dissected inHL3. Preps were stained with monoclonal anti-kinesin heavy chain (SUK4) or anti-dynein heavy chain (2C-11) at 1:20 (Developmental Studies Hybridoma Bank). Images were

captured with a Zeiss Pascal laser scanning confocal microscope (Carl Zeiss MicroImaging, Inc.) using the accompanying Zeiss PASCAL software.

Electron microscopy: Wandering 3rd instar larvae expressing HttQ138-mRFP were dissected, fixed, and processed for electron microscopy as previously described (Akbergenova and Bykhovskaia 2009). Briefly, filleted larvae were fixed in 1% glutaraldehyde, 4% formaldehyde, 0.1 M sodium cacodylate for 2 h at room temperature and then 4°C overnight. After washing in 0.1 M sodium cacodylate, 0.1 M sucrose, samples were post-fixed for 1 h in 1% osmium tetroxide, dehydrated through a graded series of ethanol and acetone, and embedded in Embed 812 epoxy resin (Electron Microscopy Sciences). Thin sections (70–90 nm) were collected on Formvar/carbon coated copper slot grids, and contrasted with lead citrate. For immuno-EM, samples were fixed for 20 min in 4% paraformaldehyde in PBS, blocked for 1 h in 1% BSA in PBS, followed by incubation for 3 h in anti-RFP antibody and then 2 h in a doubly-conjugated Alexa Fluor 594 and 1.4 nm nanogold secondary antibody (Nanoprobes). The gold signal was enhanced for 7 min using Gold Enhance (Nanoprobes), followed by a second 1 h fixation in 1% glutaraldehyde and 4% paraformaldehyde, and then embedded and sectioned as above. Thin sections (70-90 nm) were imaged at 80 kV on an FEI Tecnai G2 Spirit electron microscope equipped with an AMT CCD camera.

Results

Q138Htt expression decreases mitochondrial velocity, processivity, and flux: Individual mitochondria tagged with GFP were imaged in live, intact, third instar larvae expressing either Q138Htt-RFP or Q15Htt-RFP under the C380 motor neuron driver. Mitochondria were then tracked by hand to determine x,y,t coordinates used to calculate velocity, stops, etc. In these experiments, a low expression, adult viable, Q138Htt-RFP line was used that had one to two

aggregates per 50 µm imaging region. This expression pattern allowed imaging of transport

kinetics in the absence of large immobile aggregates, though such aggregates were present

elsewhere in the axon. We find that there is an aggregation- independent decrease in velocity

and processivity for both anterograde and retrograde moving mitochondria (Figure 1 A-D). The

increased pause rate can likely be attributed to soluble Q138Htt disrupting transport, considering

we see only a modest increase of several seconds in the duration of these pauses (Figure 1 C, D).

While aggregate-dependent changes in pause duration can last several minutes or hours at the

sites of aggregates (Figure 2A). Flux measurements indicate a decrease in mitochondrial flux

caused by Q138Htt expression (Figure 1 E, F). Flux is likely reduced by aggregated Q138Htt, as

the cumulative effect of aggregates along the axon undoubtedly affects the region in which we

are imaging, even if aggregates are not immediately present. Q138Htt aggregate concentration

increases proximal to the CNS, thus, anterograde flux would be predicted to be affected more by

aggregates in an aggregate-dependent model for reduced flux. Indeed, we see a greater decrease

in the anterograde flux than in retrograde flux of mitochondria induced by Q138Htt expression

(Figure 1 E, F).

Q138Htt aggregates do not completely block organelle FAT: The C380-GAL4 motor neuron

driver expresses in all motor neurons, and thus, imaging of one axonal bundle contains 10-30

cells, based on the number of unique mitochondrial tracks seen in time-lapse images. In z-stack

projections of transport series, mitochondria which appear to bypass an aggregate may actually

be in an adjacent cell that does not contain the aggregate. To accurately determine which

mitochondrial tracks were impacted by the presence of aggregates, we co-expressed mito-GFP

and Q138Htt-RFP under the CCAP-GAL4 (Crustacean cardioacceleratory peptide) driver, which

only expresses in one neuron per hemisegment, and thus one cell per axon bundle (Park,

Schroeder et al. 2003; Wang and Schwarz 2009). Figure 4 A and B shows the narrow expression pattern of CCAP-GAL4, where only one cell is expressing Q138Htt in an entire axon bundle stained for dynein.

Interestingly, when we measure transport in single CCAP motor neurons at the sites of aggregates, we found the majority of motile mitochondria are not blocked by aggregates (Figure 2A). Roughly 90% of mitochondria moved past large Q138Htt aggregates that exceed the diameter of the axon, while only 10% became trapped at the site of aggregation. About 20 % of mitochondria which eventually passed the aggregates had increased pause durations upstream of aggregates for 5 to 600 seconds before passing. This longer pause duration represents a unique state of movement compared to the normal two second pauses that occur along wild-type axons, or stationary phases that last in excess of three hours (which is the current time limit we can monitor a stationary mitochondria). This unique state of 'intermediate pausing' can terminate in complete stoppage (at least for the duration of imaging, about 2-3 hours) or continued transport in the imprinted direction of motion.

Vesicles are also able to bypass Q138Htt aggregates. Imaging of syt-1-GFP tagged synaptic vesicles and ANF-GFP tagged dense core vesicles at the sites of Q138Htt aggregates yields similar results to mitochondria, demonstrating that ~90% of vesicles bypass aggregates and ~10% become trapped (Figure 2 B, C). However, they differ slightly in the manner in which they are trapped: mitochondria are trapped on the sides of aggregates; synaptic vesicles are trapped within aggregates; and dense core vesicles display both patterns (Figure 2 A-C). The variation in response to these aggregates may indicate either a varied response from molecular motors associated with different cargos, properties of the cargos or cargo adapters, or a steric

size bias. We do not see any bias toward anterograde or retrograde moving organelles of any class in their probability of passing or become trapped in aggregates.

Aggregate effects on cargos are not dependent on co-localization with soluble Q138Htt: What makes one particular organelle bypass an aggregate while another organelle of the same class becomes trapped? Because not all synaptic vesicles were trapped by aggregates and not all synaptic vesicles co-localize with soluble Q138Htt during transport, we asked if the presence of Q138Htt on cargos is correlated with a particular cargo becoming trapped in an aggregate. We find no such dependence on soluble HttQ138 co-localization for any organelle. Figure 3A shows an example where two synaptic vesicle puncta are trapped at the site of a bleached Q138Htt aggregate, and neither shows co-localization with soluble Q138Htt. Figure 3B shows a mitochondrion, which has passed the aggregate to the left, despite co-localizing with soluble Q138Htt. Additionally, both dense core vesicles and synaptic vesicles become trapped in aggregates, although dense core vesicles very rarely co-localize with Q15Htt or Q138Htt (Figure 2C, Chapter 3 Figure1).

Cargo association with aggregates is not dependent on FAT: If molecular motors or other proteins that mediate FAT are involved in trapping organelles in aggregates we would not expect to see the same pattern of co-aggregation in the cell body where FAT is not occurring. However, we see similar aggregation in the cell body, whereby synaptic vesicles are co-localized within Q138Htt aggregates and mitochondria are at the edges of aggregates (Figure 3 C, D). This suggests neither the axonal transport machinery nor FAT itself is required to mediate the interaction between Q138Htt aggregates and organelles. Interestingly, we observe reduced co-localization between soluble Q138Htt and soluble synaptic vesicles in cell bodies compared to

axons, suggesting that the interaction between soluble Htt and synaptic vesicles is partially mediated by the FAT machinery (Figure 3 D).

Dynein motors do not concentrate at the site of aggregates: To test the model that Q138Htt aggregates may trap molecular motors via direct interactions with Htt and indirect interactions with FAT cargos, we probed for localization of kinesin and dynein heavy chains at the sites of aggregation. We did not see significant amounts of motor proteins at the sites of aggregation (Figure 4 A, B). We were also unable to view co-localization of the two proteins in transport, due to the low density of motor proteins on cargos undergoing transport, which may be as low as one motor per organelle (Howard, Hudspeth et al. 1989; Toyoshima, Yu et al. 1992). As a positive control for the kinesin antibody in CCAP neurons, we temporally restricted expression of UAS-KHC-GFP to second instar larvae for 18 hours and observed formation of large GFP positive accumulations and axonal swelling that were recognized by the kinesin antibody (Figure 4C). This data argues that monomeric Q138Htt does not bind motor proteins directly in a 1:1 stoichiometric ratio, nor do Q138Htt aggregates significantly titrate soluble motors away from the available pool. Vesicles and other organelles trapped in aggregates are presumably still bound by motor proteins, but this is not likely to drastically reduce the available motor pool.

Vesicular and vacuolar organelles are found inside and around aggregates: Consistent with our fluorescent imaging data, EM data suggests that aggregates can trap vesicles and vacuolar organelles inside and around aggregates, but not mitochondria (Figure 5 C). The pattern of aggregation and association with membrane bound organelles is similar in both the cell body and axon (Figure 5 A, B). This data also suggests that these aggregate structures contain a dense substance that may represent amyloid.

Discussion

Here, we examine the effects of Q138Htt on axonal transport by differentiating the contributions of soluble versus aggregated Q138Htt on transport of mitochondria, synaptic vesicles, and dense core vesicles. We show that in the absence of aggregates, we see decreased transport of mitochondria caused by soluble Q138Htt (Figure 1A-D). Studies in squid axoplasm suggest a possible mechanism for this aggregation independent defect whereby polyQexHtt can active the cJun N-terminal kinase (JNK) pathway, resulting in phosphorylation of the neuron specific JNK3. Phosphorylated JNK3 then phosphorylates and inhibits kinesin-1 and thereby inhibits mitochondrial transport (Morfini, You et al. 2009).

We also observe defects in flux and organelle accumulation which are directly caused by aggregated Q138Htt. The large aggregates that form in polyglutamine expansion diseases are known to impede axonal transport (Lee, Yoshihara et al. 2004; Morfini, Pigino et al. 2005), but it is unclear to what extent these aggregates affect various classes of organelles, and if they do so through specific binding interactions or indiscriminately by sterically blocking transport. Comparing the effects of aggregates on three separate cargos, we observe that cargos are differentially affected by aggregates. This result may be partly explained by steric properties of the cargos. Mitochondria (~500 nm diameter) may be trapped outside of aggregates because of space constraints between the cell membrane and the side of aggregate, while smaller organelles like synaptic vesicles (~40 nm diameter) are able to wedge between the cell membrane and the aggregate. Intermediately sized dense core vesicles (~100 nm diameter), demonstrate both accumulation patterns. For all cargos tested, the vast majority of organelles are able to bypass even large aggregates, demonstrating that aggregates do not represent complete blockages of transport (Figure 2). This raises the question of what is different about a small percentage of

cargos that make them susceptible to being immobilized by aggregates. Possible explanations include dependence on the exact microtubule track they are on, associated scaffolds or regulator proteins, the health of the motors or cargos, or a stochastic mechanism. We tested the hypothesis that cargos which become trapped are associated with soluble Q138Htt molecules and find that there is no dependence on the presence of Q138Htt on an individual cargo becoming trapped in an aggregate (Figure 3). One caveat here is that endogenous *Drosophila* Htt is present in our experiments and may contribute to cargo association within aggregates. It will be necessary to conduct experiments where we move the microscope stage to follow the movement of a single mitochondrion past several aggregates over a longer time course to determine if the ability to pass aggregates is consistent and retained by a specific organelle, or if this occurs randomly.

Mitochondria stop at locations of local energy demand and calcium buffering, and in wild-type axons ~ 40% of mitochondria are stationary (Cai and Sheng 2009). It is possible, given the distance at which these mitochondria stop from aggregates, that they are not becoming entangled in the aggregate, but stopping to fill local energy demands for protein degradation processes (Kalchman, Graham et al. 1996). This hypothesis is supported by the observation that some mitochondria pause for three to six minutes at the sites of aggregates before passing, arguing they may be pausing to buffer calcium or generate ATP. This effect would still be aggregate-dependent, because said duration of pausing is not seen in normal wild-type axons.

Another possible explanation for the accumulation of a subset of mitochondria is they are weak or old, and unable to generate the force or membrane bending required to squeeze past an aggregate. Mitochondrial dysfunction has been implicated in contributing to neurotoxicity in many ways, including defective energy metabolism, excitotoxicity, and release of caspases (Gu, Gash et al. 1996; Lee, Yoshihara et al. 2004; Oliveira 2010; Chen 2011). Whether the

mitochondria are healthy or sick when they become stuck, they are susceptible to failure if trapped at the sites of aggregates for several hours or days. These mitochondria may break down and release ROS species and caspases causing neurodegeneration, which has been previously suggested (Kiechle, Dedeoglu et al. 2002; Chang, Rintoul et al. 2006). The recent development of genetically encoded mitochondrial calcium sensors will help evaluate this model (Akimzhanov and Boehning 2011).

Another popular model for polyQ-Htt toxicity suggests that Q138Htt aggregates accumulate motor proteins and reduce the pool of soluble motors available to transport other cargos, thus causing global axonal transport defects. This has been demonstrated in biochemical fractionation experiments showing that polyQ-Htt expression in cultured mammalian neurons caused soluble motor proteins kinesin and dynactin to redistribute to the insoluble fraction along with aggregated Htt, and this effect is correlated with decreased neural culture viability (Trushina, Dyer et al. 2004). However, the insoluble fraction enriched in motors also contained cytoskeletal components, mitochondria, and soluble Htt, which may have an increased association with the motor proteins resulting in a shift in solubility. Additionally, this does not specifically show increased motor concentration at sites of aggregates, and these experiments were not done in axons. Similar results to our observations were obtained from brain lysates of mice expressing a 109 glutamine repeat in full-length mammalian Htt. Lysates were probed for an interaction between Htt and kinesin or dynein by immunoprecipitation and subcellular fractionation, and no interaction with soluble or aggregated Htt[Q109] was found (Morfini, You et al. 2009). Similarly, we do not observe direct interactions between soluble or aggregated Q138Htt and molecular motors *in vivo*.

Our data suggests fast axonal transport of organelles is altered by Q138Htt expression via aggregation- dependent and independent mechanisms. We find little evidence for organelle specific susceptibility to aggregates, because all organelles we analyzed were trapped by aggregates, albeit in slightly different patterns. Repeating similar *in vivo* imaging experiments with other polyQ expansion disease proteins and additional cargos will provide more evidence on the specificity of interactions with axonal transport blockages and cargos. Aggregates are not complete blockages of transport as the robust transport machinery can bypass them even when size constraints force apparent bending of the cell membrane, which is revealed when mitochondria pass aggregates. While we observe the majority of organelles bypass aggregates, the continued insult to neurons from reduced transport and stalled organelles along axons may contribute to the late-onset nature of HD and other neurodegenerative diseases involving aggregation. Indeed, mitochondrial transport and energy metabolism defects are likely to be important mechanisms of toxicity in HD, as defects in oxidative phosphorylation has been demonstrated to be selectively detrimental to the striatum compared to the cortex or hippocampus, suggesting relevance to the cell specific neurodegeneration seen in HD (Pickrell, Fukui et al. 2011).

Acknowledgements
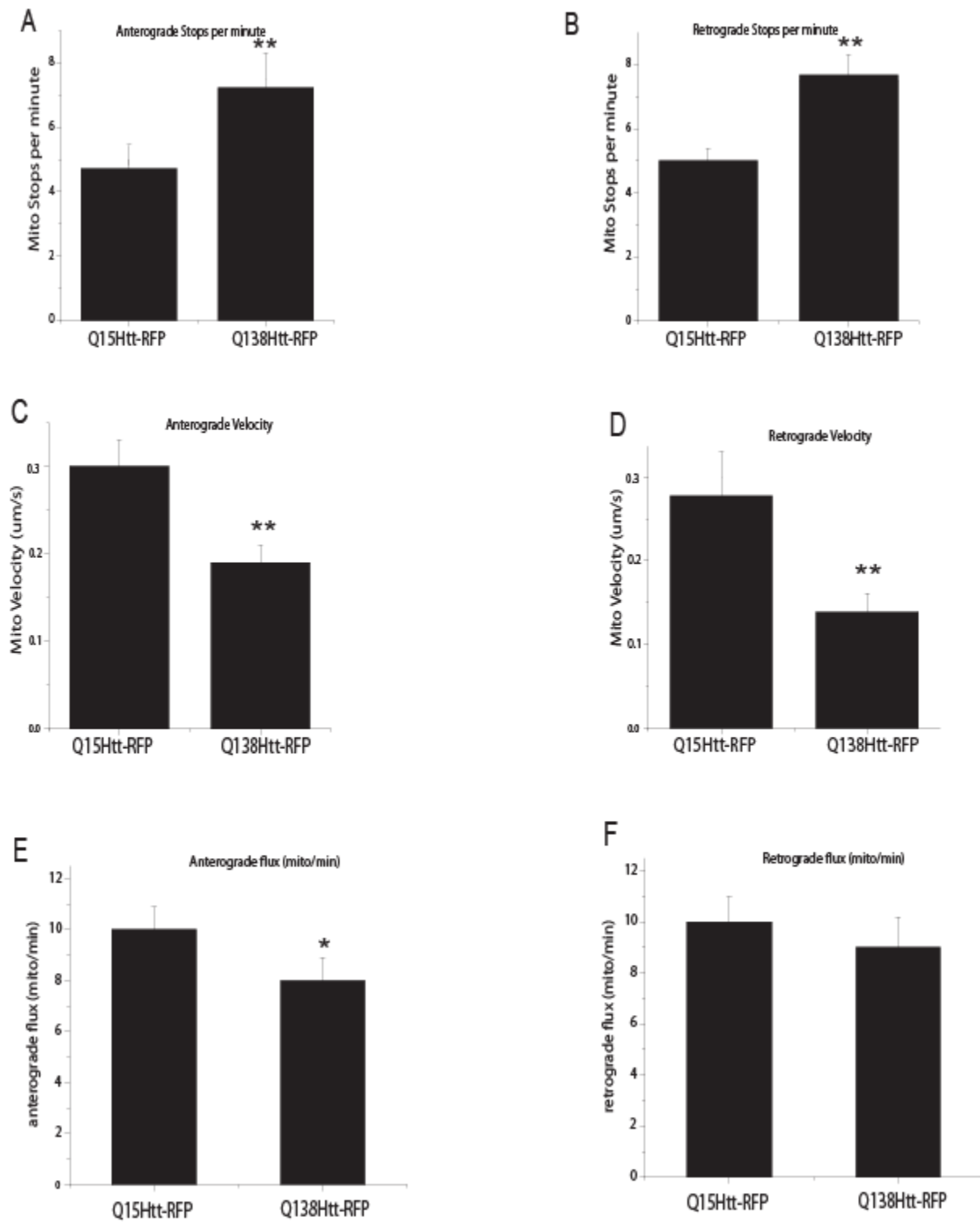
Figure 1

Figure 1. Human Q138Htt alters axonal transport of mitochondria. Co-expression of Q138Htt-RFP and mito-GFP in motor neurons allows tracking of individual mitochondria and comparison of transport kinetics. We find that there is a decrease in velocity (A, B), an increase in stops (C, D), and a decrease flux (E,F) for both anterograde and retrograde moving mitochondria. These defects in transport are primarily due to soluble Q138Htt, since tracking was done in regions of axons devoid of aggregates.

Figure 2

A
CCAP; mito-GFP;HttQ138-RFP

t=0 min post bleach   t=13 min   t=14 min

t=18 min   t=19 min   t=100 min

B
CCAP; Syt1-GFP;HttQ138-RFP

t=0 min post bleach   t=5 min   t=15 min

t=25 min   t=35 min   t=100 min

C
CCAP; ANF-GFP;HttQ138-RFP

t=0 min post bleach   t=2.5 min   t=5 min

t=15 min   t=30 min   t=100 min
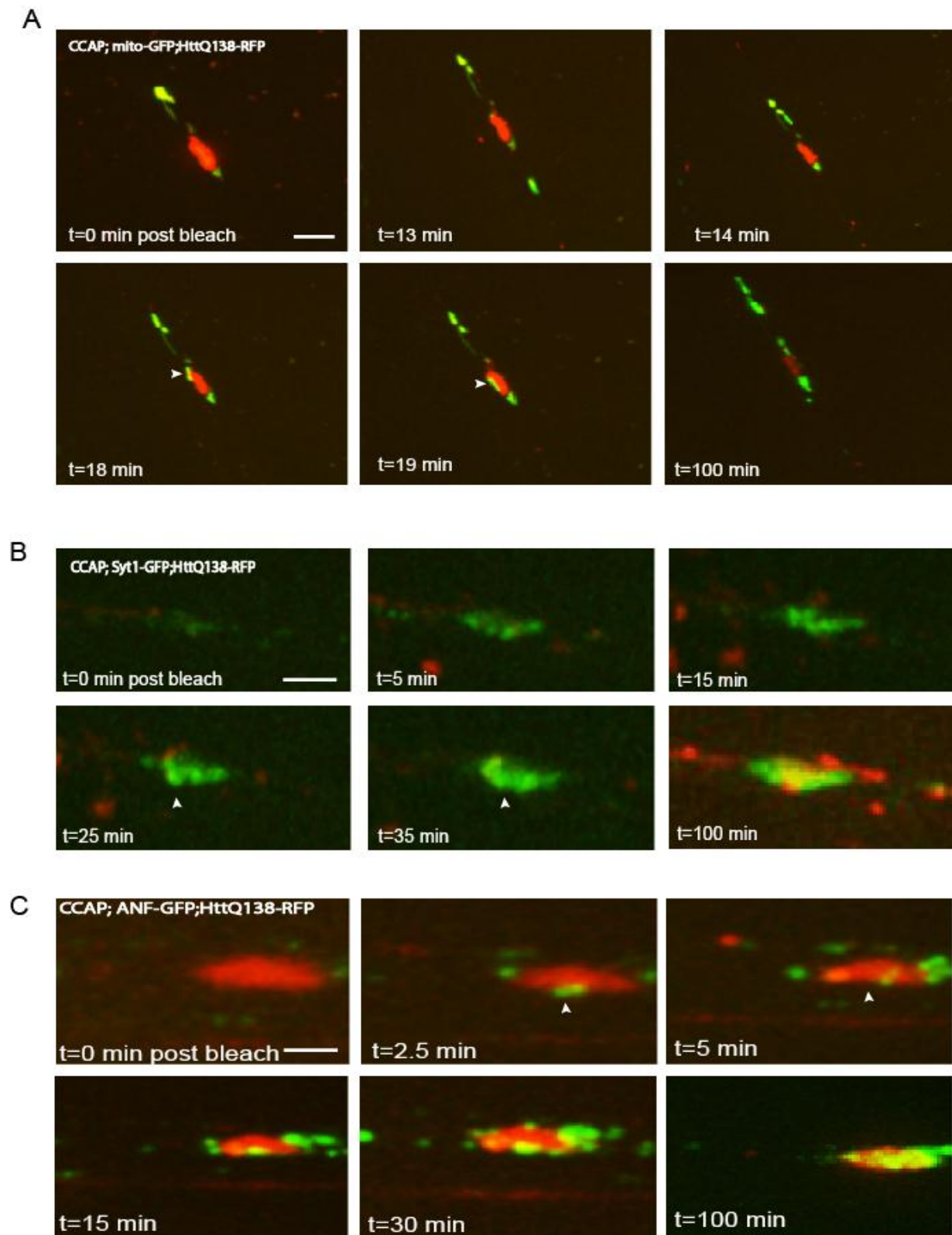
Figure 2. Q138Htt aggregates do not completely block FAT. Co-expression of Q138Htt and cargo-GFP under the CCAP driver results in aggregates in motor neurons. At the sites of aggregation HttQ138-RFP was bleached 80% and the cargo-GFP channel was bleached 100% to allow visualization of recovery of cargos at the site of aggregation. The majority of individual FAT cargos can bypass aggregates that exceed the diameter of the axon (arrows in A-C). Roughly 90% cargos pass the aggregate and 10% become trapped. Mitochondria are trapped outside the aggregates, as is seen by the aggregate entering the image from the bottom of the frame at t=13 min (A) and becomes stationary at the bottom side of the aggregate at t=14, and remains stationary until at least t=100 min (A). Conversely, the motile mitochondria marked by arrows at t=18 and t=19 min is seen passing the aggregate (A). Synaptic vesicles are trapped at the site of Q138Htt aggregation (B) and dense core vesicles trapped beside and within Q138Htt-RFP aggregates (C). Frame rate is two per minute for 20 minutes, then one per minute thereafter. Scale bar = 5 μm.
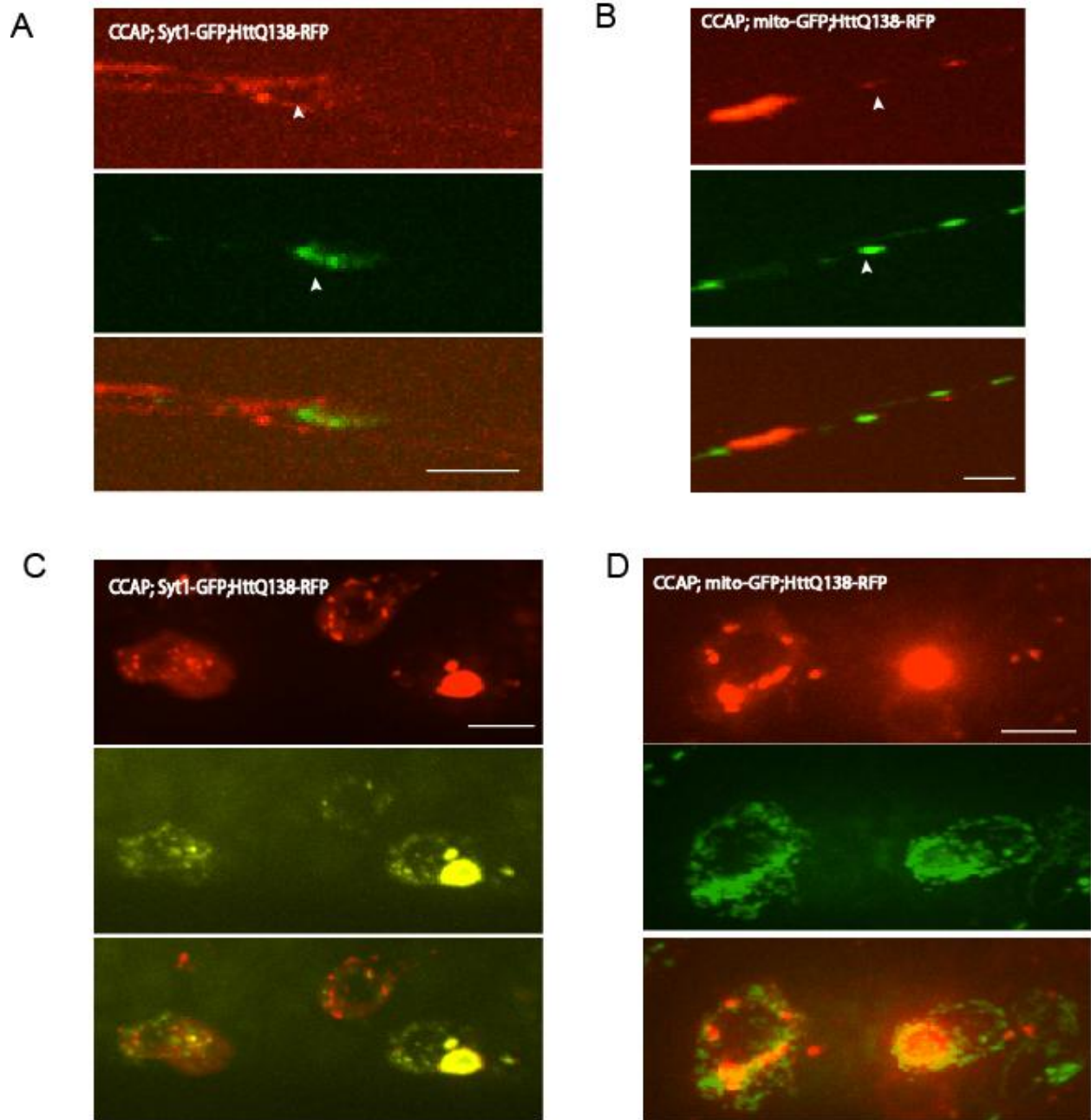
Figure 3

Figure 3. Neither co-localization with soluble Htt nor FAT mediated interactions are required for cargo accumulation into Q138Htt aggregates. Synaptic vesicles which are not bound by soluble HttQ138 are accumulated in aggregates (A). Conversely, mitochondria which are bound by soluble HttQ138 are able to bypass aggregates. This image illustrates a mitochondria moving from left to right across the image which has just passed the Htt-RFP aggregate at the left side of the image (B). In the cell body where there is not directional fast axonal transport we still observe accumulation of synaptic vesicles at the sites of aggregation (C) and mitochondria around the outsides of aggregates (D). Scale bar = 5 µm.

Figure 4

A

CCAP-Gal4; UAS-HttQ138-RFP

5 µm

anti- Kinesin Heavy Chain

Merge

B

CCAP-Gal4; UAS-HttQ138-RFP

anti -Dynein Heavy Chain

Merge

C

CCAP-GAL4; UAS-KHC-GFP

anti - Kinesin Heavy Chain

Merge
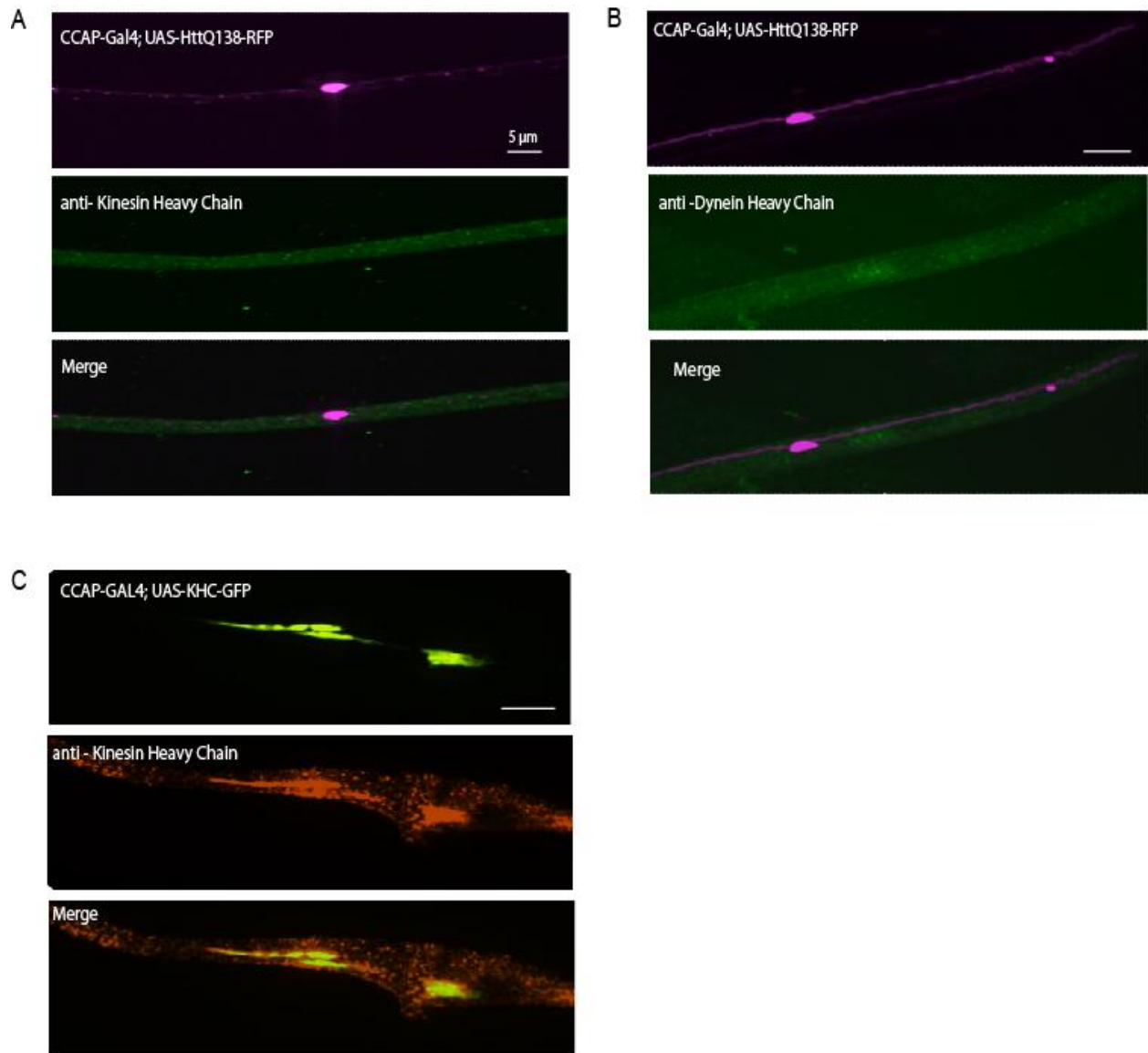
Figure 4. Dynein heavy chain and kinesin heavy chain are not concentrated at sites of aggregation. Antibodies against kinesin heavy chain (A) or dynein heavy chain (B) not show concentrated signal at HttQ138 in aggregates in CCAP neurons where aggregates clearly exceed the diameter of the cell. As a positive control for the kinesin antibody, expression of UAS-KHC-GFP in CCAP neurons shows concentration of signal at GFP positive axonal accumulations.

Figure 5

A

B

C

0.5 um
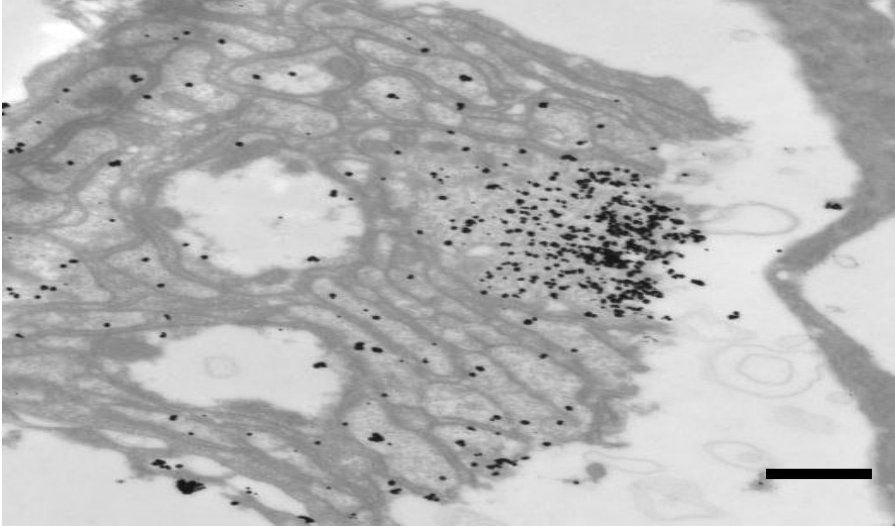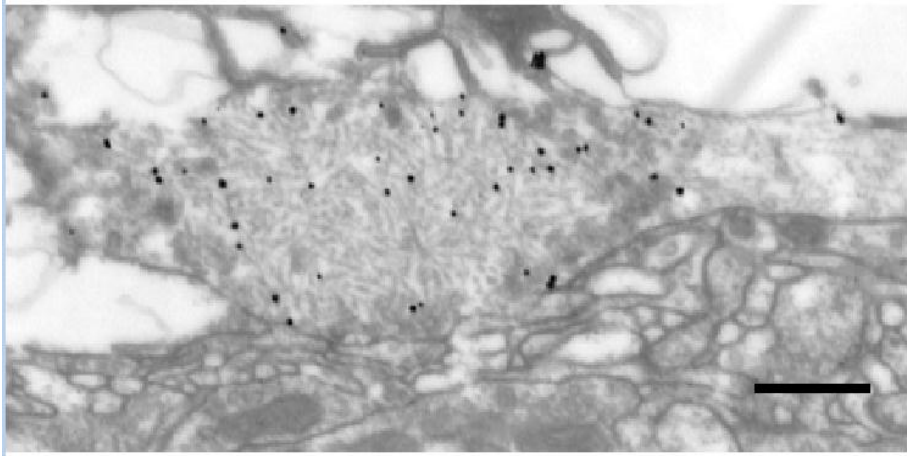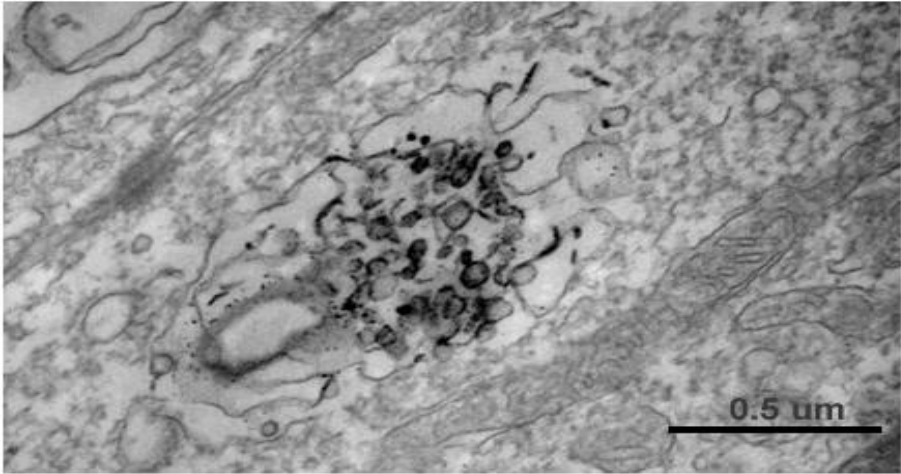
Figure 5. Aggregates contain vesicular and vacuolar-like organelles, but not mitochondria. Electron micrographs of immuno-gold labeled HttQ138 aggregates in motor neuron (A) and neuropile of the thoracic ganglia (B). Aggregates labeled by photoconversion show association with vesicular and vacuolar organelles (scale bar = 0.5 µm).

References

Akbergenova, Y. and M. Bykhovskaia (2009). "Stimulation-induced formation of the reserve pool of vesicles in Drosophila motor boutons." J Neurophysiol **101**(5): 2423-2433.

Akimzhanov, A. M. and D. Boehning (2011). "Monitoring dynamic changes in mitochondrial calcium levels during apoptosis using a genetically encoded calcium sensor." J Vis Exp(50).

Cai, Q. and Z. H. Sheng (2009). "Moving or stopping mitochondria: Miro as a traffic cop by sensing calcium." Neuron **61**(4): 493-496.

Chang, D. T., G. L. Rintoul, et al. (2006). "Mutant huntingtin aggregates impair mitochondrial movement and trafficking in cortical neurons." Neurobiol Dis.

Chang, D. T., G. L. Rintoul, et al. (2006). "Mutant huntingtin aggregates impair mitochondrial movement and trafficking in cortical neurons." Neurobiol Dis **22**(2): 388-400.

Chen, C. M. (2011). "Mitochondrial dysfunction, metabolic deficits, and increased oxidative stress in Huntington's disease." Chang Gung Med J **34**(2): 135-152.

Fuger, P., L. B. Behrends, et al. (2007). "Live imaging of synapse development and measuring protein dynamics using two-color fluorescence recovery after photo-bleaching at Drosophila synapses." Nat Protoc **2**(12): 3285-3298.

Gu, M., M. T. Gash, et al. (1996). "Mitochondrial defect in Huntington's disease caudate nucleus." Ann Neurol **39**(3): 385-389.

Gunawardena, S. and L. S. Goldstein (2001). "Disruption of axonal transport and neuronal viability by amyloid precursor protein mutations in Drosophila." Neuron **32**(3): 389-401.

Gunawardena, S., L. S. Her, et al. (2003). "Disruption of axonal transport by loss of huntingtin or expression of pathogenic polyQ proteins in Drosophila." Neuron **40**(1): 25-40.

Hoffner, G., M. L. Island, et al. (2005). "Purification of neuronal inclusions of patients with Huntington's disease reveals a broad range of N-terminal fragments of expanded huntingtin and insoluble polymers." Journal of neurochemistry **95**(1): 125-136.

Howard, J., A. J. Hudspeth, et al. (1989). "Movement of microtubules by single kinesin molecules." Nature **342**(6246): 154-158.

Hurd, D. D. and W. M. Saxton (1996). "Kinesin mutations cause motor neuron disease phenotypes by disrupting fast axonal transport in Drosophila." Genetics **144**(3): 1075-1085.

Kalchman, M. A., R. K. Graham, et al. (1996). "Huntingtin is ubiquitinated and interacts with a specific ubiquitin-conjugating enzyme." J Biol Chem **271**(32): 19385-19394.

Kiechle, T., A. Dedeoglu, et al. (2002). "Cytochrome C and caspase-9 expression in Huntington's disease." Neuromolecular Med **1**(3): 183-195.

Lee, W. C., M. Yoshihara, et al. (2004). "Cytoplasmic aggregates trap polyglutamine-containing proteins and block axonal transport in a Drosophila model of Huntington's disease." Proc Natl Acad Sci U S A **101**(9): 3224-3229.

Morfini, G., G. Pigino, et al. (2005). "Polyglutamine expansion diseases: failing to deliver." Trends Mol Med **11**(2): 64-70.

Morfini, G. A., Y. M. You, et al. (2009). "Pathogenic huntingtin inhibits fast axonal transport by activating JNK3 and phosphorylating kinesin." Nat Neurosci **12**(7): 864-871.

Nagai, Y., T. Inui, et al. (2007). "A toxic monomeric conformer of the polyglutamine protein." Nature structural & molecular biology **14**(4): 332-340.

Oliveira, J. M. (2010). "Nature and cause of mitochondrial dysfunction in Huntington's disease: focusing on huntingtin and the striatum." J Neurochem **114**(1): 1-12.

Park, J. H., A. J. Schroeder, et al. (2003). "Targeted ablation of CCAP neuropeptide-containing neurons of Drosophila causes specific defects in execution and circadian timing of ecdysis behavior." Development **130**(12): 2645-2656.

Persichetti, F., F. Trettel, et al. (1999). "Mutant huntingtin forms in vivo complexes with distinct context-dependent conformations of the polyglutamine segment." Neurobiology of disease **6**(5): 364-375.

Pickrell, A. M., H. Fukui, et al. (2011). "The striatum is highly susceptible to mitochondrial oxidative phosphorylation dysfunctions." J Neurosci **31**(27): 9895-9904.

Salinas, S., C. Proukakis, et al. (2008). "Hereditary spastic paraplegia: clinical features and pathogenetic mechanisms." Lancet Neurol **7**(12): 1127-1138.

Scherzinger, E., R. Lurz, et al. (1997). "Huntingtin-encoded polyglutamine expansions form amyloid-like protein aggregates in vitro and in vivo." Cell **90**(3): 549-558.

Sieradzan, K., D. M. Mann, et al. (1997). "Clinical presentation and patterns of regional cerebral atrophy related to the length of trinucleotide repeat expansion in patients with adult onset Huntington's disease." Neurosci Lett **225**(1): 45-48.

Sieradzan, K. A. and D. M. Mann (2001). "The selective vulnerability of nerve cells in Huntington's disease." Neuropathol Appl Neurobiol **27**(1): 1-21.

Sinadinos, C., T. Burbidge-King, et al. (2009). "Live axonal transport disruption by mutant huntingtin fragments in Drosophila motor neuron axons." Neurobiol Dis **34**(2): 389-395.

Toyoshima, I., H. Yu, et al. (1992). "Kinectin, a major kinesin-binding protein on ER." J Cell Biol **118**(5): 1121-1131.

Trushina, E., R. B. Dyer, et al. (2004). "Mutant huntingtin impairs axonal trafficking in mammalian neurons in vivo and in vitro." Mol Cell Biol **24**(18): 8195-8209.

Velier, J., M. Kim, et al. (1998). "Wild-type and mutant huntingtins function in vesicle trafficking in the secretory and endocytic pathways." Exp Neurol **152**(1): 34-40.

Wang, X. and T. L. Schwarz (2009). "Imaging axonal transport of mitochondria." Methods Enzymol **457**: 319-333.

Warita, H., Y. Itoyama, et al. (1999). "Selective impairment of fast anterograde axonal transport in the peripheral nerves of asymptomatic transgenic mice with a G93A mutant SOD1 gene." Brain Res **819**(1-2): 120-131.

Wu, L. L., Y. Fan, et al. (2010). "Huntingtin-associated protein-1 interacts with pro-brain-derived neurotrophic factor and mediates its transport and release." J Biol Chem **285**(8): 5614-5623.

Chapter 5

Conclusions and future experiments for a *Drosophila* model of Huntington's Disease

Kurt R. Weiss

Department of Biology and The Picower Institute for Learning and Memory, MIT,

Cambridge, MA 02139

Investigation of pathways involved in Htt-mediated toxicity

Conclusions: We have developed and characterized a *Drosophila* model of Huntington's Disease (HD) which allows real-time *in vivo* analysis of axonal transport and aggregation mechanisms, as well as genome-wide screening for modifiers of HD-mediated toxicity. We demonstrate that a *Drosophila* model of HD can recapitulate several aspects of the human disease, including cytoplasmic aggregation, late-onset neurodegeneration, and behavioral abnormalities. We used this model to screen for suppressors of these HD-induced phenotypes. We uncovered dosage-sensitive suppressors of mutant Htt toxicity that reduce lethality without disrupting aggregation, suggesting that pathways downstream of aggregate formation can be targeted for neuroprotection in HD. Additionally, we uncovered trends among our hits where we measured increased viability associated with decreased soluble Q138Htt, as well as measured increases in viability associated with reduced aggregation, indicating that both soluble and aggregated Htt represent toxic forms of Q138Htt. These data are consistent with the hypothesis that formation of aggregates in polyQ diseases is likely pathogenic, depending on the subcellular compartment in which aggregate formation occurs. Aggregates formed in the cell body may be neuroprotective by sequestering toxic monomeric or intermediate forms of pathogenic Htt that would otherwise enter the axon and disrupt transport or enter the nucleus and disrupt transcription.

We utilize FRAP methods to demonstrate the manner in which aggregates can disrupt transport of cargos during axonal transport. We find that aggregates are not complete blockages of fast axonal transport, as the majority of cargos are able to bypass aggregated Htt. The interaction between cargos and aggregates does not seem to be mediated by axonal transport machinery such as motors proteins, nor does it appear to be mediated by interactions between the aggregate and

soluble Q138Htt on the cargo. The exact mechanism of selective susceptibility for a subset of cargos to become trapped in aggregates will be the subject of further investigation.

Future experiments investigating Htt-mediated toxicity

Given the important role of cleavage and post-translational processing of Htt in mediating its localization and toxicity, accurate disease models should ideally reflect all possible fragments implicated in the human disorder. The problem of proper post-translational modifications is complicated in *Drosophila*, cell culture models, and even mouse models, because it is unclear if the proper kinases and caspases are expressed in the host system to fully process the Htt protein in the same manner as in human striatal neurons. For example, in *Drosophila*, there is evidence for the full-length human Htt with expanded polyglutamine (polyQexHtt) overexpression causing neurodegeneration via excitiotoxicity, though there is no aggregation or nuclear localization of this construct to suggest any proteolytic processing (Romero, Cha et al. 2008). Our *Drosophila* model consists of expression of a human polyQexHtt fragment representing the caspase-6 cleavage product known to be necessary for aggregation and nuclear entry in human HD (Davies, Turmaine et al. 1997; DiFiglia, Sapp et al. 1997; Graham, Deng et al. 2006). However, we find that this fragment is not localized to the nucleus in *Drosophila* neurons, nor is it cleaved into smaller fragments, as has been demonstrated in mouse and human striatum (Schilling, Klevytska et al. 2007). Since there is evidence for full-length, ~588 amino acid, and smaller N-terminal fragments in human HD pathology, generation of a *Drosophila* model expressing multiple forms of mutant Htt may represent a better system for characterization of HD-mediated toxicity, and characterizing domains in Htt which are necessary for toxicity.

Since phosphorylation is also known to be an essential regulator of toxicity in HD, recapitulation of biologically relevant phosphorylation states through phospho-mimetic and phospho-

incompetent mutations in Htt transgenes could represent more accurate HD models (Havel, Wang et al. 2011). One advantage of systems such as *Drosophila* lacking endogenous protease and caspase modification of Htt transgenes is that we can selectively evaluate each modification in isolation to determine the contributions of each modification on aggregation, toxicity, and localization.

Once these post-translationally modified fragments are characterized, we could conduct screens with individual fragments for specific effects on protein localization, behavioral defects, or aggregation. While incorporating multiple fragments in one model may be beneficial to evaluate effects on organismal health and protein distribution, it may also be helpful to use specific fragments which simplify the system, reduce toxicity, and increase the chances of finding rescue hits in suppressor screens.

Additional genome-wide screens for suppressors of Htt-mediated lethality and aggregation in *Drosophila* should also be carried out using RNAi collections which are now very extensive and accessible through the Vienna *Drosophila* RNAi Center. While similar RNAi screens have been carried out *in vitro*, screening *in vivo* has the advantage of immediate validation of hits, as viability is an effective and meaningful primary screening metric. One problem we have encountered in screening loss-of-function (LOF) mutations generated by EMS and deficiencies, is their dominant effects on the UAS-GAL4 system used for expression of toxic Htt transgenes. The majority of hits we have uncovered rescued viability by reducing toxic transgene expression, and similar effects might be expected with RNAi screens. Construction of Htt transgenes fused with an appropriately strong *Drosophila* transcriptional promoter element would ensure consistent gene expression and reduce false positives in these types of screens. This transcriptional element-transgene fusion would need to meet the specific criteria that it be weak

enough to allow generation of stably expressing lines, while strong enough to induce early-onset toxicity, permitting screening for suppressors.

Additionally, screening gain-of-function *Drosophila* lines for the ability to rescue Htt-mediated toxicity may improve screen hit rates. The screen from Kaltenbach et al. 2007 demonstrates that enhancer mutations are indeed effective for increasing viability in *Drosophila* HD models. We and others have had limited success screening for dominant suppressors of lethality by screening LOF mutations. Though suppressors acting through LOF represent better drug targets, it is possible, given the strong phenotype and likely dominant role of aggregation in toxicity, that LOF mutations are generally not strong enough to suppress Htt-mediated aggregation or toxicity. Thus, utilization of EP (enhancer P-element) lines in a screen for gain-of-function (GOF) suppressors of Htt-mediated aggregation and toxicity may generate more informative hits.

The use of *in vivo* imaging through the larval cuticle also expands the number of HD-mediated phenotypes we can easily screen for. In addition to assaying for viability and changes in salivary gland aggregation, as we have done previously, it is possible to screen for changes in axonal aggregation and axonal transport phenotypes. Given the ability to view these events in larval salivary glands through the cuticle in live, un-dissected larvae, one can even imagine automation of screening and image analysis.

We also demonstrate Q138Htt-mediated defects in mitochondrial fast axonal transport. In general, we observe that Q138Htt expression results in a decrease in mitochondrial flux, and fewer mitochondria appear to be present in the aggregates. It is not clear if the phenotype is caused by increased accumulation at the site of aggregates, resulting in fewer motile mitochondria along the axon, or if the defect is due to reduced associate between mitochondria and kinesin, resulting in decreased mitochondrial mobility, fission, and/or entry into axons. We

have demonstrated that wild-type Htt does increase mitochondrial motility, so establishment of a Q138Htt induced defect in motility may indicate a potential LOF associated with polyQexHtt. Thus, it will be informative to determine if polyQHtt expansion reduces the association between mitochondria and motors, or microtubules and motors. Cell-fractionation to isolate mitochondria followed by Western blot for motor protein reactivity will allow us to quantify changes in concentration of motor proteins associated with mitochondria compared with changes in the amount of tubulin associated with mitochondria. These results should reveal if decreased mitochondrial presence in axons is due to a disruption in motor-mitochondria or motor-microtubule interactions mediated by Htt (Pilling, Horiuchi et al. 2006).

In our *in vivo* imaging experiments, we observe that ~90% of motile organelles that encounter an aggregate can bypass it. We determined that the susceptibility for being trapped does not depend on the presence of soluble Q138Htt on that organelle. However, we could not elucidate the exact mechanism which regulates susceptibility of a cargo becoming trapped in an aggregate. One potential model for this selective susceptibility is that the mitochondria which become trapped are aged or defective. The recent development of genetically encoded mitochondrial calcium sensors will help evaluate this model *in vivo* (Akimzhanov and Boehning 2011). Using calcium retention as a metric for evaluating mitochondrial health, we can determine if mitochondria which show altered calcium retention are selectively susceptible to becoming trapped at the sites of aggregates. However, these assays only apply to mitochondria, while we also observe this selective susceptibility with synaptic vesicles, dense core vesicles, and soluble Q138Htt puncta. More inclusive models for selective susceptibility include cargos being on different microtubule tracks, or altered microtubule stability at the sites of aggregation. Further EM imaging and

fluorescent labeling of microtubules locally at the sites of aggregation will be necessary to evaluate microtubule health.

The endogenous function of Huntingtin

Conclusions: We have provided evidence suggesting the Huntingtin protein functions to regulate the processivity of mitochondrial and synaptic vesicles during fast axonal transport. Previous studies have suggested a role for Htt in fast axonal transport due to its association with membrane bound organelles, and evidence that Htt is a general positive regulator of fast axonal transport (DiFiglia, Sapp et al. 1995; Block-Galarza, Chase et al. 1997; Gauthier, Charrin et al. 2004). We have extended this model to demonstrate that *Drosophila* Htt (dHtt) positively regulates the movement of mitochondria and synaptic vesicles during fast axonal transport by increasing cargo processivity. This is likely accomplished by Htt acting locally on a subset of cargos to regulate the coordination of kinesin and dynein motors during fast axonal transport. Motile organelles are often bound by kinesin and dynein at the same time, and coordination between motors is essential for normal transport (Pilling, Horiuchi et al. 2006; Haghnia, Cavalli et al. 2007). In the absence of Htt, this coordination appears defective, resulting in an increase in stops and reversals in both anterograde and retrograde transport. Htt is likely acting as a scaffold to mediate interactions between regulatory signaling molecules and the motors. These interactions must take place within the first 670 amino acids of the dHtt protein, and independent of the polyglutamine tract, as we see rescue of the *dhtt* null phenotype with an N-terminal dHtt fragment lacking a polyglutamine region. In addition, we see evidence for more global effects on transport, including upregulated dynein levels and altered flux of dense core vesicles, which do not co-localize with Htt. We demonstrate similar co-localization patterns and rescue of the *dhtt* null phenotype with expression of human Htt, suggesting they are indeed functional

homologs. Additionally, we investigate the interaction between HAP1 and Htt and find that this interaction is not necessary for Htt localization to the axon, as we observe Htt-RFP localized to axons in a HAP1 deficient *milt^{92}* background.

Future experiments to elucidate the endogenous function of Htt

While we have demonstrated a defect associated with loss of dHtt in transport of mitochondria and synaptic vesicles, we have not conclusively linked this defect to any other biological process that would suggest the decrease in lifespan associated with loss of dHtt. Htt deficient *Drosophila* and conditional knockout mice are generally healthy, and show only late-onset neurodegeneration, suggesting a mild defect that only manifests with age (Dragatsis, Levine et al. 2000; Zhang, Feany et al. 2009). Phenotypes suggested by the late-onset and 'dying-back' patterns of neurodegenerative disorders are consistent with mild axonal transport defects and synaptic dysfunction.

Since the prevalent phenotypes in HD and *htt* knockouts are generally late-onset, it would be beneficial to have a system in which we could study transport defects in aged adults. The adult wing vein of *Drosophila* has recently been used to study neural injury and axonal degeneration in adult animals. This system may be used to study the effects of aggregation and loss of Htt over several days, and correlate transport defects with late-onset changes in dynein levels we observe. An adult system will be helpful in the study of many late-onset neurodegeneration mechanisms, and may also provide a more sensitive assay to uncover new phenotypes.

 In addition to waiting for late-onset phenotypes to manifest, another approach to uncover new phenotypes is to apply additional stress the system, as late-onset pathology suggests that stress is required to elucidate phenotypes. Since Htt is known to interact with vesicles, cytoskeleton

components, RAB5, and HIP14, which function in endocytosis, it is likely that Htt plays a role in some aspect of vesicle endocytosis and recycling (Caviston, Zajac et al. 2011). FM-143 fluorescent dye uptake experiments under high potassium conditions may reveal defects in endocytosis at synapses lacking Htt. Additionally, analysis of the early endosome marker, Rab5-GFP, at synapses during long trains of electrical and chemical stimulation may provide insight into the role of Htt in vesicle trafficking. By stressing the system, we may uncover a role for Htt-mediated vesicle recycling, trafficking, or endocytosis at the synapse.

While loss of Htt has been demonstrated to alter synaptic architecture, little evidence exists for defective synaptic transmission (Zhang, Feany et al. 2009; Caviston, Zajac et al. 2011) . In *Drosophila htt* null larvae, evoked responses were generally normal. However, preliminary data suggests high frequency stimulation resulted in increased failures in *dhtt* nulls compared to controls, suggesting altered nerve excitability in the absence of Htt. Voltage-clamp experiments using long stimulus trains which deplete the terminus of its primary supply of signaling molecules may reveal a defect associated with loss of Htt when synapses need to rely on vesicle recycling, reserve pool activation, and axonal transport mechanisms to replenish vesicle pools.

In addition to elucidating new phenotypes associated with the loss of dHtt, it will be necessary to further characterize the axonal transport phenotypes we have already demonstrated. One could carry out a candidate screen using mutations in known Htt interactors and components of the fast axonal transport machinery to generate stronger transport phenotypes such as distal paralysis as assayed by the 'tail flipping' phenotype. Similar methods have been applied to other transport proteins to generate synthetic transport defects (Horiuchi, Barkus et al. 2005). Thus, we might illuminate specific motors or pathways involved in Htt-mediated transport. Additionally, screens for Htt interacting proteins could be carried out by co-expressing a specific cargo-GFP and dHtt-

RFP, and screening larvae *in vivo* for genes which alter the co-localization of Htt and cargos in axons.

We demonstrate that Htt facilitates processivity of mitochondria during fast axonal transport. Specifically, we see an increase in stops and reversals of organelles associated with loss of Htt. This could indicate that Htt helps mediate interactions between organelles and motors, or between motors and microtubules. To further characterize the mechanism behind this phenotype, we will conduct co-fractionation and Western blot experiments to assay for a redistribution of motors from organelles to soluble fractions, which would suggest that Htt mediates organelle-motor interactions. Alternatively, if we observe no such redistribution, it may suggest Htt is mediating crosstalk between motors to coordinate their movement on microtubules, or between microtubules and actin. This model could be evaluated similarly by assaying for a redistribution of motors from microtubules to cytosol or actin.

It will also be helpful to characterize a wider range of cargos for defects in FAT in the *htt* mutant, including analysis of transport of proteins which are cytoplasmic, membrane-associated, secreted, anterograde biased versus retrograde biased, and especially those with well characterized transport mechanisms, including known interactions with motors and cargo adapters. This will allow better characterization of which specific aspects of FAT involve Htt and if it associates more closely with specific motors, or a specific class of cargos.

Before more transport analysis is completed, it will also be important to develop better imaging and analysis protocols to facilitate automated cargo transport imaging and quantification. Use of anesthetization, *in vivo* imaging, and the highly specific CCAP driver have vastly reduced noise and improved efficiency of this assay. However, we are limited to the use of the CCAP driver, and manual tracking of organelle movement is required. Automated tracking software has been

developed, but is still unable to accurately track *in vivo* organelle movement in complex situations such as axons (Youssef, Gude et al. 2011). Advances in software and image quality will both serve to aide automated analysis. One method to improve image quality, reduce noise, and facilitate more efficient object tracking may include utilizing photo-activatable GFP variants. This would allow us to follow and image of a small subset of cargos over much greater distance in the axon. Improved automated object tracking will have broad applications for analysis of mitochondrial dynamics, synaptic vesicle endocytosis and exocytosis, fluorescent calcium imaging, membrane restructuring, and behavioral phenotypes.

References

Akimzhanov, A. M. and D. Boehning (2011). "Monitoring dynamic changes in mitochondrial calcium levels during apoptosis using a genetically encoded calcium sensor." J Vis Exp(50).

Block-Galarza, J., K. O. Chase, et al. (1997). "Fast transport and retrograde movement of huntingtin and HAP 1 in axons." Neuroreport **8**(9-10): 2247-2251.

Caviston, J. P., A. L. Zajac, et al. (2011). "Huntingtin coordinates the dynein-mediated dynamic positioning of endosomes and lysosomes." Mol Biol Cell **22**(4): 478-492.

Davies, S. W., M. Turmaine, et al. (1997). "Formation of neuronal intranuclear inclusions underlies the neurological dysfunction in mice transgenic for the HD mutation." Cell **90**(3): 537-548.

DiFiglia, M., E. Sapp, et al. (1995). "Huntingtin is a cytoplasmic protein associated with vesicles in human and rat brain neurons." Neuron **14**(5): 1075-1081.

DiFiglia, M., E. Sapp, et al. (1997). "Aggregation of huntingtin in neuronal intranuclear inclusions and dystrophic neurites in brain." Science **277**(5334): 1990-1993.

Dragatsis, I., M. S. Levine, et al. (2000). "Inactivation of Hdh in the brain and testis results in progressive neurodegeneration and sterility in mice." Nat Genet **26**(3): 300-306.

Gauthier, L. R., B. C. Charrin, et al. (2004). "Huntingtin controls neurotrophic support and survival of neurons by enhancing BDNF vesicular transport along microtubules." Cell **118**(1): 127-138.

Graham, R. K., Y. Deng, et al. (2006). "Cleavage at the caspase-6 site is required for neuronal dysfunction and degeneration due to mutant huntingtin." Cell **125**(6): 1179-1191.

Haghnia, M., V. Cavalli, et al. (2007). "Dynactin is required for coordinated bidirectional motility, but not for dynein membrane attachment." Mol Biol Cell **18**(6): 2081-2089.

Havel, L. S., C. E. Wang, et al. (2011). "Preferential accumulation of N-terminal mutant huntingtin in the nuclei of striatal neurons is regulated by phosphorylation." Hum Mol Genet **20**(7): 1424-1437.

Horiuchi, D., R. V. Barkus, et al. (2005). "APLIP1, a kinesin binding JIP-1/JNK scaffold protein, influences the axonal transport of both vesicles and mitochondria in Drosophila." Curr Biol **15**(23): 2137-2141.

Pilling, A. D., D. Horiuchi, et al. (2006). "Kinesin-1 and Dynein are the primary motors for fast transport of mitochondria in Drosophila motor axons." Mol Biol Cell **17**(4): 2057-2068.

Romero, E., G. H. Cha, et al. (2008). "Suppression of neurodegeneration and increased neurotransmission caused by expanded full-length huntingtin accumulating in the cytoplasm." Neuron **57**(1): 27-40.

Schilling, G., A. Klevytska, et al. (2007). "Characterization of huntingtin pathologic fragments in human Huntington disease, transgenic mice, and cell models." J Neuropathol Exp Neurol **66**(4): 313-320.

Youssef, S., S. Gude, et al. (2011). "Automated tracking in live-cell time-lapse movies." Integr Biol (Camb).

Zhang, S., M. B. Feany, et al. (2009). "Inactivation of Drosophila Huntingtin affects long-term adult functioning and the pathogenesis of a Huntington's disease model." Dis Model Mech **2**(5-6): 247-266.

Supplemental Figures

Figure 1
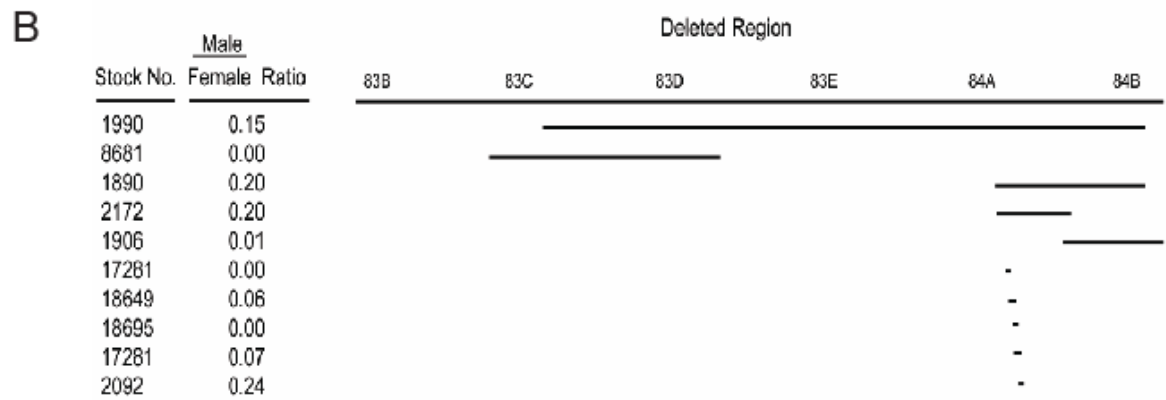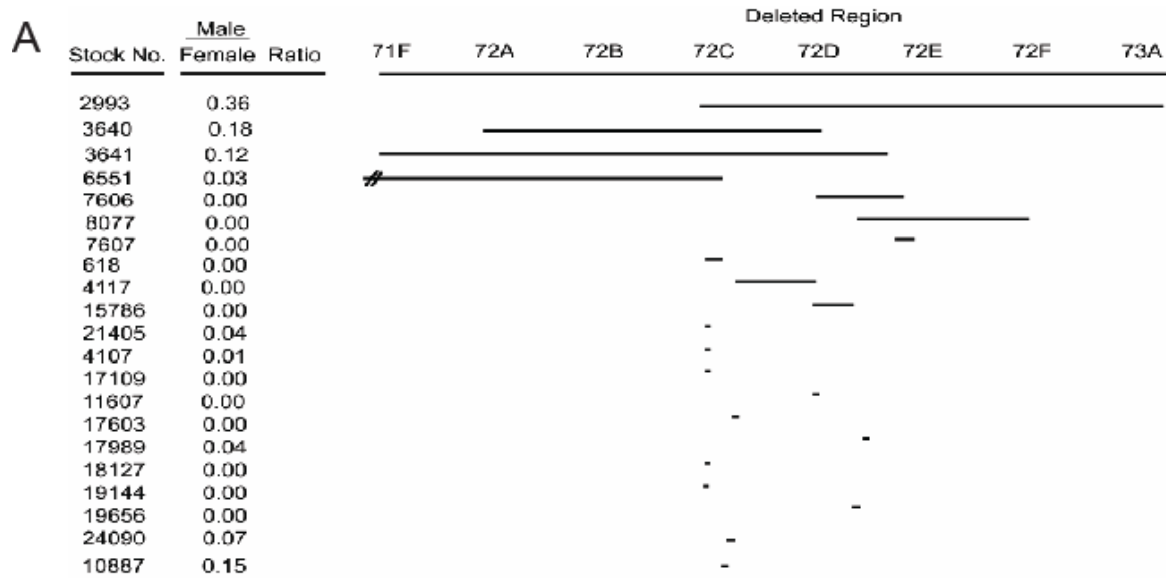
Supplemental Figure 1. Fine mapping for two genetic intervals uncovered in the initial suppressor screen for HttQ138 pupal lethality. (A) Suppressors *Df(3L)st-f13* (Bloomington stock 2993) and *Df(3L)brm11* (Bloomington stock 3640) overlap the 72C1-72D5 interval. Mapping with additional aberrations contained within the Bloomington Stock Center demonstrated stock 10887 (PBc02324) rescued HttQ138 expressing animals at 15% of expected viability. (B) Suppressor *Df(3R)Tpl10* (Bloomington stock 1990) was sub-mapped to a single genetic aberration within the region defined by stock 2092 (*lab*[14]) that increased the expected adult viability ratio to 24%.

Supplemental Table 1

Chr 2	Stock No.	Balancer	Male	Female	ratio	Aggregation
1	140	CyO	61	0	0	Yes
2	167	CyO	71	1	0.01	Yes
3	179	CyO	51	0	0	Yes
4	190	CyO	46	2	0.043	Yes
5	198	CyO	51	0	0	Yes
6	201	CyO	57	1	0.017	Yes
7	282	SM5	52	0	0	Yes
8	420	CyO	53	0	0	Yes
9	447	CyO	102	3	0.029	Yes
10	490	Cyo	55	1	0.018	Yes
11	567	CyO	68	0	0	Yes
12	740	SM1	62	1	0.016	Yes
13	754	CyO	100	2	0.02	Yes
14	757	CyO	70	1	0.014	Yes
15	781	SM6b	127	12	0.094	Yes
16	1491	CyO	50	1	0.02	not checked
17	1547	CyO	54	0	0	Yes
18	1567	Cyo	160	22	0.14	Yes
19	1702	CyO	59	0	0	Yes
20	1743	CyO	55	0	0	Yes
21	1888	CyO	52	0	0	Yes
22	2413	CyO	63	0	0	Yes
23	2583	CyO	56	1	0.017	Yes
24	2604	SM5	69	0	0	Yes
25	2892	CyO	53	1	0.018	Yes
26	3079	CyO	54	0	0	Yes
27	3084	SM1	58	0	0	Yes
28	3138	CyO	53	0	0	Yes
29	3157	SM1	72	4	0.055	Yes
30	3366	SM1	71	0	0	Yes
31	3368	CyO	53	7	0.13	No
32	3467	CyO	61	9	0.16	Less?
33	3520	CyO	65	1	0.016	Yes
34	3588	CyO	82	0	0	Yes
35	3591	CyO	49	1	0.02	Yes
36	3592	Cyo	55	0	0	Yes
37	3909	SM1	43	7	0.16	No
38	4956	CyO	51	0	0	Yes

39	4959	CyO	57	0	0	Yes
40	4960	CyO	69	1	0.014	Yes
41	4961	CyO	52	1	0.019	Yes
42	4966	CyO	56	1	0.018	Yes
43	5246	CyO	54	0	0	Yes
44	5330	Cyo	78	0	0	Yes
45	5420	CyO	60	0	0	Yes
46	5574	CyO	65	1	0.015	Yes
47	5680	CyO	50	0	0	Yes
48	5869	CyO	55	0	0	Yes
49	5879	SM6a	62	0	0	Yes
50	6283	SM5	51	1	0.02	Yes
51	6299	SM6a	50	0	0	Yes
52	6338	SM6a	54	1	0.018	Yes
53	6374	CyO	72	7	0.097	Yes
54	6455	SM6a	102	6	0.058	Yes
55	6478	SM6a	64	1	0.015	Yes
56	6507	SM6b	23	2	0.086	Yes
57	6516	SM6a	50	1	0.02	Yes
58	6608	SM6a	61	0	0	Yes
59	6609	SM6a	59	2	0.034	Yes
60	6647	SM6a	63	1	0.015	Yes
61	6779	SM6a	65	4	0.061	Yes
62	6780	SM6a	54	1	0.018	Yes
63	6865	CyO	50	0	0	Yes
64	6866	CyO	53	0	0	Yes
65	6875	SM6a	54	1	0.017	Yes
66	6917	CyO	56	0	0	Yes
67	6965	Cyo	47	1	0.021	Yes
68	7143	SM6a	56	1	0.018	Yes
69	7146	SM6a	65	0	0	Yes
70	7147	CyO	54	0	0	Yes
71	7273	CyO	52	1	0.019	Yes
72	7441	SM6a	50	0	0	Yes
73	7531	CyO	55	1	0.018	Yes
74	7875	CyO	54	1	0.019	Yes
75	7896	CyO	62	0	0	Yes
76	8469	SM6a	61	0	0	Yes
77	8672	Cyo	57	1	0.017	Yes
78	8674	Cyo	52	9	0.17	Yes
79	8835	Cyo	51	0	0	Yes
80	8836	CyO	81	2	0.025	Yes
81	9298	SM6a	55	1	0.018	Yes

82	9410	CyO	52	0	0	Yes
Ch 3	Stock No.	Balancer/Marker	male	female	ratio	Aggregation
1	383	TM3	56	5	0.017	Yes
2	439	TM2	51	2	0	Yes
3	463	TM3	58	0	0	Yes
4	600	TM3	56	0	0	Yes
5	669	TM3	66	0	0	Yes
6	823	TM3	66	0	0	Yes
7	1467	TM1	67	0	0	Yes
8	1518	MKRS	58	0	0	Yes
9	1534	MKRS	64	0	0	Yes
10	1541	TM3	59	0	0	Yes
11	1842	TM3	51	0	0	Yes
12	1884	TM3	77	8	0.05	Yes
13	1910	TM3	57	1	0	Yes
14	1920	TM2	94	5	0.05	Yes
15	1931	TM3	50	0	0	Yes
16	1962	TM3	57	0	0	Yes
17	1968	TM3	48	0	0	Yes
18	1990	TM3	40	7	0.15	Yes
19	2363	TM3	52	0	0	Yes
20	2425	TM2	56	0	0	Yes
21	2585	TM3	52	0	0	Yes
22	2612	TM3	42	25	0.52	No
23	2990	TM3	58	0	0	
24	2993	TM6B, Tb[1]	59	26	0.36	Yes
25	3007	TM3	53	0	0	Yes
26	3024	TM3	52	0	0	Yes
27	3096	TM3	14	2	0	not checked
28	3127	TM3	59	0	0	not checked
29	3128	TM3	50	1	0.02	Yes
30	3640	TM6C	120	22	0.175	Yes
31	4430	TM2	55	1	0.018	Yes
32	4431	TM2	81	1	0.01	Yes
33	4432	TM3	53	0	0	Yes
34	4500	TM3	50	0	0	Yes
35	4787	TM3	55	0	0	Yes
36	4940	TM3	55	1	0	Yes
37	4962	TM2	64	17	0.25	Mix of less and normal
38	5492	TM3	55	0	0	Yes
39	5601	TM6C	52	0	0	Yes
40	5877	TM3	56	0	0	Yes

41	5878	TM3	53	0	0	Yes
42	6411	TM3	53	0	0	Yes
43	6456	TM3	134	17	0.066	Yes
44	6457	TM3	53	0	0	Yes
45	6460	TM2	51	1	0.02	Yes
46	6471	TM3	83	0	0	Yes
47	6551	TM3	100	6	0.04	Yes
48	6649	TM3	57	5	0.035	
49	6756	TM3	51	0	0	Yes
50	6964	TM2	90	18	0.14	Yes
51	7079	TM3	54	0	0	Yes
52	7080	TM2	117	3	0.026	Yes
53	7412	TM3	53	0	0	Yes
54	7413	TM2	57	0	0	Yes
55	7443	TM3	54	1	0.018	Yes
56	8082	TM6C	74	7	0	Yes
57	8101	TM6C	61	0	0	Yes
58	8103	TM6C	55	1	0.018	Yes
59	8491	TM2	51	0	0	Yes
60	8583	TM2	69	1	0.014	Yes

Supplemental Table 1. Table showing all 166 lines from the Bloomington deficiency kit that were tested in the initial screen along with the number of viable flies and whether they had changes in salivary gland aggregation. The viability data is also represented graphically in figure 8A.

Appendix

A number of disulfide bond-free single chain antibodies were developed to the N-terminal 23 amino acids of Htt to evaluate the effects of targeting interacting proteins to Htt on aggregation. One particular intrabody, A3D2, was found to robustly reduce aggregation in the salivary gland and CNS, but not the PNS. Expression of this intrabody did not rescue pharate lethality from high expression of Q138Htt nor did it rescue the reduced lifespan induced by low expression Q138Htt. These results suggest that reducing aggregation in the salivary gland and CNS are not sufficient to rescue Q138Htt-mediated toxicity, though further characterization of this intrabody's *in vivo* effects are required.

Appendix Figure 1
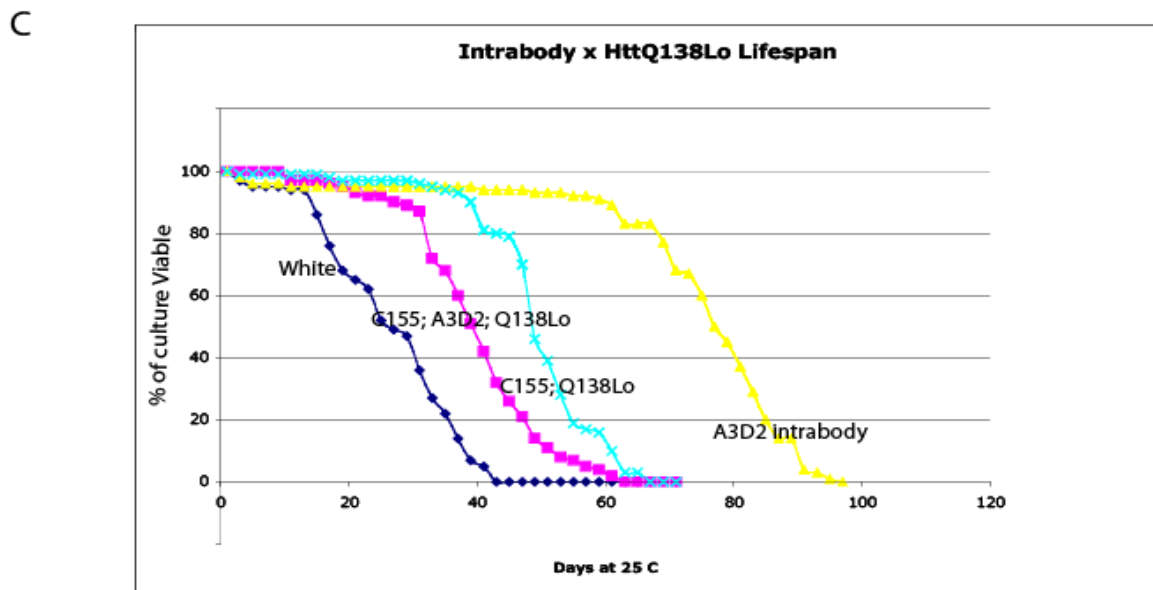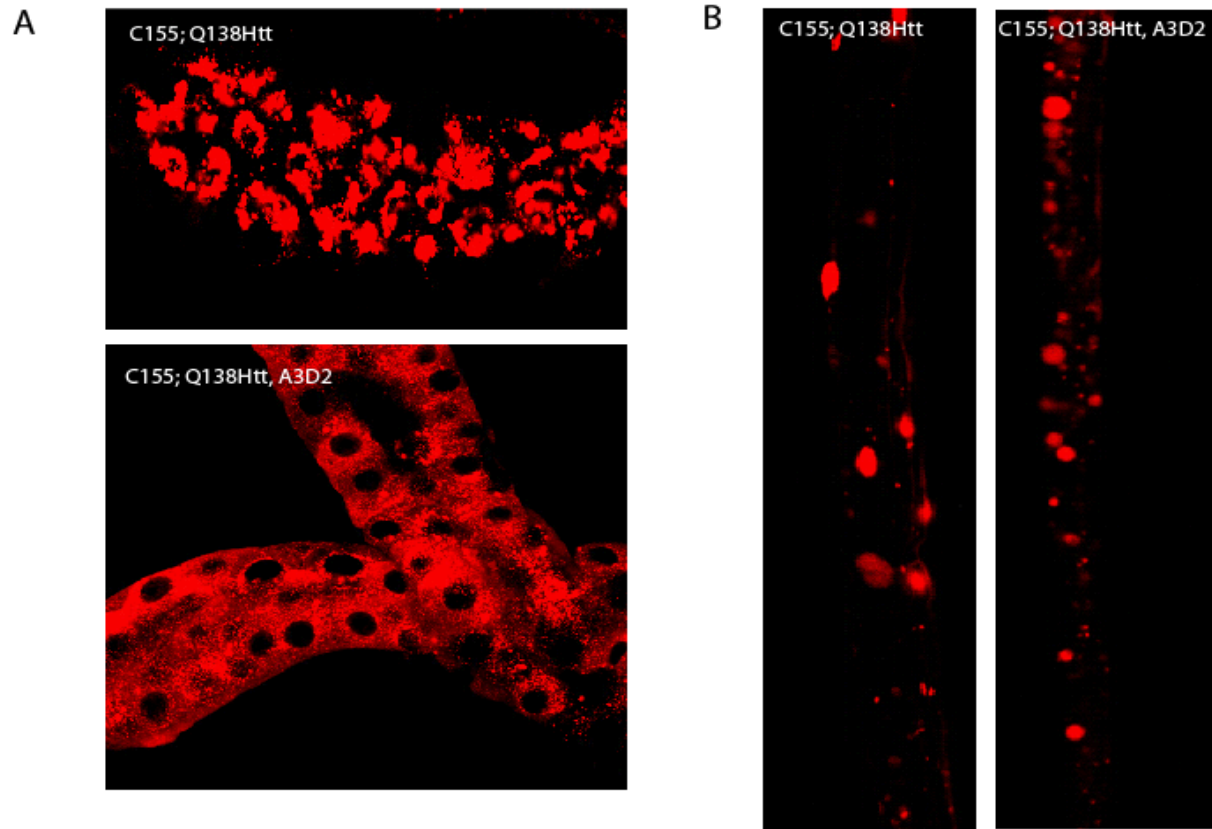
Appendix Figure 1. Intrabody. A disulfide bond free single chain intrabody (A3D2) against first 23 amino acids of Htt reduces Q138Htt-RFP aggregation in the salivary gland (A), there was no change in aggregation in the peripheral nerves (B). Co-expression of the intrabody with a low expression Q138Htt adult viable line did not significantly alter lifespan.